Development of local Coupled Cluster response methods for properties and analytic gradients of excited states in extended molecular systems

Dissertation

zur Erlangung des Doktorgrades der Naturwissenschaften (Dr. rer. nat.)
der Fakultät
- Chemie und Pharmazie -
der Universität Regensburg

vorgelegt von

Katrin Ledermüller,
geb. **Freundorfer**

aus Vilshofen an der Donau

im Jahr 2014

Promotionsgesuch eingereicht am: 10.02.2014
Die Arbeit wurde angeleitet von: Prof. Dr. Martin Schütz

Die Ergebnisse dieser Arbeit wurden bereits veröffentlicht oder zur Veröffentlichung eingereicht:

Chapter 2:

K. Ledermüller, D. Kats and M. Schütz

"Local CC2 response method based on the Laplace transform: Orbital-relaxed first-order properties for excited states"

The Journal of Chemical Physics

139, 084111 (2013), doi: 10.1063/1.4818586

Chapter 3:

K. Ledermüller and M. Schütz

"Local CC2 response method based on the Laplace transform: Analytic energy gradients for ground and excited states"

The Journal of Chemical Physics

submitted (2014)

Danksagung

An dieser Stelle möchte ich mich bei all denen bedanken, die zur Entstehung dieser Arbeit beigetragen haben. Mein besonderer Dank gilt dabei:

- Herrn *Prof. Dr. Martin Schütz* für die Möglichkeit dieses Thema zu bearbeiten sowie für die Betreuung und Unterstützung in dieser Zeit.
- Herrn *Prof. Dr. Bernhard Dick* für die freundliche Übernahme der Zweitbegutachtung.
- Der *Studienstiftung des deutschen Volkes* für die finanzielle Förderung.
- *Dr. Daniel Kats* für seine Hilfsbereitschaft.
- *Stefan Loibl* für die vielen hilfreichen Diskussionen.
- *Thomas Merz* für seine Hilfestellung bei Anwendungs- und sonstigen Fragen.
- *Klaus Ziereis* für seine schnelle und kompetente Hilfe bei Computerproblemen.
- Neben den bereits genannten aktuellen und ehemaligen Kollegen natürlich auch *Dr. Denis Usvyat*, *Dr. Keyarash Sadeghian*, *Dr. Dominik Schemmel*, *Dr. Marco Lorenz*, *Oliver Masur*, *Gero Wälz*, *David David*, *Matthias Hinreiner* und *Alexander Schinabeck* für die schöne gemeinsame Zeit am Arbeitskreis.
- *Eva S.*, *Eva W.*, *Michi*, *Oli*, *Susanne*, *Tanja* und *Tobi* für die gemeinsame Zeit während des Studiums und auch danach, die ohne sie viel langweiliger und trostloser gewesen wäre.
- Nicht zuletzt auch allen, die mich außerhalb des universitären Umfelds unterstützt haben, allen voran meinem Mann *Achim* sowie meinen Eltern *Frieda* und *Helmut*.

Contents

Chapter 1

Introduction

The excitation of electrons in molecules plays an important role for many applications in chemistry and physics. Thus, there is a need for theoretical methods based on quantum mechanics, which are able to describe such processes and complement the experimental techniques.

The behaviour of molecules in the ground state and in electronically excited states can be analysed based on the related potential energy hypersurfaces (PES).[1,2] The PES describes the energy of an eigenstate of the electronic Schrödinger equation as a function of the nuclear positions. The separation of the system into an electronic part and a nuclear part, which contributes as a parameter to the electronic part, is enabled by the Born-Oppenheimer approximation, which is one of the basic concepts in quantum chemistry.[3] This partitioning into an electronic and a nuclear part is justified by the much faster movement of the electrons compared to the movement of the nuclei. Hence, the electronic structure of a molecule can be considered at a fixed nuclear geometry and only the electronic Schrödinger equation has to be solved. After a change of the electronic structure caused by an excitation the nuclei subsequently relax due to the new potential in order to reach a stable state.

For the description of photophysical processes the PES of the ground and the excited states have to be analysed. Molecular properties calculated at particular geometries can complete the picture. Stationary points of the PES are equilibrium and transition structures of molecules, and thus of great interest in chemistry and physics as has been discussed in many publications about this topic, e.g. in the context of photochemistry and the special topic of photocatalysis.[4,5] For locating stationary points on the PES the gradient of the energy with respect to nuclear displacements has to be calculated.

Therefore, a variety of quantum chemical methods has been developed, which are able

to describe the electronic structure of molecules and to predict molecular properties. One example for a *post*-Hartree-Fock method, i.e. a method describing the correlation of the electrons based on an underlying Hartree-Fock (HF) calculation, is the Coupled Cluster (CC) method.[6–8] Excitation energies and properties of the ground and the excited states can be obtained via CC response theory.[9] A general problem of correlation methods like CC, limiting their applicability to larger molecules, is the steep scaling of the computational cost with the size of the molecules.
The aim of this thesis is the development of orbital-relaxed properties and gradients with respect to nuclear displacements within the Coupled Cluster model CC2, which are also applicable to extended molecular systems. The following sections give a short introduction to the CC2 method for the ground state (section 1.1) and electronically excited states (section 1.2). Moreover, two concepts are presented, which were used in the context of this thesis in order to reduce the computational cost, namely density fitting and local correlation methods. In section 1.3 the diagrammatic techniques are explained, which help to obtain practical equations from the common CC expressions. Finally, section 1.4 gives an outline of the thesis.

1.1 Coupled Cluster model CC2 for the ground state

1.1.1 The CC2 model

Coupled Cluster is a *post*-Hartree-Fock method describing the correlation of the electrons.[6–8] The general CC wavefunction can be written as

$$|CC\rangle = \exp(\mathbf{T})|0\rangle \tag{1.1}$$

with the Hartree-Fock reference determinant $|0\rangle$ and the cluster operator $\mathbf{T}$, which is defined as

$$\mathbf{T} = \sum_i \mathbf{T_i} \ , \quad \text{with} \quad \mathbf{T_i} = \sum_{\mu_i} t_{\mu_i} \tau_{\mu_i} \ . \tag{1.2}$$

τ_{μ_i} are excitation operators and t_{μ_i} the corresponding amplitudes. For singlet substitutions, as they occur for the electronic ground state and for singlet excited states, the

single and double excitation operators needed for the CC2 model are defined as

$$\begin{aligned} \tau_i^a &= a_{a\alpha}^\dagger a_{i\alpha} + a_{a\beta}^\dagger a_{i\beta} \ , \\ \tau_{ij}^{ab} &= \frac{1}{2}(a_{a\alpha}^\dagger a_{i\alpha} + a_{a\beta}^\dagger a_{i\beta})(a_{b\alpha}^\dagger a_{j\alpha} + a_{b\beta}^\dagger a_{j\beta}) \ , \end{aligned} \tag{1.3}$$

in terms of the elementary second quantization creation and annihilation operators $a^\dagger$ and a (the index $i\alpha$ implies a spin orbital related to a spatial orbital i times spin function α, *etc.*). The double excitation operators are symmetric with respect to the permutation of the electrons, i.e. $\tau_{ij}^{ab} = \tau_{ji}^{ba}$.
The CC ground state correlation energy is calculated as

$$E_0^{\mathrm{CC}} = \langle 0| \exp(-\mathbf{T})\mathbf{H} \exp(\mathbf{T})|0\rangle = \langle 0|\mathbf{H}|CC\rangle \ , \tag{1.4}$$

where $\mathbf{H}$ is the normal ordered Hamiltonian consisting of the Fock matrix $\mathbf{F}$ and the fluctuation potential $\mathbf{V}$,

$$\mathbf{H} = \mathbf{F} + \mathbf{V} \ . \tag{1.5}$$

By employing the Baker-Campbell-Hausdorff-expansion,

$$\exp(-\mathbf{T})\mathbf{H} \exp(\mathbf{T}) = \mathbf{H} + [\mathbf{H}, \mathbf{T}] + \frac{1}{2!}[[\mathbf{H}, \mathbf{T}], \mathbf{T}] + \frac{1}{3!}[[[\mathbf{H}, \mathbf{T}], \mathbf{T}], \mathbf{T}] + ... \ , \tag{1.6}$$

the CC equations can be written using more convenient commutator expressions.
The computationally cheapest CC model, which is also used for excited state calculations and includes dynamical correlation effects, is the CC2 model. It was proposed by Christiansen *et al.*[10] as an approximation to the well-known CCSD (CC including single and double excitations) model. The summation in the CC2 cluster operator $\mathbf{T}$ runs over single and double excitations ($\mathbf{T} = \mathbf{T_1} + \mathbf{T_2}$), thus the CC2 correlation energy can be written as

$$\begin{aligned} E_0^{\mathrm{CC2}} &= \langle 0| \exp(-\mathbf{T_1}) \exp(-\mathbf{T_2})\mathbf{H} \exp(\mathbf{T_1}) \exp(\mathbf{T_2})|0\rangle \\ &= \left\langle 0|\hat{\mathbf{H}} + [\hat{\mathbf{H}}, \mathbf{T_2}]|0\right\rangle \ . \end{aligned} \tag{1.7}$$

The correlation energy is explicitly labeled with the superscript CC2 to avoid confusion with the full energy including the HF contribution, which will occur in chapter 3. Operators decorated with a hat represent operators similarity transformed by the exponent

of the singles cluster operator $\mathbf{T_1}$, e.g.

$$\hat{\mathbf{H}} = \exp(-\mathbf{T_1})\mathbf{H}\exp(\mathbf{T_1}) \ . \tag{1.8}$$

A consequence of the similarity transformed operators is the occurrence of *dressed* integrals, which will be discussed in section 1.1.4. The CC2 amplitudes are determined by the equations

$$\begin{aligned} \Omega_{\mu_1} &= \left\langle \tilde{\mu}_1 \left| \hat{\mathbf{H}} + \left[\hat{\mathbf{H}}, \mathbf{T_2}\right] \right| 0 \right\rangle = 0 \ , \\ \Omega_{\mu_2} &= \left\langle \tilde{\mu}_2 \left| \hat{\mathbf{H}} + [\mathbf{F}, \mathbf{T_2}] \right| 0 \right\rangle = 0 \ . \end{aligned} \tag{1.9}$$

$\langle\tilde{\mu}_1|$ and $\langle\tilde{\mu}_2|$ are contravariant configuration state functions (CSFs) projecting onto the singles and doubles manifold.[11] The covariant `ket` and contravariant `bra` CSFs for singlet states are defined as

$$\begin{aligned} |\Phi_i^a\rangle &= \tau_i^a|0\rangle \ , & |\Phi_{ij}^{ab}\rangle &= \tau_{ij}^{ab}|0\rangle \ , \\ \langle\tilde{\Phi}_i^a| &= \frac{1}{2}\langle\Phi_i^a| \ , & \langle\tilde{\Phi}_{ij}^{ab}| &= \frac{1}{6}\left(2\langle\Phi_{ij}^{ab}| + \langle\Phi_{ji}^{ab}|\right) \ . \end{aligned} \tag{1.10}$$

The amplitudes related to double substitutions are correct only to first order with respect to a Møller-Plesset (MP) partitioning of the Hamiltonian, whereas the full $\exp(\mathbf{T_1})$ part of the CC ansatz is retained to provide partial orbital relaxation.

1.1.2 Density fitting approximation

Compared to computationally cheap methods, like density functional theory (DFT), canonical CC2, although being one of the cheapest CC models, is computationally rather expensive and the scaling behaviour of the computational cost with molecular size $\mathcal{N}$ is $\mathcal{O}(\mathcal{N}^5)$. Therefore, for extended molecular systems DFT might be the sole applicable method for the calculation of excited states, although it is unreliable and often fails qualitatively, if charge transfer (CT) states, Rydberg states or excitations of extended π systems are involved.[12–14] In order to reduce the computational cost of CC2 for ground and excited state calculations the density fitting approximation (DF)[15–17] is applied to the four-index two-electron integrals,

$$(mn|pq) = \int \Phi_m^*(r_1)\Phi_p^*(r_2)r_{12}^{-1}\Phi_n(r_1)\Phi_q(r_2)dr_1dr_2 \ . \tag{1.11}$$

Within this approximation the four-index integrals are decomposed into three-index objects, i.e.

$$(mn|pq) \approx \sum_P (mn|P) c_{pq}^P \ , \qquad \text{with} \qquad c_{pq}^P = \sum_Q \left(J^{-1}\right)_{PQ} (Q|pq) \ . \tag{1.12}$$

The fitting coefficients c_{pq}^P are determined by the minimization of an error functional. The capital letters P, Q index the auxiliary fitting functions and $J_{PQ} = (P|Q)$ is an element of their Coulomb matrix. The indices $m, n, p, \ldots$ denote general molecular orbitals.

There are highly efficient CC2 and scaled opposite-spin (SOS) CC2 implementations using this approach for properties and analytic gradients of the ground state and excited states.[18–23] However, DF reduces only the prefactor, but not the scaling with molecular size $\mathcal{N}$: canonical DF-CC2 still scales as $\mathcal{O}(\mathcal{N}^5)$.

1.1.3 Local approximations

For a further reduction of the computational cost the application of local approximations to DF-CC2 has been proposed.[24–29] The basic idea of local methods is to utilize the short-range nature of the dynamic electron correlation in nonmetallic systems, but this is only possible in a basis of spatially localized orbitals. The canonical orbitals resulting from a Hartree-Fock calculation are completely delocalized and thus inappropriate for local methods. A spatially localized basis can e.g. consist of localized molecular orbitals (LMOs) to span the occupied space, and projected atomic orbitals (PAOs) for the virtual space.[30,31] The molecular orbitals (MO) are in general expanded in a non-orthogonal atomic orbital (AO) basis χ_μ with the metric $S_{\mu\nu}^{\mathrm{AO}} = \langle \chi_\mu | \chi_\nu \rangle$,

$$\phi_p = \sum_\mu \chi_\mu C_{\mu p}. \tag{1.13}$$

AOs are labeled by greek letters. The LMO coefficient matrix $\mathbf{L}$ is obtained from the canonical occupied coefficients via unitary transformation,

$$L_{\mu i} = \sum_{\bar{i}} C_{\mu \bar{i}}^{\mathrm{o}} W_{\bar{i} i} \ , \tag{1.14}$$

with the occupied part of the canonical coefficient matrix $\mathbf{C^o}$. For canonical occupied orbitals the indices $\bar{i}, \bar{j}, \ldots$ are used, for LMOs the indices $i, j, \ldots$ Different choices for

the unitary matrix $\mathbf{W}$ are possible, in the following it is assumed, that the Pipek-Mezey procedure is used, which minimizes the number of atoms on which the LMO is located.[32] Another well-known localization scheme is the Boys procedure, which maximizes the distance between the orbital centroids.[33] The PAOs, which span the virtual space, are obtained via projection of the atomic orbitals onto the virtual space[30] with the projector matrix $\mathbf{P}$,

$$P_{\mu r} = \sum_{a\nu\rho} C^{v}_{\mu a} C^{v\dagger}_{a\nu} S^{\mathrm{AO}}_{\nu\rho} \delta_{\rho r} = \sum_{a} C^{v}_{\mu a} Q_{ar} \ . \tag{1.15}$$

$\mathbf{C^v}$ is the virtual part of the canonical coefficient matrix and $\mathbf{Q}$ the matrix, which transforms from canonical to PAO basis. For canonical virtual orbitals the indices $a, b, \ldots$ are used, for PAOs the indices $r, s, \ldots$ The LMOs are mutually orthogonal, while the PAOs are orthogonal to the LMOs, but not mutually. The metric $\mathbf{S}$ of the PAOs is obtained as

$$\mathbf{S} = \mathbf{P}^{\dagger}\mathbf{S}^{\mathrm{AO}}\mathbf{P} = \mathbf{Q}^{\dagger}\mathbf{Q} \ . \tag{1.16}$$

In the spatially localized LMO/PAO basis local approximations can be introduced. In local CC2 methods the singles quantities remain unrestricted, whereas the doubles are restricted to excitations from LMOs ij on a truncated pair list to PAOs in the corresponding pair domain $[ij]$.[24,26] For the electronic ground state the restrictions are obtained straightforwardly from distance criteria. The LMO pair list for the electronic ground state contains all pairs of LMOs up to a particular LMO interorbital distance R_g. The domains truncating the pair-specific virtual space are obtained by unifying the corresponding orbital domains, which are built by applying the Boughton Pulay procedure.[34] The BP orbital domain $[i]$ comprises the PAOs arising from AOs, which considerably contribute to the particular LMO i. The LMO interorbital distances for the construction of the pair list are measured as the closest distance between the two sets of nuclei related to the relevant BP domains.

1.1.4 Dressed integrals

Dressed integrals occur due to the operators, which are similarity transformed by the exponent of the singles cluster operator $\mathbf{T_1}$, c.f. eq. (1.8). They are calculated as

$$(mn\hat{|}pq) = \sum_{\mu\nu\rho\sigma} (\mu\nu|\rho\sigma)\Lambda^p_{\mu m}\Lambda^h_{\nu n}\Lambda^p_{\rho p}\Lambda^h_{\sigma q} \ , \tag{1.17}$$

with the coefficient matrices $\mathbf{\Lambda^p}$ and $\mathbf{\Lambda^h}$ in LMO/PAO basis, which contain the singles ground state amplitudes t_{μ_1},

$$\begin{aligned} \Lambda^p_{\mu r} &= P_{\mu r} - \sum_{ir'} L_{\mu i} t^i_{r'} S_{r'r} \ , & \Lambda^p_{\mu i} &= L_{\mu i} \ , \\ \Lambda^h_{\mu r} &= P_{\mu r} \ , & \Lambda^h_{\mu i} &= L_{\mu i} + \sum_r P_{\mu r} t^i_r \ . \end{aligned} \tag{1.18}$$

As discussed in section IIA of Ref. 29, for the Fock matrix internal and external dressing are distinguished. The Fock matrix contains the one-electron integrals $h_{\mu\nu}$ and the two-electron integrals $(\mu\nu|\rho\sigma)$. Internal dressing refers to the use of the coefficient matrices $\mathbf{\Lambda^p}$ and $\mathbf{\Lambda^h}$ in the contraction with the two-electron integrals inside the Fock matrix,

$$\hat{f}_{\mu\nu} = h_{\mu\nu} + 2\sum_{k\rho\sigma} \Lambda^p_{\rho k}\Lambda^h_{\sigma k}[(\mu\nu|\rho\sigma) - 0.5(\mu\rho|\sigma\nu)] \ . \tag{1.19}$$

Internal dressing actually involves contractions with the fluctuation potential (evident, when the similarity transformation with $\exp(\mathbf{T_1})$ is carried out after the Hamiltonian is written in normal ordered form) and is therefore of first-order. External dressing, on the other hand, means using these coefficient matrices for the transformation of the (internally dressed) Fock matrix $\hat{f}_{\mu\nu}$ to the MO basis,

$$\hat{f}_{pq} = \sum_{\mu\nu} \hat{f}_{\mu\nu}\Lambda^p_{\mu p}\Lambda^h_{\nu q} \ , \tag{1.20}$$

and is of zeroth-order.

Dressed integrals and other objects containing such integrals are labeled by a hat. If not explicitly stated otherwise, $\hat{f}_{pq}$ implies internal and external dressing.

1.2 CC2 for excited states

Time-dependent (TD) response theory is a widely-used and general framework providing access to excitation energies and other properties of excited states for various wavefunction approaches. It starts from the time-dependent Schrödinger equation, which contains a time dependent-perturbation. The use of TD response theory is well established *e.g.* in the context of Hartree-Fock (TD-HF),[35] density functional (TD-DFT),[12,36] or Coupled Cluster theory (TD-CC).[9,37–39] Also TD response methods for non-conventional, variational Coupled Cluster ansätze have been discussed.[40,41] A detailed description of the traditional, non-variational Coupled Cluster linear response theory can be found in reference 9.

First, an appropriate time-averaged quasienergy Lagrangian has to be specified,[42–44] from which then the linear response function is obtained by differentiation (rather than from the time-averaged quasienergy itself, as for variational methods). The excitation energies are obtained as a property of the electronic ground state, namely as the poles of the linear response function, i.e. the frequency-dependent polarizability (FDP). Applied to CC, the result is, that the excitation energies are obtained as the eigenvalues of the Jacobian $\mathbf{A}$,

$$A_{\mu_i \nu_j} = \frac{\partial \Omega_{\mu_i}}{\partial t_{\nu_j}} \ . \tag{1.21}$$

The CC response function differs from the exact one, but the additional terms do not affect the location of the poles. Thus CC theory reproduces the exact pole structure, from which the excitation energies of the system are obtained. The equation-of-motion Coupled Cluster (EOM-CC) method,[45–49] approaches excited states from the CI perspective, but has close relationships to TD-CC response. The excitation energies and densities of TD-CC response and EOM-CC are equivalent.

There is a hierarchy of CC models employed in the context of TD-CC response theory, differing in the level of truncation of the cluster operator, and in simplifications made in the CC amplitude equations based on many-body perturbation theory.[50] The CC2 model, which is in the focus of this thesis, is the computationally cheapest model of this hierarchy, which does not neglect dynamical correlation effects.[10] The CC2 model produces rather accurate results for excited states, provided that they are dominated by singles substitutions.

Canonical[18–21] as well as local[24–28] CC2 response methods were presented for the calcu-

lation of excitation energies and orbital-unrelaxed first-order properties. Canonical and local implementations both use the densitiy fitting approximation (cf. section 1.1.2) to decompose the four-index integrals into three-index quantities. The methods were developed for singlet and triplet excited states, which both play an important role in spectroscopy.

1.2.1 Singlet excited states

The CC2 Jacobian for singlet excited states takes the form

$$A_{\mu_i\nu_j} = \begin{pmatrix} \langle\tilde{\mu}_1|[\hat{\mathbf{H}},\tau_{\nu_1}] + [[\hat{\mathbf{H}},\tau_{\nu_1}],\mathbf{T_2}])|0\rangle & \langle\tilde{\mu}_1|[\hat{\mathbf{H}},\tau_{\nu_2}]|0\rangle \\ \langle\tilde{\mu}_2|[\hat{\mathbf{H}},\tau_{\nu_1}]|0\rangle & \langle\tilde{\mu}_2|[\mathbf{F},\tau_{\nu_2}]|0\rangle \end{pmatrix} . \tag{1.22}$$

τ_{μ_i} are the singlet excitation operators defined in eq. (1.3), and $\langle\tilde{\mu}_i|$ the contravariant CSFs for singlet states defined in eq. (1.10). For excitation energies it is sufficient to solve the right eigenvalue problem,

$$\mathbf{A}R^f = \omega_f \mathbf{M}R^f \ , \tag{1.23}$$

to obtain the right eigenvector R^f and excitation energy ω_f for state f. $\mathbf{M}$ is the metric of contra- and covariant CSFs. The Jacobian is not symmetric, thus for the calculation of properties also the left eigenvalue problem,

$$\tilde{L}^f\mathbf{A} = \omega_f \tilde{L}^f\mathbf{M} \ , \tag{1.24}$$

has to be solved to obtain the contravariant left eigenvector $\tilde{L}^f$. Details about solving these equation systems and the corresponding working equations can be found in Ref. 24 and 25 for the DF-LCC2 method and in Ref. 26 and 27 for the LT-DF-LCC2 method. The differences between these two local CC2 methods will be discussed in section 1.2.3. Details about the calculation of properties will be discussed in chapter 2.

1.2.2 Triplet excited states

Triplet excited states were introduced into the canonical DF-CC2 response method in Ref. 20, and later also implemented in the framework of the local LT-DF-LCC2 method.[28] For triplet substitutions the excitation operators τ for single and double excitations are

defined as

$$\begin{aligned} \tau_i^a &= a^\dagger_{a\alpha} a_{i\alpha} - a^\dagger_{a\beta} a_{i\beta} \ , \\ \tau_{ij}^{ab} &= (a^\dagger_{a\alpha} a_{i\alpha} - a^\dagger_{a\beta} a_{i\beta})(a^\dagger_{b\alpha} a_{j\alpha} + a^\dagger_{b\beta} a_{j\beta}) \ . \end{aligned} \tag{1.25}$$

Contrary to the singlet case, the triplet double substitution operators have no permutational symmetry ($\tau_{ij}^{ab} \neq \tau_{ji}^{ba}$), but they are linearly dependent according to

$$\tau_{ij}^{ab} + \tau_{ji}^{ba} + \tau_{ji}^{ab} + \tau_{ij}^{ba} = 0. \tag{1.26}$$

To get rid of these redundancies symmetrized operators of the form

$$\begin{aligned} \overset{(+)}{\tau}{}_{ij}^{ab} &= \tau_{ij}^{ab} + \tau_{ji}^{ba}, \quad \forall \ a > b, \ i > j \ , \\ \overset{(-)}{\tau}{}_{ij}^{ab} &= \tau_{ij}^{ab} - \tau_{ji}^{ba}, \quad \forall \ (ai) > (bj) \ , \end{aligned} \tag{1.27}$$

are introduced, which fulfill the symmetry relations

$$\overset{(+)}{\tau}{}_{ij}^{ab} = \overset{(+)}{\tau}{}_{ji}^{ba} = -\overset{(+)}{\tau}{}_{ij}^{ba} = -\overset{(+)}{\tau}{}_{ji}^{ab} \qquad \text{and} \qquad \overset{(-)}{\tau}{}_{ij}^{ab} = -\overset{(-)}{\tau}{}_{ji}^{ba}. \tag{1.28}$$

The covariant `ket` and contravariant `bra` CSFs for triplet states are defined as

$$\begin{aligned} |\Phi_i^a\rangle &= \tau_i^a |0\rangle \ , & |\overset{(+)}{\Phi}{}_{ij}^{ab}\rangle &= \overset{(+)}{\tau}{}_{ij}^{ab} |0\rangle \ , & |\overset{(-)}{\Phi}{}_{ij}^{ab}\rangle &= \overset{(-)}{\tau}{}_{ij}^{ab} |0\rangle \ , \\ \langle\tilde{\Phi}_i^a| &= \frac{1}{2}\langle\Phi_i^a| \ , & \langle\overset{(+)}{\tilde{\Phi}}{}_{ij}^{ab}| &= \frac{1}{8}\langle\overset{(+)}{\Phi}{}_{ij}^{ab}| \ , & \langle\overset{(-)}{\tilde{\Phi}}{}_{ij}^{ab}| &= \frac{1}{8}\langle\overset{(-)}{\Phi}{}_{ij}^{ab}| \ , \end{aligned} \tag{1.29}$$

and the triplet singles and doubles cluster operators $\mathbf{U_1}$ and $\mathbf{U_2}$ as

$$\mathbf{U_1} = \sum_{ia} u_a^i \tau_i^a, \qquad \text{and} \qquad \mathbf{U_2} = \sum_{a>b,i>j} \overset{(+)}{U}{}_{ab}^{ij} \overset{(+)}{\tau}{}_{ij}^{ab} + \sum_{(ai)>(bj)} \overset{(-)}{U}{}_{ab}^{ij} \overset{(-)}{\tau}{}_{ij}^{ab} \ . \tag{1.30}$$

Thus the Jacobian $\mathbf{A}$, for which the right (and for properties also the left) eigenvalue equation system has to be solved, takes for triplet excited states the form

$$A_{\mu_i\nu_j} = \begin{pmatrix} \langle\tilde{\mu}_1|[\hat{\mathbf{H}},\tau_{\nu_1}]+[[\hat{\mathbf{H}},\tau_{\nu_1}],\mathbf{T_2}]|0\rangle & \langle\tilde{\mu}_1|[\hat{\mathbf{H}},\overset{(+)}{\tau}_{\nu_2}]|0\rangle & \langle\tilde{\mu}_1|[\hat{\mathbf{H}},\overset{(-)}{\tau}_{\nu_2}]|0\rangle \\ \langle\overset{(+)}{\tilde{\mu}}_2|[\hat{\mathbf{H}},\tau_{\nu_1}]|0\rangle & \langle\overset{(+)}{\tilde{\mu}}_2|[\mathbf{F},\overset{(+)}{\tau}_{\nu_2}]|0\rangle & 0 \\ \langle\overset{(-)}{\tilde{\mu}}_2|[\hat{\mathbf{H}},\tau_{\nu_1}]|0\rangle & 0 & \langle\overset{(-)}{\tilde{\mu}}_2|[\mathbf{F},\overset{(-)}{\tau}_{\nu_2}]|0\rangle \end{pmatrix} . \quad (1.31)$$

The cluster operator $\mathbf{T}$ refers to the ground state and therefore contains singlet excitation operators. The working equations for the left and right matrix-vector products in the context of the LT-DF-LCC2 method can be found in Ref. 28.

1.2.3 The local CC2 response methods DF-LCC2 and LT-DF-LCC2

The *a priori* specification of local approximations is rather straightforward for ground state amplitudes, but more intricate for eigenvectors of excited states, which can have Rydberg or CT character.[24,26,51,52] Two local CC2 response methods were developed (both including density fitting), which are discussed in the following. Within both methods the local basis is spanned by LMOs and PAOs and restricted pair lists and domains are introduced only for the doubles quantities, the singles remain unrestricted. The latter is important due to the neglect of explicit orbital relaxation in the (time-averaged) Lagrangian, which otherwise would cause fictitious additional poles originating from the underlying time-dependent Hartree Fock solution.[9] Explicit orbital relaxation is added afterwards for the calulation of orbital-relaxed properties and energy gradients as will be demonstrated in the chapters 2 and 3.

DF-LCC2

The DF-LCC2 method was developed for excitation energies[24] and first-order properties.[25] As discussed in detail in section IIB of Ref. 24, it determines the local approximations by an *a priori* analysis of the untruncated CIS (configuration interaction singles) wavefunction of the state of interest, which can be calculated quite simply and fast.
The first step towards the excited state pair list is to determine a list of important LMOs. For every LMO a weight is calculated based on the CIS coefficients and the LMOs are added to the list of important LMOs in order of their weights, starting with the highest one, until the sum of their corresponding weights reaches a threshold κ_e. The remaining

LMOs with low weights are neglected. The CIS wavefunction is normalized, thus setting $\kappa_e = 1$ leads to a full list of important LMOs. The final excited state pair list comprises all pairs of LMOs on this list of important orbitals, all other pairs of LMOs up to a certain interorbital distance R_{ex}, and the pairs of the ground state pair list.
The excited state pair domains $[ij]$, which restrict the virtual space for double excitations from the corresponding pair of LMOs ij, are obtained by unifying the excited state orbital domains $[i]$ and $[j]$. For an important LMO i the excited state orbital domain $[i]$ is the union of the corresponding ground state orbital domain and an additional domain. This additional domain is obtained by applying the Boughton Pulay procedure[34] to orbitals, which are constructed using the CIS coefficients. For unimportant orbitals the excited state orbital domain is equal to the ground state domain.
Within the DF-LCC2 method the singles and doubles eigenvalue equations have to be solved explicitely, it is not possible to construct an effective singles eigenvalue problem as can be done in canonical CC2 (cf. next paragraph). Moreover, the *a priori* approximations obtained from the CIS wavefunction cause problems, if the simpler theory provides qualitatively wrong wavefunctions for the excited states. Hence, another local CC2 method called LT-DF-LCC2 was developed, which employs the Laplace transformation. In this method the eigenvalue equations are reduced to an effective singles eigenvalue problem like in canonical CC2 and multistate calculations with state-specific local approximations are enabled.[26–28]

LT-DF-LCC2

In the following the Einstein convention is employed for conciseness, i.e. repeated indices are implicitly summed up. Summations are only written explicitly, if it is necessary for clarity.
The concept of partitioning the eigenvalue equations using Laplace transformation is applied to the right and left eigenvalue equations and to the equations determining the Lagrange multipliers $\tilde{\lambda}^{\mathbf{0}}$ and $\tilde{\lambda}^{\mathbf{f}}$, which will be introduced in chapter 2. The formalism was derived for MP2,[53] and adopted for local MP2[54] and CC2[26] methods. In the following the approach is explained using the example of the right eigenvalue equation system for singlet excited states. The right eigenvalue problem for the singlet Jacobian leads to a set of equations for the singles part of the eigenvector R_{μ_1}, and a set of equations for

the doubles part R_{μ_2},

$$\begin{aligned} A_{\mu_1\nu_1}R_{\nu_1} + A_{\mu_1\nu_2}R_{\nu_2} &= \omega R_{\nu_1}M_{\nu_1\mu_1} \ , \\ A_{\mu_2\nu_1}R_{\nu_1} + A_{\mu_2\nu_2}R_{\nu_2} &= \omega R_{\nu_2}M_{\nu_2\mu_2} \ . \end{aligned} \tag{1.32}$$

In canonical basis the doubles-doubles part of the Jacobian is diagonal,

$$A_{\mu_2\nu_2} = \Delta\epsilon_{\mu_2}\delta_{\mu_2\nu_2} \ , \quad \text{with} \quad \Delta\epsilon^{ab}_{\bar{i}\bar{j}} = \epsilon_a + \epsilon_b - \epsilon_{\bar{i}} - \epsilon_{\bar{j}} \ . \tag{1.33}$$

ϵ_p is the energy of the canonical orbital p and $\delta_{\mu_2\nu_2}$ is 1 for $\mu_2 = \nu_2$ and 0 otherwise. Hence, an effective singles eigenvalue problem can be formulated and the doubles can be calculated on-the-fly,

$$\begin{aligned} R_{\mu_2} &= \frac{A_{\mu_2\nu_1}R_{\nu_1}}{\omega - \Delta\epsilon_{\mu_2}} \ , \\ A^{\text{eff}}_{\mu_1\nu_1}(\omega)R_{\nu_1} &= A_{\mu_1\nu_1}R_{\nu_1} + A_{\mu_1\xi_2}\frac{A_{\xi_2\nu_1}R_{\nu_1}}{\omega - \Delta\epsilon_{\xi_2}} = \omega M_{\mu_1\nu_1}R_{\nu_1} \ . \end{aligned} \tag{1.34}$$

The Laplace transform (LT) identity,

$$\frac{1}{x} = \int_0^\infty \exp(-xt)dt \approx \sum_{q=1}^{n_q} \mathrm{w}_q \exp(-t_q x) \ , \tag{1.35}$$

can be employed to evaluate the denominator of the doubles expression and to calculate the doubles part on-the-fly,[26,53]

$$A^{\text{eff}}_{\mu_1\nu_1}(\omega)R_{\nu_1} \approx A_{\mu_1\nu_1}R_{\nu_1} - A_{\mu_1\xi_2}\sum_{q=1}^{n_q} \mathrm{w}_q e^{-\Delta\epsilon_{\xi_2}t_q}e^{\omega t_q}A_{\xi_2\nu_1}R_{\nu_1} \ . \tag{1.36}$$

This partitioning allows the formulation of the eigenvalue equation with local orbitals i, j, r, s for the doubles, i.e.

$$\begin{aligned} A^{\text{eff}}_{\mu_1\nu_1}(\omega)R_{\nu_1} &= A_{\mu_1\nu_1}R_{\nu_1} \\ &\quad -A_{\mu_1 irjs}\sum_{q=1}^{n_q} \mathrm{sgn}(\mathrm{w}_q)e^{\omega t_q}Y^{\mathrm{v}}_{rt}(q)Y^{\mathrm{v}}_{su}(q)(A_{ktlu\nu_1}R_{\nu_1})X^{\mathrm{o}}_{ki}(q)X^{\mathrm{o}}_{lj}(q) \\ &= \omega M_{\mu_1\nu_1}R_{\nu_1} \ . \end{aligned} \tag{1.37}$$

Thus, the Laplace transform identity can be utilized to decompose the eigenvalue prob-

lem into an effective singles eigenvalue problem without losing the sparsity of the matrices in the local basis. The doubles can be calculated directly in the local basis as

$$\begin{aligned} R_{rs}^{ij} &= -V_{rt}^{ij} V_{su}^{ij} (1 + \mathcal{P}_{ij}\mathcal{P}_{tu}) \sum_{q=1}^{n_q} \mathrm{sgn}(\mathrm{w}_q) e^{\omega t_q} \\ &\quad \times X_{tv'}^{\mathrm{v}}(q) V_{v'v}^{\dagger} X_{uw'}^{\mathrm{v}}(q) V_{w'w}^{\dagger} (\hat{B}_{vk}^{P} \hat{c}_{wl}^{P}) X_{ki}^{\mathrm{o}}(q) X_{lj}^{\mathrm{o}}(q) \ , \end{aligned} \tag{1.38}$$

with the permutation operator $\mathcal{P}_{pq}$, which permutes the orbital indices p and q, and an intermediate quantity $\hat{B}_{ai}^{P}$, which depends on the singles vector R_{ν_1} (working equations can be found in Ref. 26, section IIB). Thus, in this local CC2 response method based on Laplace transform, denoted as LT-DF-LCC2, just an effective eigenvalue problem in the space of the untruncated singles determinants has to be solved (as in the canonical case) and the doubles part does not enter the Davidson diagonalization explicitly.
The quadrature point dependent matrices $X_{ij}^{\mathrm{o}}(q)$, $X_{rs}^{\mathrm{v}}(q)$ and $Y_{rs}^{\mathrm{v}}(q)$ appearing in eqs. (1.37) and (1.38) were defined in Ref. 54 as

$$\begin{aligned} X_{ij}^{\mathrm{o}}(q) &= W_{\bar{i}i}^{\dagger} e^{(\epsilon_{\bar{i}} - \epsilon_F) t_q + \frac{1}{4}\ln|\mathrm{w}_q|} W_{\bar{i}j}, \\ X_{rs}^{\mathrm{v}}(q) &= Q_{ra}^{\dagger} e^{(-\epsilon_a + \epsilon_F) t_q + \frac{1}{4}\ln|\mathrm{w}_q|} Q_{as}, \\ Y_{rs}^{\mathrm{v}}(q) &= V_{rt} X_{tu}^{\mathrm{v}}(q) V_{us}^{\dagger}. \end{aligned} \tag{1.39}$$

with the matrices $\mathbf{W}$, transforming from occupied canonical orbitals to LMOs, and $\mathbf{Q}$, transforming from virtual canonical orbitals to PAOs, which were already introduced in section 1.1.3. $\mathbf{V^{ij}}$ is the pseudoinverse of the corresponding PAO metric $\mathbf{S^{ij}_{PAO}}$. ϵ_F contains the energy difference between the highest occupied molecular orbital (HOMO) and the lowest unoccupied molecular orbital (LUMO),

$$\epsilon_F = \frac{\epsilon_{HOMO} - \epsilon_{LUMO}}{2} \ , \tag{1.40}$$

and cancels in equation (1.37), but ensures that the exponential factor is for positive t_q always smaller than 1.
The quadrature points t_q and the corresponding weights w_q are obtained by a Simplex optimization procedure.[26,54] It has been shown, that only a small number n_q of Laplace quadrature points is needed to reach sufficient accuracy.[26,28,29,54]
The LT approach can analogously be applied to triplet excited states,[28] with the effective

singles eigenvalue problem

$$A^{\text{eff}}_{\mu_1\nu_1}(\omega)R_{\nu_1} = A_{\mu_1\nu_1}R_{\nu_1} + \frac{(\overset{(+)}{A}_{\mu_1\xi_2}\overset{(+)}{A}_{\xi_2\nu_1} + \overset{(-)}{A}_{\mu_1\xi_2}\overset{(-)}{A}_{\xi_2\nu_1})R_{\nu_1}}{\omega - \Delta\epsilon_{\xi_2}} = \omega M_{\mu_1\nu_1}R_{\nu_1} \ . \tag{1.41}$$

The doubles can be calculated directly in the local basis as

$$\begin{aligned}
\overset{(+)}{R}{}^{ij}_{rs} &= -V^{ij}_{rt}V^{ij}_{su}\frac{(1-\mathcal{P}_{ij})(1-\mathcal{P}_{tu})}{2}\sum_{q=1}^{n_q}\text{sgn}(\text{w}_q)e^{\omega t_q} \\
&\quad \times X^{\text{v}}_{tv'}(q)V^{\dagger}_{v'v}X^{\text{v}}_{uw'}(q)V^{\dagger}_{w'w}(\hat{B}^P_{vk}\hat{c}^P_{wl})X^{\text{o}}_{ki}(q)X^{\text{o}}_{lj}(q) \ , \\
\overset{(-)}{R}{}^{ij}_{rs} &= -V^{ij}_{rt}V^{ij}_{su}\frac{(1-\mathcal{P}_{ij}\mathcal{P}_{tu})}{2}\sum_{q=1}^{n_q}\text{sgn}(\text{w}_q)e^{\omega t_q} \\
&\quad \times X^{\text{v}}_{tv'}(q)V^{\dagger}_{v'v}X^{\text{v}}_{uw'}(q)V^{\dagger}_{w'w}(\hat{B}^P_{vk}\hat{c}^P_{wl})X^{\text{o}}_{ki}(q)X^{\text{o}}_{lj}(q) \ ,
\end{aligned} \tag{1.42}$$

with the quantity $\hat{B}^P_{ai}$ depending on the singles vector R_{ν_1} (details and working equations can be found in Ref. 28, section IIA).

In LT-DF-LCC2 calculations adaptive, state-specific local approximations are employed for excited state doubles quantities, as explained in detail in section IIC of Ref. 26. As in the DF-LCC2 method the excited state pair lists usually contain all pairs of LMOs on the list of important orbitals, all other pairs of LMOs up to a certain interorbital distance R_{ex}, and all pairs of the ground state list. The size of the list of important LMOs is, as for DF-LCC2, regulated via a threshold κ_e, but the criterion is not constructed using the CIS coefficients. It is obtained by a Löwdin like analysis of the untruncated diagonal pair doubles part U^{ii}_{rs} of the actual approximation U_{μ_2} to the eigenvector for each individual state.

The excited state domains are obtained in an adaptive procedure, also based on analysis of the actual approximation to the eigenvector. The orbital domains are determined by specifying an ordered list of important centers for each important LMO. The ground state domains then are augmented with further centers from this list until a threshold is reached by the least-squares optimization procedure introduced in section IIC of Ref. 26. For unimportant orbitals the excited state orbital domain is equal to the ground state domain. The excited state pair domains are obtained by unifying the corresponding excited state orbital domains.

Contrary to the DF-LCC2 method, the local approximations are state-specific and re-

specified in every Davidson-refresh, thus they allow the eigenvectors to change their character during the Davidson process. If two states come energetically close, the local approximations of these states are unified. Thus, the LT-DF-LCC2 method is a multistate method in the same sense as canonical CC2.

1.3 Coupled Cluster diagrams

Starting from the common CC expressions based on the normal ordered second quantized operators and the particle-hole-formalism practical equations can be developed by employing diagrammatic techniques.[55] In the context of this thesis CC diagrams were used to obtain the starting equations for the Lagrangians, from which properties and the gradient with respect to nuclear displacements are obtained by differentiation as explained in detail in the chapters 2 and 3. The following outline is a revised version of section 2.4 in Ref. 56.
Operators are depicted as vertical interaction lines, which are connected by horizontal lines, that start or end at the vertex of an operator. Every vertex has an incoming and an outgoing horizontal line, symbolizing the action of the operator on an electron. The one-electron operators, i.e. the Fock and single excitation operators, have one vertex, the two-electron operators, i.e. the fluctuation and the double excitation operators, have two vertices. In literature, the diagrams are often rotated by 90° compared to the diagrams in this thesis, which were obtained from the program `ccgen`.[57]
Starting from the Baker-Campbell-Hausdorff-expansion (eq. (1.6)) of the normal ordered second quantized Hamiltonian it can be demonstrated, that in CC theory only those diagrams contribute, in which all operators are connected by horizontal lines. There are some rules for the evaluation of such diagrams:

1. Horizontal lines pointing from the left to the right are hole lines representing occupied orbitals denoted with the indices i, j, k and so on. Horizontal lines pointing to the left are particle lines representing virtual orbitals denoted with the indices r, s, t and so on. Lines, which start or end at a bare excitation operator τ_{μ_i}, are dashed.

2. Every vertical line contributes an integral or an amplitude to the final expression, except for the lines, which represent a bare excitation operator τ_{μ_i}. An element of the Fock matrix would be $\langle out|F|in\rangle$, where *out* stands for the outgoing line and

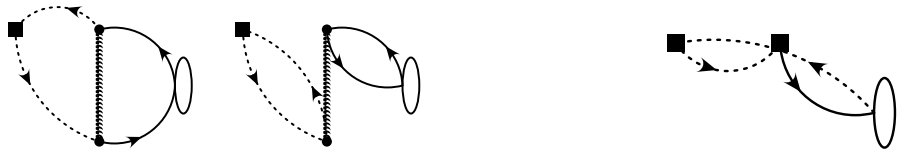

(a) Diagrams contributing to $\langle\Phi_r^i|[V,T_1]|0\rangle$.

(b) One of the diagrams contributing to $\langle\Phi_r^i|[F,T_1]|0\rangle$.

Figure 1.1: Examples of CC diagrams.

in for the incoming one. The two-electron integrals are constructed following the scheme $(out_1\ in_1 \mid out_2\ in_2)$, where the indices 1 and 2 denote the vertex.

3. The summation runs over all internal lines, i.e. the lines which are not connected to a bare excitation operator τ_{μ_i}.

4. The sign of a diagram is $(-1)^{h+l}$, where h is the number of hole lines and l the number of loops.

5. Every loop contributes a factor of 2. But if a loop directly links a singlet and a triplet vertex (without an operator in between), the factor is 0 and the diagram does not contribute. The vertices of the Hamiltonian are singlet vertices. The triplet double excitation operators have one triplet and one singlet vertex, cf. eq. (1.25).

6. The projected atomic orbitals (PAOs), which are used in this work for spanning the virtual space in the local basis, are not mutually orthogonal. Thus each particle line, which directly links the `ket` (on the right) with the `bra` (on the left) without an operator in between, contributes an element of the PAO overlap matrix $\mathbf{S}$.

The procedure is in the following demonstrated for the examplary term $\langle\Phi_a^i|[V,T_1]|0\rangle$. There are two diagrams corresponding to this term, which are shown in figure 1.1(a). According to the first rule the hole lines are denoted as i and k, and the particle lines as r and s. The operators V and T_1 contribute an integral and an amplitude to the expression (rule 2). The `bra` side does not contribute an amplitude, because only the bare excitation operator τ_r^i is involved. The summation runs over all internal lines, that means all lines except the ones coming from τ_r^i (rule 3). For the chosen example the two sums

$$\sum_{sk}(ki|rs)t_s^k \qquad \text{and} \qquad \sum_{sk}(ri|ks)t_s^k \tag{1.43}$$

are obtained. Applying the rules 4 to 6 yields the final expressions for the term $\langle\Phi_a^i|[V,T_1]|0\rangle$, depending on the spin symmetry of $\langle\Phi_r^i|$. If $\langle\Phi_r^i|$ is a singlet CSF, the result is

$$-2\sum_{sk}(ki|rs)t_s^k + 4\sum_{sk}(ri|ks)t_s^k \ . \tag{1.44}$$

If $\langle\Phi_r^i|$ is a triplet CSF, the second diagram does not contribute, because one of the singlet vertices of V is directly connected with the triplet vertex of the excitation operator τ_r^i, and the result is

$$-2\sum_{sk}(ki|rs)t_s^k \ . \tag{1.45}$$

The diagrams are constructed for integrals projecting on covariant CSFs. Thus for the projection on the contravariant *bra*-function $\langle\tilde{\Phi}_r^i|$, as done in the context of this thesis, the resulting terms in eqs. (1.44) and (1.45) have to be multiplied with 0.5 according to eqs. (1.10) and (1.29).
An example, where the PAO overlap matrix must be taken into account according to rule 6 is the diagram shown in figure 1.1(b). This diagram contributes to the term $\langle\Phi_a^i|[F,T_1]|0\rangle$ and yields for singlet and for triplet excitations the expression

$$-2\sum_{kr'}S_{rr'}t_{r'}^k f_{ki} \ , \tag{1.46}$$

which has to be multiplied with 0.5, if the contravariant *bra*-CSF $\langle\tilde{\Phi}_r^i|$ is used.

1.4 Structure of the thesis

After this short introduction of basic concepts and theories, the calculation of orbital-relaxed properties and gradients with respect to nuclear displacements will be discussed in the following chapters.
First, in chapter 2 explicit orbital relaxation is introduced and the formalism for orbital-relaxed first-order properties of the ground state and the excited states within the local CC2 methods is derived. The accuracy and efficiency of the implementation will also be discussed. Gradients with respect to nuclear displacements are in the focus of chapter 3. Again the derivation of the formalism is followed by an analysis of the accuracy and efficiency of the implementation. Finally, chapter 4 gives a short summary of the thesis.

Chapter 2

Orbital-relaxed first-order properties

The content of this chapter has already been published in the Journal of Chemical Physics, Ref. 29. Parts of the text are identical to the publication. The manuscript was revised concerning the context given in this thesis, i.e. basic principles, which were discussed in chapter 1 were shortened or omitted, while other aspects are discussed more detailed.
Daniel Kats mainly derived and partly implemented the working equations for the Z-CPL and Z-CPHF equations of the electronic ground state (sections 2.2.1-2.2.3). The completion of this work and the testing of the code for the ground state, as well as the derivation of the formalism for excited states and the implementation and testing of the corresponding code were realized by the author.

2.1 Introduction

The calculation of excited state properties is very useful for the interpretation or prediction of the photophysical behaviour of molecules. For example, a large change in the dipole moment compared to the electronic ground state indicates a charge transfer (CT) excitation, which may enable other reaction paths than a local excitation.
In the framework of the TD-CC response theory first-order properties of individual excited states are obtained as the derivatives of the corresponding time-independent excited state Lagrangians with respect to the strength of a time-independent perturbation. These Lagrangians are necessary because CC is non-variational and involve the total energy of the related excited state, i.e. the ground-state energy plus the corre-

sponding excitation energy, which is within the TD-CC theory obtained as eigenvalue of the Jacobian.[9] For an explicit inclusion of orbital-relaxation effects these Lagrangians are augmented by additional conditions related to the orbitals.
LT-DF-LCC2 excitation energies, transition moments and orbital-unrelaxed properties were implemented into the MOLPRO program package[58] earlier and enable calculations for extended molecular systems consisting of hundred or more atoms.[26–28] The method is now extended in so far that the orbitals are allowed to relax with respect to the perturbation, i.e., orbital-relaxed first-order properties for the LT-DF-LCC2 method are presented. This is a major step on the way towards analytic gradients with respect to nuclear displacements, which will be discussed in chapter 3.

This chapter is organized as follows: First the formalism for the calculation of orbital-relaxed ground state properties is discussed in section 2.2. The approach is then applied to singlet and triplet excited states in sections 2.3 and 2.4. The orbital-relaxed densities for the ground state and excited states are discussed in detail in section 2.5. Section 2.6 comprises the results of the test calculations concerning the accuracy of the method and the results of an exemplary application. Section 2.7 summarizes the chapter.

2.2 The electronic ground state

2.2.1 The Lagrangian

The Einstein convention introduced in section 1.2.3 will be employed throughout the rest of the thesis, i.e. repeated indices are implicitly summed up. Summations are only written explicitly, if it is necessary for clarity. The formalism is derived for an orthonormal basis of molecular orbitals (MOs) and the transformation to the basis of nonorthogonal PAOs is performed *a posteriori*, as done in earlier work on the LMP2 gradient.[59] The MOs are expanded in an AO-basis with the metric $\mathbf{S}^{\mathrm{AO}}$, cf. eq. (1.13),

$$\phi_p = \chi_\mu C_{\mu p}. \tag{2.1}$$

The composite coefficient matrix $\mathbf{C} = (\mathbf{L}|\mathbf{C}^{\mathrm{v}})$ concatenates the LMO coefficient matrix $\mathbf{L}$ and the coefficient matrix of the canonical virtuals $\mathbf{C}^{\mathrm{v}}$. As introduced in chapter 1, LMOs are labeled with the indices $i, j, \ldots$, and canonical virtuals with $a, b, \ldots$ General molecular orbitals are indexed by $m, n, \ldots$, and PAOs by $r, s, \ldots$ In order to reduce the computational cost the density fitting approximation[15–17] is employed to decompose the

four-index integrals into three-index objects as discussed in section 1.1.2.

Properties are obtained as derivatives of the time-independent Lagrangian for the energy of the related state with respect to the strength of a time-independent perturbation. The time-independent perturbation $\mathbf{V_0}$, which is contained in the Hamiltonian,

$$\mathbf{H} = \mathbf{F} + \mathbf{V} + \mathbf{V_0} \ , \tag{2.2}$$

is e.g. an applied electric field. In this case the corresponding property is the dipole moment. $\mathbf{V_0}$ consists of a Hermitian perturbation operator $\mathbf{X}$ describing the observable, and the corresponding perturbation strength ϵ_X,

$$\mathbf{V_0} = \sum_X \epsilon_X \mathbf{X} = \sum_{pq} \left[\mathbf{v_0}\right]_{pq} \tau_q^p \ , \tag{2.3}$$

with the matrix elements

$$\left[\mathbf{v_0}\right]_{pq} = \sum_X X_{pq} \epsilon_X \ . \tag{2.4}$$

The general time-independent local CC2 Lagrangian for the electronic ground state without orbital relaxation, which was also used in previous work,[25,27,28] reads

$$\mathcal{L}_0^{\mathrm{CC2}\prime} \ = \ E_0^{\mathrm{CC2}} + \tilde{\lambda}_{\mu_i}^0 \Omega_{\mu_i}. \tag{2.5}$$

It includes the ground state correlation energy E_0^{CC2} and the amplitude equations $\mathbf{\Omega}$ as defined in eqs. (1.7) and (1.9). The Lagrangian is required to be stationary with respect to all parameters, i.e. the amplitudes $\mathbf{t}$ and multipliers $\tilde{\lambda}^{\mathbf{0}}$. As dicussed earlier,[25,29] differentiation of $\mathcal{L}_0'$ with respect to the amplitudes yields the equations, which determine the multipliers,

$$-\eta_{\nu_j} = \tilde{\lambda}_{\mu_i}^0 A_{\mu_i \nu_j} \ , \tag{2.6}$$

with

$$\eta_{\nu_j} = \frac{\partial E_0^{\mathrm{CC2}}}{\partial t_{\nu_j}} \ , \tag{2.7}$$

and the Jacobian $\mathbf{A}$, which was defined in eq. (1.21) as

$$A_{\mu_i\nu_j} = \frac{\partial \Omega_{\mu_i}}{\partial t_{\nu_j}} \ . \tag{2.8}$$

Eq. (1.7) for the CC2 ground state energy and eq. (1.9) for the CC2 amplitudes of the unperturbed system are extended by the perturbation $\mathbf{V_0}$, which is contained in the Hamiltonian $\mathbf{H}$ according to eq. (2.2), and explicitly arises in the second term of Ω_{μ_2},

$$\Omega_{\mu_2} \ = \ \left\langle \tilde{\mu}_2 \left| \hat{\mathbf{H}} + \left[\mathbf{F} + \hat{\mathbf{V}}_\mathbf{0}, \mathbf{T_2} \right] \right| 0 \right\rangle = 0 \ . \tag{2.9}$$

Differentiating the Lagrangian $\mathcal{L}_0^{\mathrm{CC2}'}$ with respect to the perturbation strength ϵ_X yields the orbital-unrelaxed dipole moment of the electronic ground state, which was presented in the context of the local CC2 methods earlier.[25,27,28]

The local CC2 Lagrangian for the electronic ground state including orbital relaxation reads

$$\mathcal{L}_0^{\mathrm{CC2}} \ = \ \mathcal{L}_0^{\mathrm{CC2}'} + z_{ij}^{loc,0} r_{ij} + z_{ai}^0 [\mathbf{f} + \mathbf{v_0}]_{ai} + x_{pq}^0 \left[\mathbf{C}^\dagger \mathbf{S}^{\mathrm{AO}} \mathbf{C} - \mathbf{1} \right]_{pq} \ . \tag{2.10}$$

$[\mathbf{f} + \mathbf{v_0}]_{ai}$ are the occupied-virtual matrix elements of the perturbed Fock operator $[\mathbf{F} + \mathbf{V_0}]$. Compared to the orbital-unrelaxed Lagrangian $\mathcal{L}_0^{\mathrm{CC2}'}$, $\mathcal{L}_0^{\mathrm{CC2}}$ contains further conditions, namely the localization, Brillouin, and orthonormality conditions. The related Lagrange multipliers are $z_{ij}^{loc,0}$, z_{ai}^0, and x_{pq}^0, respectively. The multipliers x_{pq}^0 related to the orthogonality condition are redundant, since $\mathbf{x^0} = \mathbf{x^{0\dagger}}$. This will be resolved later. By choosing Pipek-Mezey localization[32] the localization conditions r_{ij} become

$$r_{ij} = \sum_A [S_{ii}^A - S_{jj}^A] S_{ij}^A = 0 \quad \text{for all} \quad i > j, \tag{2.11}$$

with the matrix $\mathbf{S^A}$ being defined as

$$S_{kl}^A = \sum_{\mu \in A} \sum_\nu [L_{\mu k} S_{\mu\nu}^{\mathrm{AO}} L_{\nu l} + L_{\mu l} S_{\mu\nu}^{\mathrm{AO}} L_{\nu k}] \ . \tag{2.12}$$

The summation over μ is restricted to basis functions centered on atom A.
Explicitly including the Brillouin condition in the Lagrangian $\mathcal{L}_0^{\mathrm{CC2}}$ leads to a different treatment of the perturbation inside the term $\mathcal{L}_0^{\mathrm{CC2}'}$ compared to the orbital-unrelaxed

case. This will be discussed in detail in section 2.5, because it affects the density, which is needed for the calculation of the properties. Yet, it does not affect the determination of the additional Lagrange multipliers in $\mathcal{L}_0^{\mathrm{CC2}}$, which will be discussed in the following section.

2.2.2 Linear z-vector equations

Differentiation of the orbital-relaxed Lagrangian $\mathcal{L}_0^{\mathrm{CC2}}$ with respect to orbital variations yields the linear *z-vector equations*, from which the multipliers $\mathbf{z^0}$, $\mathbf{z^{loc,0}}$, and $\mathbf{x^0}$ are obtained. The derivation proceeds in an analogous way as for the LMP2 gradient:[59,60] the variations of the orbitals in the presence of the perturbation $\mathbf{V_0}$ are described by the coefficient matrix

$$C_{\mu p}(\mathbf{V_0}) \;=\; C_{\mu q}(\mathbf{0}) O_{qp}(\mathbf{V_0}), \tag{2.13}$$

where $\mathbf{C}(\mathbf{0})$ are the coefficients of the optimized orbitals without perturbation and the matrix $\mathbf{O}(\mathbf{V_0})$ describes the rotation of the orbitals caused by the perturbation $\mathbf{V_0}$, with $\mathbf{O}(\mathbf{0}) = \mathbf{1}$.
The derivative of the Lagrangian with respect to the variation of the orbitals can be partitioned into four contributions,

$$\left(\frac{\partial \mathcal{L}_0^{\mathrm{CC2}}}{\partial O_{pq}}\right)_{\mathbf{V}_0=0} = [\mathbf{B^0} + \tilde{\mathbf{B}}(\mathbf{z^0}) + \mathbf{b}(\mathbf{z^{loc,0}}) + 2\mathbf{x^0}]_{pq} = 0 \;, \tag{2.14}$$

with

$$\begin{aligned}
[\mathbf{B^0}]_{pq} &= \left(\frac{\partial}{\partial O_{pq}} \mathcal{L}_0^{\mathrm{CC2}\prime}\right)_{\mathbf{V}_0=0} , \\
[\tilde{\mathbf{B}}(\mathbf{z^0})]_{pq} &= \left(\frac{\partial}{\partial O_{pq}} z^0_{ai} f_{ai}\right)_{\mathbf{V}_0=0} , \\
[\mathbf{b}(\mathbf{z^{loc,0}})]_{pi} &= \left(\frac{\partial}{\partial O_{pi}} z^{loc,0}_{kl} r_{kl}\right)_{\mathbf{V}_0=0} .
\end{aligned} \tag{2.15}$$

The derivation of $\mathbf{B^0}$ will be discussed in detail in the next section. The quantities $\tilde{\mathbf{B}}(\mathbf{z^0})$ and $\mathbf{b}(\mathbf{z^{loc,0}})$ are identical to the quantities $\tilde{\mathbf{A}}$, and $\mathbf{a}(\mathbf{z^{loc}})$ given explicitly in eqs. (29)

and (39), of Ref. 59, i.e.

$$\begin{aligned}\tilde{\mathbf{B}}(\mathbf{z^0}) &= \mathbf{f}\bar{\mathbf{z}}^{\mathbf{0}} + \mathbf{g}(\bar{\mathbf{z}}^{\mathbf{0}})\mathbf{d}^{\mathrm{HF}} \ , \\ \left[\mathbf{b}(\mathbf{z^{loc,0}})\right]_{pi} &= \sum_{k>l}\left(\frac{\partial r_{kl}}{\partial O_{pi}}\right)_{\mathbf{V}_0=0} z_{kl}^{loc,0} \ , \end{aligned} \tag{2.16}$$

with

$$\begin{aligned}\bar{\mathbf{z}}^{\mathbf{0}} &= \mathbf{z^0} + \mathbf{z^{0\dagger}} \ , \\ d_{ij}^{\mathrm{HF}} &= 2\delta_{ij} \ , \\ g(\bar{z}^0)_{pq} &= ((pq|mn) - 0.5(pn|mq))\bar{z}^0_{mn} \ , \\ \left(\frac{\partial r_{kl}}{\partial O_{pi}}\right)_{\mathbf{V}_0=0} &= \sum_A \big[2(S^A_{pk}\delta_{ik} - S^A_{pl}\delta_{il})S^A_{kl} \\ &\quad + (S^A_{kk} - S^A_{ll})(S^A_{pl}\delta_{ik} + S^A_{pk}\delta_{il})\big] \ . \end{aligned} \tag{2.17}$$

The stationarity of $\mathcal{L}_0^{\mathrm{CC2}}$ with respect to the orbital variations O_{pq}, eq. (2.14), and the relation $\mathbf{x^0} = \mathbf{x^{0\dagger}}$ are employed to obtain the linear *z-vector equations*,

$$(1 - \mathcal{P}_{pq})[\mathbf{B^0} + \tilde{\mathbf{B}}(\mathbf{z^0}) + \mathbf{b}(\mathbf{z^{loc,0}})]_{pq} = 0 \ , \tag{2.18}$$

from which $\mathbf{z^0}$ and $\mathbf{z^{loc,0}}$ are obtained. As shown in Ref. 59, the *z-vector equations* can be decoupled further into the Z-CPL (coupled perturbed localization), and the Z-CPHF (coupled perturbed Hartree Fock) equations. The Z-CPL equations, which are obtained by considering the occupied-occupied part of eq. (2.18),

$$B^0_{ij} - B^0_{ji} + \sum_{k>l}\left(\left(\frac{\partial r_{kl}}{\partial O_{ij}}\right)_{\mathbf{V}_0=0} - \left(\frac{\partial r_{kl}}{\partial O_{ji}}\right)_{\mathbf{V}_0=0}\right) z_{kl}^{loc,0} = 0 \ , \tag{2.19}$$

have to be solved first, since the solutions, i.e. the multipliers $\mathbf{z^{loc,0}}$, appear in the Z-CPHF equations,

$$B^0_{ai} - B^0_{ia} + [\mathbf{b}(\mathbf{z^{loc,0}}) + \mathbf{f}\mathbf{z^0} - \mathbf{z^0}\mathbf{f} + 2\mathbf{g}(\bar{\mathbf{z}}^{\mathbf{0}})]_{ai} = 0 \ . \tag{2.20}$$

The Z-CPHF equations are obtained from the external-occupied part of eq. (2.18), and determine the multipliers $\mathbf{z^0}$. Knowing the multipliers $\mathbf{z^{loc,0}}$ and $\mathbf{z^0}$ the multipliers $\mathbf{x^0}$

for the orthogonality condition can be calculated as

$$x^0_{pq} = -\frac{1}{4}(1+\mathcal{P}_{pq})[\mathbf{B^0} + \tilde{\mathbf{B}}(\mathbf{z^0}) + \mathbf{b}(\mathbf{z^{loc,0}})]_{pq} \ . \tag{2.21}$$

The $\mathbf{x^0}$ are not needed for the calculation of properties, but for the gradient with respect to nuclear displacements in chapter 3.

2.2.3 Calculation of the intermediate $\mathbf{B^0}$

The quantity $\mathbf{B^0}$ is obtained by differentiation according to eq. (2.15). It comprises three parts,

$$B^0_{pq} \ = \ C_{\mu p} B^0_{\mu i} + C_{\mu p} B^0_{\mu r} Q_{ra} + C_{\mu p} S^{\mathrm{AO}}_{\mu\rho} \delta_{\rho r} B^0_{r\nu} C^v_{\nu a} \ , \tag{2.22}$$

with the intermediates $B^0_{\mu i}$ and $B^0_{\mu r}$ simply being the partial derivatives of $\mathcal{L}_0^{\mathrm{CC2}\prime}$ with respect to O_{pq} for $q = i$ and $q = r$, respectively. The third term involving $B^0_{r\nu}$ originates from the dependence of the multipliers and amplitudes in the local basis on the coefficients $\mathbf{C}$ via the transformation matrix $\mathbf{Q}$.

The direct partial derivatives

Practical equations for the Lagrangian, which are the starting point for the derivatives, were obtained via diagrammatic techniques following the rules in section 1.3. The diagrams for the correlation energy E_0^{CC2} and the amplitude condition $\tilde{\lambda}^0_{\mu_i}\Omega_{\mu_i}$ are shown in appendix A, figure A.1 and A.2, respectively. For the ground state correlation energy one obtains

$$E_0^{\mathrm{CC2}} = 2 f_{ir} t^i_r + (ir|js)[\tilde{t}^{ij}_{rs} + 2 t^i_r t^j_s - t^j_r t^i_s] \ , \tag{2.23}$$

and for the amplitude equations

$$\begin{aligned} \tilde{\lambda}^0_{\mu_i}\Omega_{\mu_i} \ = \ & \tilde{\lambda}^{i,0}_r \hat{f}_{ri} - \tilde{\lambda}^{i,0}_r S_{rr'} \tilde{t}^{kj}_{sr'} (ks\hat{|}ji) + \tilde{\lambda}^{i,0}_r \tilde{t}^{ki}_{st} (ks\hat{|}rt) + \tilde{\lambda}^{i,0}_r S_{rr'} \tilde{t}^{ik}_{r's} \hat{f}_{ks} \\ & + \tilde{\lambda}^{ij,0}_{rs} (ri\hat{|}sj) - 2\tilde{\lambda}^{ij,0}_{rs} S_{rr'} S_{bb'} f_{kj} t^{ik}_{r's'} + 2\tilde{\lambda}^{ij,0}_{rs} S_{rr'} f_{st} t^{ij}_{r't} \ . \end{aligned} \tag{2.24}$$

How to obtain the direct partial derivatives, which contribute to $B^0_{\mu i}$ and $B^0_{\mu r}$, is in the following demonstrated for the exemplary term $\tilde{\lambda}^{i,0}_r \hat{f}_{ri}$, which originates from the general expression $\tilde{\lambda}^0_{\mu_1}\langle\tilde{\mu}_1|\hat{F}|0\rangle$ in the amplitude condition. First the dressing of the

orbital coefficients is written explicitly, i.e. using eq. (1.18) for $\mathbf{\Lambda^h}$ and $\mathbf{\Lambda^p}$. For a better distinction between dressed and undressed coefficients inside the integrals the dressed ones are in eqs. (2.25) - (2.27) explicitly labeled by a tilde. For the exemplary term this yields

$$\tilde{\lambda}^{i,0}_r \hat{f}_{\tilde{r}\tilde{i}} = \tilde{\lambda}^{i,0}_r \hat{f}_{ri} + \tilde{\lambda}^{i,0}_r \hat{f}_{rs} t^i_s - \tilde{\lambda}^{i,0}_r \hat{f}_{ji} S_{rr'} t^j_{r'} - \tilde{\lambda}^{i,0}_r \hat{f}_{js} S_{rr'} t^j_{r'} t^i_s \ , \tag{2.25}$$

with the elements of the dressed Fock matrix on the right-hand side being dressed only internally, i.e., according to the discussion in section 1.1.4,

$$\hat{f}_{pq} = C_{\mu p} C_{\nu q} \left(h_{\mu\nu} + 2 \left[(\mu\nu|\hat{k\tilde{k}}) - 0.5(\mu\tilde{\hat{k}}|k\nu) \right] \right) = h_{pq} + 2(pq|\hat{|}k\tilde{\hat{k}}) \ . \tag{2.26}$$

$B^0_{\mu i}$ and $B^0_{\mu r}$ of eq. (2.22) are obtained as the direct partial derivatives with respect to the orbital variations O_{pq} for $q = i$ and $q = r$, respectively. For a Fock matrix element f_{pq} also the coefficients occuring inside for the 4-index integrals have to be taken into account, thus the contributions from the exemplary term to the working equations for $B^0_{\mu i}$ and $B^0_{\mu r}$ are

$$\begin{aligned}
\left(\frac{\partial(\tilde{\lambda}^{i,0}_r \hat{f}_{\tilde{r}\tilde{i}})}{\partial O_{pq}} \right)_{q=i} &= \tilde{\lambda}^{i,0}_r \hat{f}_{r\mu} - \tilde{\lambda}^{j,0}_r \hat{f}_{\mu j} S_{rr'} t^{i}_{r'} - \tilde{\lambda}^{i,0}_r \hat{f}_{j\mu} S_{rr'} t^{j}_{r'} - \tilde{\lambda}^{j,0}_r \hat{f}_{\mu s} S_{rr'} t^{i}_{r'} t^{j}_{s} \\
&\quad + 2\tilde{\lambda}^{k,0}_s (\tilde{s}\tilde{\hat{k}}|\hat{|}\mu i) + 2\tilde{\lambda}^{k,0}_s (\tilde{s}\tilde{\hat{k}}|\hat{|}i\mu) + 2\tilde{\lambda}^{k,0}_s t^i_r (\tilde{s}\tilde{\hat{k}}|\hat{|}\mu r) \ , \\
\left(\frac{\partial(\tilde{\lambda}^{i,0}_r \hat{f}_{\tilde{r}\tilde{i}})}{\partial O_{pq}} \right)_{q=r} &= \tilde{\lambda}^{i,0}_r \hat{f}_{\mu i} + \tilde{\lambda}^{i,0}_r \hat{f}_{\mu s} t^i_s + \tilde{\lambda}^{i,0}_s \hat{f}_{s\mu} t^i_r - \tilde{\lambda}^{j,0}_s \hat{f}_{i\mu} S_{ss'} t^i_{s'} t^j_r \\
&\quad + 2\tilde{\lambda}^{i,0}_s t^k_r (\tilde{s}\tilde{\hat{i}}|\hat{|}k\mu) \ .
\end{aligned} \tag{2.27}$$

The entire working equations obtained via this procedure for $B^0_{\mu i}$ and $B^0_{\mu r}$ are

$$\begin{aligned}
B^0_{\mu i} &= 2f_{\mu r} t^i_r + \hat{f}_{\mu r} d'_{ir} + \hat{f}_{r\mu} d'_{ri} + \hat{f}_{k\mu} d'_{ki} + \hat{f}_{\mu k} d'_{ik} + 2g(\bar{d})_{\mu i} + 2g(d')_{\mu r} t^i_r + \bar{\mathcal{D}}^{\xi}_{ik}(\lambda^0) f_{k\mu} \\
&\quad + (\mu r|Q) \left[\bar{V}^Q_{ir} + 4t^i_r b^Q - 2t^j_r \bar{c}^Q_{ji} \right] - (\mu\hat{k}|Q) V^Q_{ir} S_{rr'} \tilde{\lambda}^{k,0}_{r'} \\
&\quad + 2N_{\mu i} + d'_{ik} N_{\mu k} + \hat{\bar{N}}_{\mu i} + \tilde{\lambda}^{i,0}_{r'} S_{r'r} M_{\mu r} + \hat{\bar{M}}_{\mu r} S_{rr'} t^i_{r'} \ ,
\end{aligned} \tag{2.28}$$

$$\begin{aligned}
B^0_{\mu r} &= 2f_{k\mu} t^k_r + \hat{f}_{k\mu} d'_{kr} + \hat{f}_{\mu k} d'_{rk} + \hat{f}_{\mu s} d'_{rs} + \hat{f}_{s\mu} d'_{sr} + 2g(d'^{\dagger})_{\mu k} t^k_r + \bar{\mathcal{D}}^{\xi}_{rs}(\lambda^0) f_{s\mu} \ , \\
&\quad + (k\mu|Q) \left[\bar{V}^Q_{kr} + 4t^k_r b^Q - 2t^j_r \bar{c}^Q_{jk} \right] + (s\mu\hat{|}Q) V^Q_{kr} \tilde{\lambda}^{k,0}_s \\
&\quad + N_{\mu k} \tilde{\lambda}^{k,0}_r + \hat{\bar{N}}_{\mu k} t^k_r - 2M_{\mu r} - \hat{\bar{M}}_{ra} + d'_{sr} S_{ss'} M_{\mu s'} \ .
\end{aligned} \tag{2.29}$$

Here and in all following working equations the density fitting approximation is employed and the doubles amplitudes and multipliers are restricted to pair-lists and domains. The intermediates needed for calculating $B^0_{\mu i}$, $B^0_{\mu r}$ and $B^0_{r\mu}$ (*vide infra*) are

$$\begin{aligned}
b^Q &= c^Q_{ir} t^i_r \ , & \bar{c}^Q_{ij} &= c^Q_{ir} t^j_r \ , \\
V^Q_{ir} &= \tilde{t}^{ij}_{rs} c^{js}_Q \ , & \hat{\bar{V}}^Q_{ir} &= \tilde{\lambda}^{ij,0}_{rs} \hat{c}^{sj}_Q \ , \\
\bar{V}^Q_{ir} &= \tilde{t}^{ij}_{rs} (\tilde{\lambda}^{j,0}_t \hat{c}^P_{ts} - S_{ss'} \tilde{\lambda}^{k,0}_{s'} \hat{c}^P_{jk}) \ , & X(\lambda^0 T)_{ir} &= \tilde{\lambda}^{j,0}_s S_{ss'} \tilde{t}^{ji}_{s'r} \ , \\
d'_{ij} &= -\tilde{\lambda}^{j,0}_r S_{rr'} t^i_{r'} \ , & d'_{rs} &= \tilde{\lambda}^{k,0}_r t^k_s \ , \\
d'_{ir} &= t^k_r d'_{ik} + X(\lambda^0 T)_{ir} \ , & d'_{ri} &= \tilde{\lambda}^{i,0}_r \ , \\
d^{(s)} &= 2 t^i_a L_{\mu i} C^v_{\nu a} \ , & d &= d^{(s)} + \mathcal{D}^{\xi}(\lambda^0) + d' \ , \\
g(d)_{pq} &= ((pq|rs) - 0.5(ps|rq)) d_{rs} \ . & & \qquad (2.30)
\end{aligned}$$

A bar indicates symmetrized densities, e.g. $\bar{d} = d + d^\dagger$. All $\hat{f}$ are dressed only internally, the density $\mathcal{D}^{\xi}(\lambda^0)$ will be discussed in detail in section 2.5, eq. (2.81). The intermediates including half transformed integrals are defined as

$$\begin{aligned}
(i\mu|Q) &= (\nu\mu|Q)\Lambda^p_{\nu i} \ , & (\mu i\hat{|}Q) &= (\mu\nu|Q)\Lambda^h_{\nu i} \ , \\
(\mu r|Q) &= (\mu\nu|Q)\Lambda^h_{\nu r} \ , & (r\mu\hat{|}Q) &= (\nu\mu|Q)\Lambda^p_{\nu r} \ , \\
M_{\mu r} &= -V^Q_{kr}(k\mu|Q) \ , & N_{\mu i} &= V^Q_{kr}(\mu r|Q) \ , \\
\hat{\bar{M}}_{\mu r} &= -2\hat{\bar{V}}^Q_{kr}(\mu k\hat{|}Q) \ , & \hat{\bar{N}}_{\mu i} &= 2\hat{\bar{V}}^Q_{kr}(r\mu\hat{|}Q) \ . \qquad (2.31)
\end{aligned}$$

The derivatives originating from Q_{ar}

The third term in eq. (2.22) involving $B^0_{r\nu}$ originates from the dependence of the multipliers and amplitudes in local basis on the coefficients $\mathbf{C}$ via the transformation matrix $\mathbf{Q} = \mathbf{C}^{\mathbf{v}\dagger}\mathbf{S}^{\mathrm{AO}}$, i.e.

$$\begin{aligned}
C_{\mu p} S^{\mathrm{AO}}_{\mu\rho} \delta_{\rho r} B^0_{r\nu} C^v_{\nu a} = &\sum_{\mu_i} \left[\left(\frac{\partial \mathcal{L}^{\mathrm{CC2}'}_0}{\partial \tilde{\lambda}^0_{\mu_i}} \right) \left(\frac{\partial \tilde{\lambda}^0_{\mu_i}}{\partial O_{pq}} \right) \right]_{\mathbf{V}_0 = 0} \\
&+ \sum_{\mu_i} \left[\left(\frac{\partial \mathcal{L}^{\mathrm{CC2}'}_0}{\partial t_{\mu_i}} \right) \left(\frac{\partial t_{\mu_i}}{\partial O_{pq}} \right) \right]_{\mathbf{V}_0 = 0} \ , \qquad (2.32)
\end{aligned}$$

with $\tilde{\lambda}^0_{\mu_i}$ and t_{μ_i} representing the ground state multipliers and amplitudes related to singles ($i = 1$) and doubles ($i = 2$) substitutions, respectively, in local occupied and canonical virtual orbital basis, e.g. $t_{\mu_2} \equiv t^{ij}_{ab}$. The derivatives have to be calculated for

the doubles parts of $\tilde{\lambda}^0_{\mu_i}$ and t_{μ_i} only, which are restricted to pair lists and domains in local basis. Hence, the amplitude and multiplier residual vectors only vanish in local basis within the pair domains, but not outside. Consequently, they are non-zero in the canonical basis. The singles parts, on the other hand, are unrestricted, and the derivatives of $\mathcal{L}_0^{\mathrm{CC2}'}$ with respect to singles amplitudes t_a^i or multipliers $\tilde{\lambda}_a^{i,0}$ are zero in local and in canonical basis.
The derivative of a doubles quantity, e.g. of the amplitude t_{ab}^{ij}, with respect to the orbital variations is

$$\left(\frac{\partial t_{ab}^{ij}}{\partial O_{pq}}\right)_{\mathbf{V}_0=0} = \left(\frac{\partial (Q_{ar} t_{rt}^{ij} Q_{bt})}{\partial O_{pq}}\right)_{\mathbf{V}_0=0} = 2\delta_{qa} C_{\mu p} S^{AO}_{\mu\nu} \delta_{\nu r} t_{rt}^{ij} Q_{bt} \ . \tag{2.33}$$

Thus eq. (2.32) can be written as

$$\begin{aligned}\sum_{\mu_2} \left[\left(\frac{\partial \mathcal{L}_0^{\mathrm{CC2}'}}{\partial t_{\mu_2}}\right)\left(\frac{\partial t_{\mu_2}}{\partial O_{pq}}\right) + \left(\frac{\partial \mathcal{L}_0^{\mathrm{CC2}'}}{\partial \tilde{\lambda}^0_{\mu_2}}\right)\left(\frac{\partial \tilde{\lambda}^0_{\mu_2}}{\partial O_{pq}}\right)\right]_{\mathbf{V}=0} \\ = 2C_{\mu p} S^{AO}_{\mu\rho} \delta_{\rho r} \left[t_{rt}^{ji} Q_{bt} \left(\frac{\partial \mathcal{L}_0^{\mathrm{CC2}'}}{\partial t_{ab}^{ij}}\right) + \tilde{\lambda}_{rt}^{ji,0} Q_{bt} \left(\frac{\partial \mathcal{L}_0^{\mathrm{CC2}'}}{\partial \tilde{\lambda}_{ab}^{ij,0}}\right)\right] = C_{\mu p} S^{\mathrm{AO}}_{\mu\rho} \delta_{\rho r} B^0_{r\nu} C^v_{\nu a} \ .\end{aligned} \tag{2.34}$$

The derivative of $\mathcal{L}_0^{\mathrm{CC2}'}$ with respect to the amplitudes $\mathbf{t}$ yields the equations for the multipliers and the derivative with respect to the Lagrange multipliers $\tilde{\boldsymbol{\lambda}}^{\mathbf{0}}$ the amplitude residual equations,

$$\begin{aligned}\left(\frac{\partial \mathcal{L}_0^{\mathrm{CC2}'}}{\partial t_{ab}^{ij}}\right) &= [\eta + \tilde{\boldsymbol{\lambda}}^{\mathbf{0}}\mathbf{A}]^{ij}_{ab} \\ &= (1 + \mathcal{P}_{ab}\mathcal{P}_{ij}) \Big\{ f_{ca} \tilde{\lambda}_{cb}^{ij,0} - \tilde{\lambda}_{ab}^{ik,0} f_{jk} \\ &\qquad + (1 - \frac{1}{2}\mathcal{P}_{ij}) \big[(ia|jb) + \hat{G}_{ab}^{ij}(\tilde{\lambda}^0) + \tilde{\lambda}_a^{i,0} \hat{f}_{jb}\big] \Big\} \ , \\ \left(\frac{\partial \mathcal{L}_0^{\mathrm{CC2}'}}{\partial \tilde{\lambda}_{ab}^{ij,0}}\right) &= \Omega_{ab}^{ij} \\ &= (1 + \mathcal{P}_{ab}\mathcal{P}_{ij}) \left\{ \frac{1}{2}(ai\hat{|}bj) + t_{ac}^{ij} f_{bc} - f_{ki} t_{ab}^{kj} \right\} \ ,\end{aligned} \tag{2.35}$$

with η as defined in eq. (2.7) and

$$\hat{G}^{ij}_{ab}(\tilde{\lambda}^0) = \tilde{\lambda}^{i,0}_c(ca\hat{|}jb) - \tilde{\lambda}^{k,0}_a(ik\hat{|}jb) \ . \tag{2.36}$$

Employing these expressions the working equation for $B^0_{r\mu}$ is finally obtained starting from eq. (2.34) as

$$\begin{aligned} B^0_{r\mu} &= -\hat{\bar{M}}_{\nu r}\hat{C}_{\nu\mu} - 2M_{\mu r} + \bar{M}_{\mu r} + \breve{M}_{\mu r} + \bar{\mathcal{D}}^{\xi}_{rt}(\lambda^0)f_{t\mu} + X(\lambda^0 T)_{jr}\hat{f}_{j\mu} \\ &\quad + \left(X(\hat{f}_{it})_{jr}\tilde{\lambda}^{j,0}_u + M_{\rho r}\Lambda^h_{\rho k}\tilde{\lambda}^{k,0}_u + \bar{d}^D_{ru}(f_{st}) - \bar{d}^f_{ru}\right)\delta_{u\nu}S^{\mathrm{AO}}_{\nu\mu} \ , \end{aligned} \tag{2.37}$$

with the intermediates given in eqs. (2.30) and (2.31) and

$$\begin{aligned} \hat{C}_{\mu\nu} &= \delta_{\mu\nu} - L_{\mu k}t^k_r\delta_{r\rho}S^{\mathrm{AO}}_{\rho\nu} \ , & X(\hat{f}_{jt})_{ir} &= \hat{f}_{jt}\tilde{t}^{ji}_{tr} \ , \\ d^f_{ru} &= 2\tilde{\lambda}^{ji,0}_{rt'}S_{t't}\left(f_{ki}t^{kj}_{tu} + f_{kj}t^{ik}_{tu}\right) \ , & d^D_{ru}(f_{st}) &= 2\tilde{\lambda}^{ji,0}_{rs}f_{st}t^{ij}_{tu} \ , \\ \bar{M}_{\mu r} &= \bar{V}^Q_{kr}(Q|k\mu) \ , & \breve{M}_{\mu r} &= V^Q_{kr}\tilde{\lambda}^{k,0}_s(Q\hat{|}s\mu). \end{aligned} \tag{2.38}$$

2.2.4 Calculation of properties

Differentiation of the Lagrangian $\mathcal{L}^{\mathrm{CC2}}_0$ given in eq. (2.10) with respect to the strength ϵ_X of the perturbation $\mathbf{V_0}$ finally yields the orbital-relaxed property $\langle X\rangle^{rel}_0$, e.g. the orbital-relaxed dipole moment in the case of an electric field. $\langle X\rangle^{rel}_0$ can generally be written as the trace of the density matrix, backtransformed to AO basis, with the integrals $X^{\mathrm{AO}}_{\mu\nu} = \langle\chi_\mu|\mathbf{X}|\chi_\nu\rangle$ representing the operator $\mathbf{X}$ in the AO basis, i.e. as

$$\langle X\rangle^{rel}_0 = \left(\frac{\partial\mathcal{L}^{\mathrm{CC2}}_0}{\partial\epsilon_X}\right) = \mathrm{tr}[\mathbf{X}^{\mathrm{AO}}(\mathcal{D}^0_{\mathrm{AO}} + z^0_{\mathrm{AO}})] \ . \tag{2.39}$$

z^0_{AO} are the multipliers for the Brillouin condition transformed to AO basis. The explicit form of the density $\mathcal{D}^0_{\mathrm{AO}}$ will be derived in section 2.5. As can be seen, the multipliers $\mathbf{x^0}$ are not needed for the calculation of the dipole moments. The multipliers $\mathbf{z^{loc,0}}$ do not occur explicitly in eq. (2.39), but in the Z-CPHF equations, which determine the multipliers $\mathbf{z^0}$.

2.3 Singlet excited states

Details about the LT-DF-LCC2 method for properties of singlet excited states without orbital relaxation were presented earlier.[27] To obtain excitation energies and properties of an excited state f the left and right eigenvalue equations for the Jacobian $\mathbf{A}$ have to be solved. The contravariant left eigenvector $\tilde{L}^f$ and the covariant right eigenvector R^f are both needed for the calculation of properties, cf. section 1.2.1. The resulting eigenvalues ω are the excitation energies of the system.

2.3.1 The Lagrangian

The local CC2 Lagrangian for an excited state f including orbital relaxation can be written as

$$\begin{aligned}\mathcal{L}_{f'} &= E_0^{\mathrm{CC2}} + \tilde{L}^f \mathbf{A} R^f + \tilde{\lambda}_{\mu_i}^{f'} \Omega_{\mu_i} - \omega_f [\tilde{L}^f \mathbf{M} R^f - \mathbf{1}] \\ &\quad + z_{ij}^{loc,f'} r_{ij} + z_{ai}^{f'} [\mathbf{f} + \mathbf{v_0}]_{ai} + x_{pq}^{f'} \left[\mathbf{C}^\dagger \mathbf{S}^{\mathrm{AO}} \mathbf{C} - \mathbf{1}\right]_{pq} . \end{aligned} \tag{2.40}$$

The sum of the first two terms represents the CC2 energy of the excited state f, the third term is the condition for the ground state amplitudes $\mathbf{t}$. The fourth term enforces the orthogonality of left and right eigenvector ($\mathbf{M}$ is the metric of the co- and contravariant CSFs). Analogously to the orbital-relaxed ground state Lagrangian, the remaining terms represent the localization, Brillouin and orbital-orthogonality conditions, respectively. The ground state quantities are calculated only once in the beginning, thus only the difference to the ground state ($\mathcal{L}_f = \mathcal{L}_{f'} - \mathcal{L}_0^{\mathrm{CC2}}$) has to be considered for the particular excited state,

$$\begin{aligned}\mathcal{L}_f &= \tilde{L}^f \mathbf{A} R^f + \tilde{\lambda}_{\mu_i}^{f} \Omega_{\mu_i} - \omega_f [\tilde{L}^f \mathbf{M} R^f - \mathbf{1}] \\ &\quad + z_{ij}^{loc,f} r_{ij} + z_{ai}^{f} [\mathbf{f} + \mathbf{v_0}]_{ai} + x_{pq}^{f} \left[\mathbf{C}^\dagger \mathbf{S}^{\mathrm{AO}} \mathbf{C} - \mathbf{1}\right]_{pq} . \end{aligned} \tag{2.41}$$

The corresponding Lagrange multipliers are defined as

$$\begin{aligned} \tilde{\lambda}^f &= \tilde{\lambda}^{f'} - \tilde{\lambda}^0 , & x^f &= x^{f'} - x^0 , \\ z^f &= z^{f'} - z^0 , & z^{loc,f} &= z^{loc,f'} - z^{loc,0} . \end{aligned} \tag{2.42}$$

For conciseness the state index f is omitted for L, R, and ω in the following. Differentiation of the Lagrangian $\mathcal{L}_f$ with respect to the amplitudes $\mathbf{t}$ yields the equation

determining the multipliers $\tilde{\lambda}^{\mathbf{f}}$,

$$\begin{aligned} &[\tilde{\mathbf{L}}\mathbf{D}\mathbf{R} + \tilde{\lambda}^{\mathbf{f}}\mathbf{A}]_{\mu_i} = 0 \\ &\text{with} \quad D_{\mu_i\sigma_k\nu_j} = \frac{\partial A_{\mu_i\nu_j}}{\partial t_{\sigma_k}} \ . \end{aligned} \tag{2.43}$$

The corresponding working equations were published in Ref. 27.

2.3.2 Linear z-vector equations

Analogously to the ground state, the stationarity of $\mathcal{L}_f$ with respect to the orbital variations, i.e.

$$\begin{aligned} 0 \ = \ \Bigg(\frac{\partial}{\partial O_{pq}} \Big[&\tilde{L}\mathbf{A}R + \tilde{\lambda}^{\mathbf{f}}\mathbf{\Omega} - \omega[\tilde{L}\mathbf{M}R - \mathbf{1}] \\ &+ z_{ij}^{loc,f} r_{ij} + z_{ai}^{f}[\mathbf{f} + \mathbf{v_0}]_{ai} + x_{pq}^{f}\left[\mathbf{C}^{\dagger}\mathbf{S}\mathbf{C} - \mathbf{1}\right]_{pq} \Big] \Bigg)_{\mathbf{V}_0=0} \ , \end{aligned} \tag{2.44}$$

yields the *z-vector equations*,

$$0 \ = \ (1 - \mathcal{P}_{pq})[\mathbf{B}^{\mathbf{f}} + \tilde{\mathbf{B}}(\mathbf{z}^{\mathbf{f}}) + \mathbf{b}(\mathbf{z}^{\mathbf{loc,f}})]_{pq}, \tag{2.45}$$

and a set of equations for $\mathbf{x}^{\mathbf{f}}$,

$$x_{pq}^{f} = -\frac{1}{4}(1 + \mathcal{P}_{pq})[\mathbf{B}^{\mathbf{f}} + \tilde{\mathbf{B}}(\mathbf{z}^{\mathbf{f}}) + \mathbf{b}(\mathbf{z}^{\mathbf{loc,f}})]_{pq} \ , \tag{2.46}$$

corresponding to the ground state eqs. (2.18) and (2.21), respectively. Eq. (2.45) again decouples into the Z-CPL equations,

$$B_{ij}^{f} - B_{ji}^{f} + \sum_{k>l} \left(\left(\frac{\partial r_{kl}}{\partial O_{ij}} \right)_{\mathbf{V}_0=0} - \left(\frac{\partial r_{kl}}{\partial O_{ji}} \right)_{\mathbf{V}_0=0} \right) z_{kl}^{loc,f} = 0 \ , \tag{2.47}$$

determining $\mathbf{z}^{\mathbf{loc,f}}$, and the Z-CPHF equations,

$$B_{ai}^{f} - B_{ia}^{f} + [\mathbf{b}(\mathbf{z}^{\mathbf{loc,f}}) + \mathbf{f}\mathbf{z}^{\mathbf{f}} - \mathbf{z}^{\mathbf{f}}\mathbf{f} + 2\mathbf{g}(\bar{\mathbf{z}}^{\mathbf{f}})]_{ai} = 0 \ , \tag{2.48}$$

determining $\mathbf{z}^{\mathbf{f}}$, corresponding to eqs. (2.19) and (2.20) for the ground state. Apart from the different right hand side $\mathbf{B}^{\mathbf{f}}$, these equations are equivalent to those of the ground

state. The quantities $\tilde{\mathbf{B}}(\mathbf{z}^{\mathbf{f}})$ and $\mathbf{b}(\mathbf{z}^{\mathbf{loc,f}})$ are defined according to eq. (2.15), and $\mathbf{B}^{\mathbf{f}}$ as

$$[\mathbf{B}^{\mathbf{f}}]_{pq} = \left(\frac{\partial \mathcal{L}'_f}{\partial O_{pq}}\right)_{\mathbf{v}_0=0} = C_{\mu p} B^f_{\mu i} + C_{\mu p} B^f_{\mu r} Q_{ra} + C_{\mu p} S^{\mathrm{AO}}_{\mu\rho} \delta_{\rho r} B^f_{r\nu} C^v_{\nu a} \ ,$$
$$\text{with} \quad \mathcal{L}'_f = \tilde{\mathbf{L}}\mathbf{A}\mathbf{R} + \tilde{\lambda}^{\mathbf{f}}\mathbf{\Omega} - \omega[\tilde{\mathbf{L}}\mathbf{M}\mathbf{R} - \mathbf{1}] \ . \tag{2.49}$$

Analogously to the ground state the terms including $B^f_{\mu i}$ and $B^f_{\mu r}$ arise from the direct partial derivatives with respect to O_{pq} for $q = i$ and $q = r$, respectively. The term including $B^f_{r\nu}$ has its origin in the dependence of the doubles amplitudes, eigenvectors and Lagrange multipliers $\tilde{\lambda}^{\mathbf{f}}$ on the orbital variations (cf. eqs. (2.32) and (2.33) for the ground state).
The practical equations for the Lagrangian, from which the derivation starts, are again obtained employing diagrammatic techniques as explained in section 1.3. Starting from the diagrams shown in figure A.3 (in appendix A) for the excitation energy $\omega = \tilde{L}\mathbf{A}R$ the expression

$$\begin{aligned}
\tilde{L}\mathbf{A}R = &- \tilde{L}^k_r \hat{f}_{ik} S_{rr'} R^i_{r'} + \tilde{L}^i_r \hat{f}_{rs} R^i_s + 2\tilde{L}^k_s (ir\hat{|}sk) R^i_r - \tilde{L}^i_t (lr|ks) S_{tt'} \tilde{t}^{kl}_{st'} R^i_r \\
&- \tilde{L}^k_r (is|lt) S_{rr'} \tilde{t}^{kl}_{st} R^i_{r'} + 2\tilde{L}^k_s (lt|ir) S_{ss'} \tilde{t}^{kl}_{s't} R^i_r - \tilde{L}^k_s (lr|it) S_{ss'} \tilde{t}^{kl}_{s't} R^i_r \\
&+ \tilde{L}^i_r \hat{f}_{js} S_{rr'} \tilde{R}^{ij}_{r's} + \tilde{L}^i_t (tr\hat{|}js) \tilde{R}^{ij}_{rs} - \tilde{L}^k_r (ik\hat{|}js) S_{rr'} \tilde{R}^{ij}_{rs} + 2\tilde{L}^{ik}_{st} (tk\hat{|}sr) R^i_r \\
&- 2\tilde{L}^{kl}_{rs} (sl\hat{|}ik) S_{rr'} R^i_{r'} + 2\tilde{L}^{ij}_{rs} f_{st} S_{rr'} R^{ij}_{r't} - 2\tilde{L}^{ik}_{rs} S_{rr'} S_{ss'} f_{jk} R^{ij}_{r's'} \ ,
\end{aligned} \tag{2.50}$$

is obtained, and for the orthogonality condition of the eigenvectors from figure A.4 the expression

$$\tilde{L}\mathbf{M}R = \tilde{L}^i_r S_{rr'} R^i_{r'} + \tilde{L}^{ij}_{rs} S_{rr'} S_{ss'} R^{ij}_{r's'} \ . \tag{2.51}$$

The terms originating from the amplitude condition $\tilde{\lambda}^f_{\mu_i} \Omega_{\mu_i}$ are the same as for the ground state in eq. (2.24), with replacing the ground state multipliers $\tilde{\lambda}^{\mathbf{0}}$ by the excited state multipliers $\tilde{\lambda}^{\mathbf{f}}$.

As discussed for the ground state, only the derivatives of the Lagrangian with respect to the doubles quantities have to be considered for the term including $B^f_{r\nu}$ in eq. (2.49). The derivative of the Lagrangian $\mathcal{L}'_f$ with respect to the amplitudes $\mathbf{t}$ yields the equations for the multipliers, with respect to the multipliers $\tilde{\lambda}^{\mathbf{f}}$ the amplitude equations, with respect to the right eigenvector $\mathbf{R}^{\mathbf{f}}$ the left eigenvalue equation, and with respect to the

left eigenvector $\tilde{\mathbf{L}}^{\mathbf{f}}$ the right eigenvalue equation,

$$\begin{aligned}
\left(\frac{\partial \mathcal{L}'_f}{\partial t_{ab}^{ij}}\right) &= [\tilde{\mathbf{L}}\mathbf{D}\mathbf{R} + \tilde{\lambda}^{\mathbf{f}}\mathbf{A}]_{ab}^{ij} \\
&= (1+\mathcal{P}_{ab}\mathcal{P}_{ij})\Big\{ f_{ca}\tilde{\lambda}_{cb}^{ij,f} - \tilde{\lambda}_{ab}^{ik,f} f_{jk} \\
&\qquad +(1-\frac{1}{2}\mathcal{P}_{ij})\Big[-\tilde{L}_b^k R_c^k(jc|ia) + 2\tilde{L}_a^i R_c^k(jb|kc) - \tilde{L}_a^i R_c^k(jc|kb) \\
&\qquad\qquad -\tilde{L}_c^i R_c^k(ka|jb) + \hat{G}_{ab}^{ij}(\tilde{\lambda}^f) + \tilde{\lambda}_a^{i,f}\hat{f}_{jb}\Big]\Big\} \ , \qquad (2.52) \\
\left(\frac{\partial \mathcal{L}'_f}{\partial \tilde{\lambda}_{ab}^{ij,f}}\right) &= \Omega_{ab}^{ij} \\
&= (1+\mathcal{P}_{ab}\mathcal{P}_{ij})\left\{ \frac{1}{2}(ai\hat{|}bj) + t_{ac}^{ij} f_{bc} - f_{ki} t_{ab}^{kj} \right\} \ , \qquad (2.53) \\
\left(\frac{\partial \mathcal{L}'_f}{\partial R_{ab}^{ij}}\right) &= [\tilde{\mathbf{L}}\mathbf{A} - \omega\tilde{\mathbf{L}}]_{ab}^{ij} \\
&= (1+\mathcal{P}_{ab}\mathcal{P}_{ij})\Big\{ \tilde{L}_{ac}^{ij} f_{cb} - \tilde{L}_{ab}^{ik} f_{jk} - \frac{1}{2}\omega\tilde{L}_{ab}^{ij} \\
&\qquad +(1-\frac{1}{2}\mathcal{P}_{ij})\left[\tilde{L}_a^i \hat{f}_{jb} + \tilde{L}_c^i(ca\hat{|}jb) - \tilde{L}_a^k(ik\hat{|}jb)\right]\Big\} \ , \qquad (2.54) \\
\left(\frac{\partial \mathcal{L}'_f}{\partial \tilde{L}_{ab}^{ij}}\right) &= [\mathbf{A}\mathbf{R} - \omega\mathbf{R}]_{ab}^{ij} \\
&= (1+\mathcal{P}_{ab}\mathcal{P}_{ij})\left[(ac\hat{|}bj)R_c^i - (ki\hat{|}bj)R_a^k + f_{ac}R_{cb}^{ij} - R_{ab}^{ik} f_{kj} - \frac{1}{2}\omega R_{ab}^{ij}\right] \ . \qquad (2.55)
\end{aligned}$$

Adapting eq. (2.34) for excited states, i.e.

$$\begin{aligned}
2C_{\mu p}S_{\mu\rho}^{AO}\delta_{\rho r}\Bigg[& t_{rt}^{ji} Q_{bt}\left(\frac{\partial \mathcal{L}'_f}{\partial t_{ab}^{ij}}\right) + \tilde{\lambda}_{rt}^{ji,f} Q_{bt}\left(\frac{\partial \mathcal{L}'_f}{\partial \tilde{\lambda}_{ab}^{ij,f}}\right) \\
& + R_{rt}^{ji} Q_{bt}\left(\frac{\partial \mathcal{L}'_f}{\partial R_{ab}^{ij}}\right) + \tilde{L}_{rt}^{ji} Q_{bt}\left(\frac{\partial \mathcal{L}'_f}{\partial \tilde{L}_{ab}^{ij}}\right)\Bigg] = C_{\mu p}S_{\mu\rho}^{\mathrm{AO}}\delta_{\rho r}B_{r\nu}^f C_{\nu a}^v \ , \qquad (2.56)
\end{aligned}$$

leads to the working equation for the intermediate $B^f_{r\mu}$,

$$\begin{aligned}
B^f_{r\mu} &= (X(\lambda^f T)_{jr} + d^{LR2}_{jr})\hat{f}_{j\mu} + (\bar{\mathcal{D}}^{\xi}_{tr}(\lambda^f) + \bar{\mathcal{D}}^{\eta}_{tr})f_{t\mu} \\
&\quad + (j\mu|Q)\left[V^Q_{kr}d^L_{jk} + 2X(LT)_{jr}{}^R b^Q - X(LT)_{kr}{}^R\bar{c}^Q_{kj}\right] + (j\mu\tilde{\tilde{|}}Q)V^Q_{jr} + (j\mu\hat{\tilde{|}}Q)^R V^Q_{jr} \\
&\quad - \bar{M}_{\mu r} - {}^{LR\bar{V}}M_{\mu r} - \hat{\bar{M}}_{\nu r}\hat{C}_{\nu\mu} - {}^{LW}M_{\nu r}\hat{C}_{\nu\mu} - \tilde{M}_{\nu r}\hat{C}_{\nu\mu} \\
&\quad + \big\{-\bar{d}^f_{ru} - \bar{d}^{f(LR)}_{ru} + \bar{d}^D_{ru}(f_{st}) + \bar{d}^{D(LR)}_{ru}(f_{st}) - \omega\bar{\mathcal{D}}^{\eta}_{ru} \\
&\qquad + X(\hat{f}_{it})_{jr}\tilde{\lambda}^{j,f}_u + {}^R X(\hat{f}_{it})_{jr}\tilde{L}^j_u \\
&\qquad + 2\tilde{L}^j_u V^Q_{jr}(ks|Q)R^k_s - \tilde{L}^j_u\tilde{t}^{ji}_{rs}(ks|Q)^R\bar{c}^Q_{ik} \\
&\qquad + M_{\rho r}P_{\rho t}d^L_{ut} + {}^R M_{\rho r}\Lambda^h_{\rho k}\tilde{L}^k_u + {}^L M_{\rho r}L_{\rho k}R^k_u + M_{\rho r}\Lambda^h_{\rho k}\tilde{\lambda}^{k,f}_u\big\}\,\delta_{u\nu}S^{\mathrm{AO}}_{\nu\mu}\ , \qquad (2.57)
\end{aligned}$$

while $B^f_{\mu i}$ and $B^f_{\mu r}$ are obtained as the direct partial derivatives of $\mathcal{L}'_f$ with respect to the orbital variations for $q = i$ and $q = r$, respectively,

$$\begin{aligned}
B^f_{\mu i} &= \hat{f}_{\mu k}(d^L_{ik} + d'_{ik}) + \hat{f}_{k\mu}(d^L_{ki} + d'_{ki}) + \hat{f}_{s\mu}d'_{si} + \hat{f}_{\mu s}(d^L_{is} + d^{LR2}_{is} + d'_{is}) \\
&\quad + f_{k\mu}(\bar{\mathcal{D}}^{\xi}_{ik}(\lambda^f) + \bar{\mathcal{D}}^{\eta}_{ik}) \\
&\quad + 2g(\bar{d}^L + \bar{d}^{LR2} + \bar{\mathcal{D}}^{\xi}(\lambda^f) + \bar{\mathcal{D}}^{\eta} + \bar{d}')_{\mu i} + 2g(d^L + d^{LR2} + d')_{\mu s}t^i_s \\
&\quad + (k\mu|Q)\left[-{}^{LR}\bar{c}^Q_{ik} - 2^L V^Q_{ir}S_{rr'}R^k_{r'}\right] \\
&\quad + (\mu k\hat{\tilde{|}}Q)\left[-{}^{LR}\bar{c}^Q_{ki} - \tilde{L}^k_r S_{rr'}{}^R V^Q_{ir'} + 2d^{Lt}_{ik}\ {}^R b^Q - V^Q_{is}S_{ss'}\tilde{\lambda}^{k,f}_{s'}\right] \\
&\quad + (\mu i\tilde{|}Q)\left[2^L b^Q + 2^X b^Q\right] + (\mu l\tilde{|}Q)\left[-d^{Lt}_{ik}\hat{c}^Q_{l\bar{k}} - {}^X\bar{c}^Q_{li} - \tilde{L}^l_s S_{ss'}V^Q_{is'}\right] \\
&\quad + 2(i\mu\hat{\tilde{|}}Q)^R b^Q + (\mu r|Q)\left[\bar{V}^Q_{ir} - X(LT)_{lr}{}^R\bar{c}^Q_{li} + 2X(LT)_{ir}{}^R b^Q\right] \\
&\quad + {}^{LR\bar{V}}N_{\mu i} + {}^{LW}N_{\mu i} + \hat{\bar{N}}_{\mu i} + (d^L_{ik} + d'_{ik})N_{\mu k} + d^{Lt}_{ik}\ {}^R N_{\mu k} \\
&\quad + \tilde{M}_{\mu s}S_{ss'}t^i_{s'} + {}^{LW}M_{\mu s}S_{ss'}t^i_{s'} + {}^L M_{\mu s}S_{ss'}R^i_{s'} + M_{\mu s}S_{ss'}\tilde{\lambda}^{i,f}_{s'} \\
&\quad + \hat{\bar{M}}_{\mu s}S_{ss'}t^i_{s'} + {}^R M_{\mu s}S_{ss'}\tilde{L}^i_{s'}\ , \qquad (2.58)
\end{aligned}$$

$$
\begin{aligned}
B^f_{\mu r} &= \hat{f}_{k\mu}(d^L_{kr} + d'_{kr} + d^{LR2}_{kr}) + \hat{f}_{\mu k} d'_{rk} + \hat{f}_{s\mu}(d^L_{sr} + d'_{sr}) + \hat{f}_{\mu s}(d^L_{rs} + d'_{rs}) \\
&+ f_{\mu s}(\bar{\mathcal{D}}^{\xi}_{rs}(\lambda^f) + \bar{\mathcal{D}}^{\eta}_{rs}) + 2g(d^L + d^{LR2} + d')_{k\mu} t^k_r \\
&+ (i\mu|Q)\Big[d^L_{ik} V^Q_{kr} - 2^L V^Q_{ks} S_{ss'} R^i_{s'} t^k_r + \bar{V}^Q_{ir} + 2^L b^Q R^i_r - {}^{LR}\bar{c}^Q_{ki} t^k_r \\
&\qquad + 2^X b^Q R^i_r - {}^X\bar{c}^Q_{li} R^l_r + 2X(LT)_{ir}\, {}^R b^Q - X(LT)_{lr}\, {}^R\bar{c}^Q_{li}\Big] \\
&+ 2(\mu k\hat{|}Q)\tilde{L}^{kR}_r b^Q - (\mu i\tilde{|}Q)\tilde{L}^k_r \hat{c}^Q_{i\bar{k}} + (i\breve{\mu}\breve{|}Q) V^Q_{ir} \\
&+ (k\mu\hat{\tilde{|}}Q)\left[{}^R V^Q_{kr} - \hat{c}^Q_{i\bar{k}} R^i_r + 2t^k_r\ {}^R b^Q\right] \\
&+ ({}^{LW}N_{\mu k} + \hat{\tilde{N}}_{\mu k}) t^k_r + {}^R N_{\mu k}\tilde{L}^k_r + {}^L N_{\mu k} R^k_r + N_{\mu k}\tilde{\lambda}^k_r \\
&- {}^{LR\bar{V}}M_{\mu r} - {}^{LW}M_{\mu r} - \hat{\tilde{M}}_{\mu r} - \tilde{M}_{\mu r} + M_{\mu s} S_{ss'} d^L_{s'r} \\
&+ {}^R M_{\mu s} S_{ss'} d^{Lt}_{s'r} + M_{\mu s} S_{ss'} d'_{s'r}\ .
\end{aligned} \tag{2.59}
$$

Again, all $\hat{f}$ are dressed only internally. The intermediates including 3-index quantities are

$$
\begin{aligned}
{}^R b^Q &= c^Q_{ir} R^i_r\ , & {}^R\bar{c}^Q_{ij} &= c^Q_{ir} R^j_r\ , \\
{}^X b^Q &= c^Q_{ir} X(LT)_{ir}\ , & {}^X\bar{c}^Q_{ij} &= c^Q_{ir} X(LT)_{jr}\ , \\
{}^L b^Q &= \hat{c}^Q_{ri}\tilde{L}^i_r\ , & {}^{LR}\bar{c}^Q_{ij} &= \tilde{L}^i_s \hat{c}^Q_{sr} R^j_r\ , \\
V^Q_{ir} &= \tilde{t}^{ij}_{rs} c^Q_{js}\ , & \hat{\bar{V}}^Q_{ir} &= \tilde{\lambda}^{ij,f}_{rs}\hat{c}^Q_{sj}\ , \\
{}^R V^Q_{ir} &= \tilde{R}^{ij}_{rs} c^Q_{js}\ , & {}^L V^Q_{ir} &= \tilde{L}^{ij}_{rs}\hat{c}^Q_{sj}\ , \\
{}^L W^Q_{ir} &= \tilde{L}^{ij}_{rs}(R^j_t \hat{c}^Q_{st} - S_{ss'} R^k_{s'}\hat{c}^Q_{kj})\ , & {}^{LR}\bar{V}^Q_{ir} &= \tilde{R}^{ij}_{rs}(\tilde{L}^j_t \hat{c}^Q_{ts} - S_{ss'}\tilde{L}^k_{s'}\hat{c}^Q_{jk})\ , \\
\hat{\bar{B}}^Q_{ir} &= \lambda^{i,f}_s \hat{c}^Q_{sr} - S_{rr'}\lambda^{k,f}_{r'}\hat{c}^Q_{ik}\ , & \hat{\bar{B}}'^Q_{ir} &= d^L_{ki} c^Q_{kr} - S_{rr'} d^L_{r's} c^Q_{is}\ , \\
\bar{V}^Q_{ir} &= \tilde{t}^{ij}_{rs}(\hat{\bar{B}}^Q_{js} + \hat{\bar{B}}'^Q_{js})\ .
\end{aligned} \tag{2.60}
$$

The intermediates including half-transformed integrals are

$$
\begin{aligned}
(\mu i\tilde{|}Q) &= (\mu s|Q)R^i_s \ , & (i\mu\hat{\tilde{|}}Q) &= (s\mu\hat{|}Q)\tilde{L}^i_s \ , \\
(i\mu\breve{\tilde{|}}Q) &= (s\mu\hat{|}Q)\tilde{\lambda}^{i,f}_s \ , & \tilde{M}_{\mu r} &= -2^L V^Q_{kr}(\mu k\tilde{|}Q) \ , \\
M_{\mu r} &= -(k\mu|Q)V^Q_{kr} \ , & N_{\mu i} &= V^Q_{is}(\mu s|Q) \ , \\
{}^R M_{\mu r} &= -(k\mu|Q)\,{}^R V^Q_{kr} \ , & {}^R N_{\mu i} &= {}^R V^Q_{is}(\mu s|Q) \ , \\
{}^{LR\bar{V}} M_{\mu r} &= -(k\mu|Q)\,{}^{LR}\bar{V}^Q_{kr} \ , & {}^{LR\bar{V}} N_{\mu i} &= {}^{LR}\bar{V}^Q_{is}(\mu s|Q) \ , \\
{}^L M_{\mu r} &= -2(\mu k\hat{|}Q)\,{}^L V^Q_{kr} \ , & {}^L N_{\mu i} &= 2\,{}^L V^Q_{is}(s\mu\hat{|}Q) \ , \\
{}^{LW} M_{\mu r} &= -2(\mu k\hat{|}Q)\,{}^L W^Q_{kr} \ , & {}^{LW} N_{\mu i} &= 2\,{}^L W^Q_{is}(s\mu\hat{|}Q) \ , \\
\hat{\bar{M}}_{\mu r} &= -2(\mu k\hat{|}Q)\hat{\bar{V}}^Q_{kr} \ , & \hat{\bar{L}}_{\mu i} &= 2\hat{\bar{V}}^Q_{is}(s\mu\hat{|}Q) \ , \\
\bar{M}_{\mu r} &= -(k\mu|Q)\bar{V}^Q_{kr} \ . & & \qquad (2.61)
\end{aligned}
$$

The densities $\mathcal{D}^{\xi}(\lambda^f)$ and $\mathcal{D}^{\eta}$ will be discussed in section 2.5, eqs. (2.81) and (2.82). The remaining intermediates are

$$
\begin{aligned}
X(LT)_{ir} &= \tilde{L}^j_s S_{ss'}\tilde{t}^{ji}_{s'r} \ , & X(\lambda^f T)_{ir} &= \tilde{\lambda}^{j,f}_s S_{ss'}\tilde{t}^{ji}_{s'r} \ , \\
d'_{ij} &= -\tilde{\lambda}^{j,f}_s S_{ss'} t^i_{s'} \ , & d'_{ri} &= \tilde{\lambda}^{i,f}_r \ , \\
d'_{ir} &= t^k_r d'_{ik} + X(\lambda^f T)_{ir} \ , & d'_{rs} &= \tilde{\lambda}^{k,f}_r t^k_s \ , \\
d^{Lt}_{ij} &= -\tilde{L}^j_s S_{ss'} t^i_{s'} \ , & d^{Lt}_{rs} &= \tilde{L}^k_r t^k_s \ , \\
d^{L}_{ij} &= -\tilde{L}^j_s S_{ss'} R^i_{s'} \ , & d^{L}_{rs} &= \tilde{L}^k_r R^k_s \ , \\
d^{L}_{ir} &= -\tilde{L}^k_s S_{ss'}(R^i_{s'} t^k_r + R^k_r t^i_{s'}) \ , & d^{LR2}_{ir} &= \tilde{L}^k_s S_{ss'}\tilde{R}^{ji}_{s'r} \ , \\
d^{f}_{ru} &= 2\tilde{\lambda}^{ji,f}_{rt'} S_{t't}(f_{ki}t^{kj}_{tu} + f_{kj}t^{ik}_{tu}) \ , & d^{f(LR)}_{ru} &= 2\tilde{L}^{ji}_{rt'} S_{t't}(f_{ki}R^{kj}_{tu} + f_{kj}R^{ik}_{tu}) \ , \\
d^{D}_{ru}(f) &= 2\tilde{\lambda}^{ji,f}_{rs} f_{st} t^{ij}_{tu} \ , & d^{D(LR)}_{ru}(f) &= 2\tilde{L}^{ji}_{rs} f_{st} R^{ij}_{tu} \ , \\
{}^R X(\hat{f}_{it})_{jr} &= \hat{f}_{it}\tilde{R}^{ij}_{tr} \ . & & \qquad (2.62)
\end{aligned}
$$

2.3.3 Calculation of properties

Orbital-relaxed properties, e.g. the dipole moment, are obtained by differentiation of the Lagrangian $\mathcal{L}_{f'}$ in eq. (2.40) with respect to the perturbation strength ϵ_X,

$$\begin{aligned}\langle X\rangle_{f'}^{rel} &= \left(\frac{\partial \mathcal{L}_{f'}}{\partial \epsilon_X}\right) = \left(\frac{\partial (\mathcal{L}_0^{\mathrm{CC2}} + \mathcal{L}_f)}{\partial \epsilon_X}\right) = \langle X\rangle_0^{rel} + \langle X\rangle_f^{rel} \ , \\ \langle X\rangle_f^{rel} &= \left(\frac{\partial \mathcal{L}_f}{\partial \epsilon_X}\right) = \tilde{\lambda}^f \xi^X + \tilde{L}\mathbf{A}^{\mathbf{X}} R + z_{ai}^f X_{ai} \\ &= \mathrm{tr}[\mathbf{X}^{\mathrm{AO}}(\mathcal{D}_{\mathrm{AO}}^f + z_{\mathrm{AO}}^f)] \ , \end{aligned} \tag{2.63}$$

$$\text{with} \qquad A_{\mu_i\nu_j}^X = \frac{\partial A_{\mu_i\nu_j}}{\partial \epsilon_X} \qquad \text{and} \qquad \xi_{\mu_i}^X = \frac{\partial \Omega_{\mu_i}}{\partial \epsilon_X}. \tag{2.64}$$

$\langle X\rangle_0^{rel}$ is calculated according to eq. (2.39), and the explicit expression for the density $\mathcal{D}_{\mathrm{AO}}^f$ will be discussed in detail in section 2.5.

2.4 Triplet excited states

Details about the calculation of properties of triplet excited states without orbital relaxation using the LT-DF-LCC2 method were presented earlier.[28]

2.4.1 The Lagrangian

The general formulation of the local CC2 Lagrangian $\mathcal{L}_{f'}$ including orbital relaxation, given in eq. (2.40), also holds for triplet excited states and the derivation of orbital-relaxed properties proceeds in the same way. The individual terms contain triplet excitation operators, as discussed in section 1.2.1.

2.4.2 Linear z-vector equations

The formalism is the same as for singlet excited states, cf. section 2.3.2, the difference lies in the intermediates $B_{\mu i}^f$, $B_{\mu r}^f$, and $B_{r\nu}^f$ for $\mathbf{B^f}$, which is according to eq. (2.49) defined as

$$[\mathbf{B^f}]_{pq} = \left(\frac{\partial \mathcal{L}'_f}{\partial O_{pq}}\right)_{\mathbf{V}_0=0} = C_{\mu p} B_{\mu i}^f + C_{\mu p} B_{\mu r}^f Q_{ra} + C_{\mu p} S_{\mu\rho}^{\mathrm{AO}} \delta_{\rho r} B_{r\nu}^f C_{\nu a}^v \ . \tag{2.65}$$

The practical equations for the triplet terms contributing to $\mathcal{L}'_f$ are obtained starting from the diagrams in figure A.5 for the triplet excitation energy $\omega = \tilde{L}\mathbf{A}R$, and the diagrams in figure A.6 for the orthogonality condition of the eigenvectors (both figures in appendix A), as

$$\begin{aligned}
\tilde{L}\mathbf{A}R =& -\tilde{L}^k_r \hat{f}_{ik} S_{rr'} R^i_{r'} + \tilde{L}^i_r \hat{f}_{rs} R^i_s - \tilde{L}^k_s (ik\hat{|}sr) R^i_r - \tilde{L}^i_t (ls|kr) S_{tt'} \tilde{t}^{kl}_{t's} R^i_r \\
& - \tilde{L}^k_r (is|lt) S_{rr'} \tilde{t}^{kl}_{st} R^i_{r'} + \tilde{L}^k_s (lr|it) S_{ss'} t^{kl}_{ts'} R^i_r \\
& + \tilde{L}^i_r \hat{f}_{js} S_{rr'} \bar{R}^{ij}_{r's} + \tilde{L}^i_t (tr\hat{|}js) \bar{R}^{ij}_{rs} - \tilde{L}^k_r (ik\hat{|}js) S_{rr'} \bar{R}^{ij}_{rs} + \frac{1}{2} \bar{L}^{ik}_{st} (tk\hat{|}sr) R^i_r \\
& - \frac{1}{2} \tilde{L}^{kl}_{rs} (sl\hat{|}ik) S_{rr'} R^i_{r'} + f_{st} S_{rr'} \left(\overset{(+)}{\tilde{L}}{}^{ij}_{rs} \overset{(+)}{R}{}^{ij}_{r't} + 2 \overset{(-)}{\tilde{L}}{}^{ij}_{rs} \overset{(-)}{R}{}^{ij}_{r't} \right) \\
& - f_{jk} S_{rr'} S_{ss'} f_{jk} \left(\overset{(+)}{\tilde{L}}{}^{ik}_{rs} \overset{(+)}{R}{}^{ij}_{r's'} + 2 \overset{(-)}{\tilde{L}}{}^{ik}_{rs} \overset{(-)}{R}{}^{ij}_{r's'} \right) , \\
\tilde{L}\mathbf{M}R =& \tilde{L}^i_r S_{rr'} R^i_{r'} + \frac{1}{2} \overset{(+)}{\tilde{L}}{}^{ij}_{rs} S_{rr'} S_{ss'} \overset{(+)}{R}{}^{ij}_{r's'} + \overset{(-)}{\tilde{L}}{}^{ij}_{rs} S_{rr'} S_{ss'} \overset{(-)}{R}{}^{ij}_{r's'} \, .
\end{aligned} \tag{2.66}$$

The terms originating from the amplitude condition $\tilde{\lambda}^f_{\mu_i} \Omega_{\mu_i}$ are the same as for singlet states, i.e. eq. (2.24) with replacing the ground state multipliers $\tilde{\lambda}^{\mathbf{0}}$ by the excited state multipliers $\tilde{\lambda}^{\mathbf{f}}$. $\mathbf{B^f}$ is obtained as the derivative of these practical expressions for the terms in $\mathcal{L}'_f$ with respect to the orbital variations.

Analogously to singlet excited states the dependence of the Lagrange multipliers, amplitudes, left and right eigenvector on the coefficients yields the third term in eq. (2.65). Only the derivatives of the Lagrangian with respect to the doubles quantities have to be calculated. For triplet states the derivatives of the plus and minus combinations of the left and right eigenvector have to be considered,

$$\begin{aligned}
\left(\frac{\partial \mathcal{L}'_f}{\partial t^{ij}_{ab}} \right) =& (1 + \mathcal{P}_{ab}\mathcal{P}_{ij}) \left\{ \frac{1}{2} \tilde{L}^j_a (kb|ic) R^k_c + f_{ca} \tilde{\lambda}^{ij,f}_{cb} - \tilde{\lambda}^{kj,f}_{ab} f_{ik} \right. \\
& \left. + (1 - \frac{1}{2}\mathcal{P}_{ij}) \left[\hat{G}^{ij}_{ab}(\tilde{\lambda}^f) + \tilde{\lambda}^{i,f}_a \hat{f}_{jb} - \tilde{L}^i_c (jb|ka) R^k_c - \tilde{L}^k_a (jb|ic) R^k_c \right] \right\} ,
\end{aligned} \tag{2.67}$$

$$\left(\frac{\partial \mathcal{L}'_f}{\partial \tilde{\lambda}^{ij,f}_{ab}} \right) = (1 + \mathcal{P}_{ab}\mathcal{P}_{ij}) \left\{ \frac{1}{2} (ai\hat{|}bj) + t^{ij}_{ac} f_{bc} - f_{ki} t^{kj}_{ab} \right\} , \tag{2.68}$$

$$\left(\frac{\partial \mathcal{L}'_f}{\partial \overset{(+)}{R}{}^{ij}_{ab}}\right) = \frac{1}{4}(1+\mathcal{P}_{ab}\mathcal{P}_{ij})(1-\mathcal{P}_{ij})\Big\{2\tilde{L}^i_a \hat{f}_{jb} - 2\tilde{L}^k_a(jb\hat{|}ik) + 2\tilde{L}^i_c(jb\hat{|}ca) + f_{cb}\overset{(+)}{\tilde{L}}{}^{ij}_{ac} - f_{jk}\overset{(+)}{\tilde{L}}{}^{ik}_{ab} - \frac{1}{2}\omega\overset{(+)}{\tilde{L}}{}^{ij}_{ab}\Big\}\ , \tag{2.69}$$

$$\left(\frac{\partial \mathcal{L}'_f}{\partial \overset{(-)}{R}{}^{ij}_{ab}}\right) = \frac{1}{2}(1-\mathcal{P}_{ab}\mathcal{P}_{ij})\Big\{2\tilde{L}^i_a \hat{f}_{jb} - 2\tilde{L}^k_a(jb\hat{|}ik) + 2\tilde{L}^i_c(jb\hat{|}ca) + 2f_{cb}\overset{(-)}{\tilde{L}}{}^{ij}_{ac} - 2f_{jk}\overset{(-)}{\tilde{L}}{}^{ik}_{ab} - \omega\overset{(-)}{\tilde{L}}{}^{ij}_{ab}\Big\}\ , \tag{2.70}$$

$$\left(\frac{\partial \mathcal{L}'_f}{\partial \overset{(+)}{\tilde{L}}{}^{ij}_{ab}}\right) = \frac{1}{4}(1+\mathcal{P}_{ab}\mathcal{P}_{ij})(1-\mathcal{P}_{ij})\Big\{(ac\hat{|}bj)R^i_c - (ki\hat{|}bj)R^k_a + f_{bc}\overset{(+)}{R}{}^{ij}_{ac} - f_{kj}\overset{(+)}{R}{}^{ik}_{ab} - \frac{1}{2}\omega\overset{(+)}{R}{}^{ij}_{ab}\Big\}\ , \tag{2.71}$$

$$\left(\frac{\partial \mathcal{L}'_f}{\partial \overset{(-)}{\tilde{L}}{}^{ij}_{ab}}\right) = \frac{1}{2}(1-\mathcal{P}_{ab}\mathcal{P}_{ij})\Big\{(ac\hat{|}bj)R^i_c - (ki\hat{|}bj)R^k_a + 2f_{bc}\overset{(-)}{R}{}^{ij}_{ac} - 2f_{kj}\overset{(-)}{R}{}^{ik}_{ab} - \omega\overset{(-)}{R}{}^{ij}_{ab}\Big\}\ . \tag{2.72}$$

These derivatives contribute to the third term of eq.(2.49) for excited triplet states in analogy to eq. (2.32) for the ground state case. For the plus combination of a triplet doubles quantity, e.g. the right eigenvector $\overset{(+)}{R}{}^{ij}_{ab}$, the derivative is then calculated as

$$\begin{aligned}\left[\left(\frac{\partial \mathcal{L}'_f}{\partial \overset{(+)}{R}{}^{ij}_{ab}}\right)\left(\frac{\partial \overset{(+)}{R}{}^{ij}_{ab}}{\partial O_{pq}}\right)\right]_{\mathbf{V}_0=0} &= \delta_{qa}C_{p\mu}S^{AO}_{\mu\nu}\delta_{\nu r}\left(\left(\frac{\partial \mathcal{L}'_f}{\partial \overset{(+)}{R}{}^{ij}_{\rho s}}\right) - \left(\frac{\partial \mathcal{L}'_f}{\partial \overset{(+)}{R}{}^{ij}_{s\rho}}\right)\right)\overset{(+)}{R}{}^{ij}_{rs}C_{\rho a} \\ &= 2\delta_{qa}C_{p\mu}S^{AO}_{\mu\nu}\delta_{\nu r}\left(\frac{\partial \mathcal{L}'_f}{\partial \overset{(+)}{R}{}^{ij}_{\rho s}}\right)\overset{(+)}{R}{}^{ij}_{rs}C_{\rho a},\end{aligned} \tag{2.73}$$

and for a triplet quantity $\overset{(-)}{R}{}^{ij}_{ab}$ as

$$\begin{aligned}\left[\left(\frac{\partial\mathcal{L}}{\partial\overset{(-)}{R}{}^{ij}_{ab}}\right)\left(\frac{\partial\overset{(-)}{R}{}^{ij}_{ab}}{\partial O_{pq}}\right)\right]_{\mathbf{v}_0=0} &= \delta_{qa}C_{p\mu}S^{AO}_{\mu\nu}\delta_{\nu r}\left(\left(\frac{\partial\mathcal{L}'_f}{\partial\overset{(-)}{R}{}^{ij}_{\rho s}}\right)-\left(\frac{\partial\mathcal{L}'_f}{\partial\overset{(-)}{R}{}^{ji}_{s\rho}}\right)\right)\overset{(-)}{R}{}^{ij}_{rs}C_{\rho a}\\ &= 2\delta_{qa}C_{p\mu}S^{AO}_{\mu\nu}\delta_{\nu r}\left(\frac{\partial\mathcal{L}'_f}{\partial\overset{(-)}{R}{}^{ij}_{\rho s}}\right)\overset{(-)}{R}{}^{ij}_{rs}C_{\rho a}. \end{aligned} \tag{2.74}$$

Finally, the intermediate $B^f_{r\mu}$ in equation (2.49) is in local basis obtained as

$$\begin{aligned}B^f_{r\mu} =&(X(\lambda^f T)_{jr}+d^{LR2}_{jr})\hat{f}_{j\mu}+(\bar{\mathcal{D}}^{\xi}_{tr}(\lambda^f)+\bar{\mathcal{D}}^{\eta}_{tr})f_{t\mu}\\ &+(j\mu|Q)\left[V^Q_{kr}d^L_{jk}-X'(LT)_{kr}{}^R\bar{c}^Q_{kj}\right]+(j\mu\breve{\hat{|}}Q)V^Q_{jr}+(j\mu\hat{\breve{|}}Q)^RV^Q_{jr}\\ &-\bar{M}_{\mu r}-{}^{LR\bar{V}}M_{\mu r}-\hat{\bar{M}}_{\nu r}\hat{C}_{\nu\mu}-\frac{1}{4}{}^{LW}M_{\nu r}\hat{C}_{\nu\mu}-\frac{1}{4}\tilde{M}_{\nu r}\hat{C}_{\nu\mu}\\ &+\{-\bar{d}^f_{ru}-\bar{d}^{f(LR)}_{ru}+\bar{d}^D_{ru}(f_{st})+\bar{d}^{D(LR)}_{ru}(f_{st})-\omega\bar{\mathcal{D}}^{\eta}_{ru}\\ &\quad+X(\hat{f}_{it})_{jr}\tilde{\lambda}^{j,f}_u+{}^RX(\hat{f}_{it})_{jr}\tilde{L}^j_u+\tilde{L}^i_ut^{ji}_{rs}(ks|Q)^R\bar{c}^Q_{jk}\\ &\quad+M_{\rho r}P_{\rho t}d^L_{ut}+{}^RM_{\rho r}\Lambda^h_{\rho k}\tilde{L}^k_u+\frac{1}{4}{}^LM_{\rho r}L_{\rho k}R^k_u+M_{\rho r}\Lambda^h_{\rho k}\tilde{\lambda}^{k,f}_u\Big\}\delta_{u\nu}S^{\mathrm{AO}}_{\nu\mu}\ . \end{aligned} \tag{2.75}$$

The direct partial derivatives of $\mathcal{L}'_f$ with respect to the orbital variation $\mathcal{O}_{pq}$ for $q=i$ and $q=r$ yield the quantities $B^f_{\mu i}$ and $B^f_{\mu r}$, respectively. They are calculated as

$$\begin{aligned}B^f_{\mu i} =&\hat{f}_{\mu k}(d^L_{ik}+d'_{ik})+\hat{f}_{k\mu}(d^L_{ki}+d'_{ki})+\hat{f}_{s\mu}d'_{si}+\hat{f}_{\mu s}(d^L_{is}+d^{LR2}_{is}+d'_{is})\\ &+f_{k\mu}(\bar{\mathcal{D}}^{\xi}_{ik}(\lambda^f)+\bar{\mathcal{D}}^{\eta}_{ik})\\ &+2g(\bar{d}^L+\bar{d}^{LR2}+\bar{\mathcal{D}}^{\xi}(\lambda^f)+\bar{\mathcal{D}}^{\eta}+\bar{d}')_{\mu i}+2g(d^L+d^{LR2}+d')_{\mu s}t^i_s\\ &+(k\mu|Q)\left[-{}^{LR}\bar{c}^Q_{ik}-\frac{1}{2}{}^LV^Q_{ir}S_{rr'}R^k_{r'}\right]\\ &+(\mu k\hat{|}Q)\left[-{}^{LR}\bar{c}^Q_{ki}-\tilde{L}^k_rS_{rr'}{}^RV^Q_{ir'}-V^Q_{is}S_{ss'}\tilde{\lambda}^{k,f}_{s'}\right]\\ &+(\mu l\tilde{|}Q)\left[-d^{Lt}_{ik}\hat{c}^Q_{l\bar{k}}-{}^{X'}\bar{c}^Q_{li}-\tilde{L}^l_sS_{ss'}V^Q_{is'}\right]+(\mu r|Q)\left[\bar{V}^Q_{ir}-X'(LT)_{lr}{}^R\bar{c}^Q_{li}\right]\\ &+{}^{LR\bar{V}}N_{\mu i}+\frac{1}{4}{}^{LW}N_{\mu i}+\hat{\bar{N}}_{\mu i}+(d^L_{ik}+d'_{ik})N_{\mu k}+d^{Lt}_{ik}\ {}^RN_{\mu k}\\ &+\frac{1}{4}{}^{LW}M_{\mu s}S_{ss'}t^i_{s'}+\frac{1}{4}{}^LM_{\mu s}S_{ss'}R^i_{s'}+M_{\mu s}S_{ss'}\tilde{\lambda}^{i,f}_{s'}+\hat{\bar{M}}_{\mu s}S_{ss'}t^i_{s'}\\ &+{}^RM_{\mu s}S_{ss'}\tilde{L}^i_{s'}+\frac{1}{4}\tilde{M}_{\mu s}S_{ss'}t^i_{s'}\ , \end{aligned} \tag{2.76}$$

$$
\begin{aligned}
B^f_{\mu r} =& \hat{f}_{k\mu}(d^L_{kr} + d'_{kr} + d^{LR2}_{kr}) + \hat{f}_{\mu k} d'_{rk} + \hat{f}_{s\mu}(d^L_{sr} + d'_{sr}) + \hat{f}_{\mu s}(d^L_{rs} + d'_{rs}) \\
&+ f_{\mu s}(\bar{\mathcal{D}}^{\xi}_{rs}(\lambda^f) + \bar{\mathcal{D}}^{\eta}_{rs}) + 2g(d^L + d^{LR2} + d')_{k\mu} t^k_r \\
&+ (i\mu|Q)\left[d^L_{ik} V^Q_{kr} - \frac{1}{2}{}^L V^Q_{ks} S_{ss'} R^i_{s'} t^k_r + \bar{V}^Q_{ir} - {}^{LR}\bar{c}^Q_{ki} t^k_r - {}^{X'}\bar{c}^Q_{li} R^l_r - X'(LT)_{lr}\,{}^R\bar{c}^Q_{li}\right] \\
&- (\mu i\tilde{|}Q)\tilde{L}^k_r \hat{c}^Q_{i\bar{k}} + (i\mu\breve{\tilde{|}}Q) V^Q_{ir} + (k\mu\hat{\tilde{|}}Q)\left[{}^R V^Q_{kr} - \hat{c}^Q_{i\bar{k}} R^i_r\right] \\
&+ (\frac{1}{4}{}^{LW} N_{\mu k} + \hat{\tilde{N}}_{\mu k}) t^k_r + {}^R N_{\mu k} \tilde{L}^k_r + \frac{1}{4}{}^L N_{\mu k} R^k_r + N_{\mu k} \tilde{\lambda}^k_r \\
&- {}^{LR\bar{V}} M_{\mu r} - \frac{1}{4}{}^{LW} M_{\mu r} - \frac{1}{4}\tilde{M}_{\mu r} - \hat{\tilde{M}}_{\mu r} + M_{\mu s} S_{ss'} d^L_{s'r} \\
&+ {}^R M_{\mu s} S_{ss'} d^{Lt}_{s'r} + M_{\mu s} S_{ss'} d'_{s'r}. \qquad (2.77)
\end{aligned}
$$

The intermediates different from those already defined for singlet excited states in eqs. (2.60 - 2.62) are

$$
\begin{aligned}
\bar{R}^{ij}_{rs} &= 2(\overset{(+)}{R}{}^{ij}_{rs} + \overset{(-)}{R}{}^{ij}_{rs}) , & \bar{L}^{ij}_{rs} &= 2(\overset{(+)}{\tilde{L}}{}^{ij}_{rs} + \overset{(-)}{\tilde{L}}{}^{ij}_{rs}) , \\
{}^R V^Q_{ir} &= \bar{R}^{ij}_{rs} c^Q_{js} , & {}^L V^Q_{ir} &= \bar{L}^{ij}_{rs} \hat{c}^Q_{sj} , \\
{}^L W^Q_{ir} &= \bar{L}^{ji}_{sr}(R^j_t \hat{c}^Q_{st} - S_{ss'} R^k_{s'} \hat{c}^Q_{kj}) , & {}^{LR}\bar{V}^Q_{ir} &= \bar{R}^{ji}_{sr}(\tilde{L}^j_t \hat{c}^Q_{ts} - S_{ss'} \tilde{L}^k_{s'} \hat{c}^Q_{jk}) , \\
X'(LT)_{ir} &= -\tilde{L}^j_s S_{ss'} t^{ij}_{s'r} , & {}^{X'}\bar{c}^Q_{ij} &= c^Q_{ir} X'(LT)_{jr} , \\
{}^R X(\hat{f}_{it})_{jr} &= \bar{R}^{ji}_{rt} \hat{f}_{it} , & & \\
d^{f(LR)}_{ru} &= \overset{(+)}{\tilde{L}}{}^{ji}_{rt'} S_{t't}(f_{ki} \overset{(+)}{R}{}^{kj}_{tu} + f_{kj} \overset{(+)}{R}{}^{ik}_{tu}) & d^f_{ru} &= 2\tilde{\lambda}^{ji,f}_{rt'} S_{t't}(f_{ki} t^{kj}_{tu} + f_{kj} t^{ik}_{tu}) , \\
& \quad -2\overset{(-)}{\tilde{L}}{}^{ji}_{rt'} S_{t't}(f_{ki} \overset{(-)}{R}{}^{kj}_{tu} + f_{kj} \overset{(-)}{R}{}^{ik}_{tu}) , & d^{LR2}_{ir} &= \tilde{L}^j_s S_{ss'} \bar{R}^{ji}_{s'r} , \\
d^{D(LR)}_{ru}(f) &= \overset{(+)}{\tilde{L}}{}^{ji}_{rs} f_{st} \overset{(+)}{R}{}^{ij}_{tu} - 2\overset{(-)}{\tilde{L}}{}^{ji}_{rs} f_{st} \overset{(-)}{R}{}^{ij}_{tu} , & d^D_{ru}(f) &= 2\tilde{\lambda}^{ji,f}_{rs} f_{st} t^{ij}_{tu} . \qquad (2.78)
\end{aligned}
$$

The densities $\mathcal{D}^{\xi}(\lambda^f)$ and $\mathcal{D}^{\eta}$ are defined in section 2.5, eqs. (2.81) and (2.84), respectively. Again, all $\hat{f}$ are dressed only internally. All M and N quantities are defined as for the singlet case, e.g. ${}^R M_{\mu r} = -{}^R V^Q_{kr}(k\mu|Q)$, with the corresponding three-index intermediates for triplet states.

2.4.3 Calculation of properties

First-order orbital-relaxed properties are calculated according to equation (2.63), but with the corresponding density matrix $\mathcal{D}^f_{\mathrm{AO}}$ for triplet states, which is discussed explicitly in the following section.

2.5 Orbital-relaxed densities

In the following the individual density matrices are given explicitly in the LMO/PAO basis, i.e. after transformation from canonical virtuals to PAOs.
For the orbital-relaxed case the term $\mathbf{F}+\hat{\mathbf{V}}_\mathbf{0}$ in the commutator of the doubles amplitude equation Ω_{μ_2}, cf. eq. (1.9), simplifies to $\mathbf{F}+\mathbf{V_0}$, i.e., the dressed time-independent perturbation has to be replaced by the undressed one,

$$\Omega_{\mu_2} \;=\; \left\langle \tilde{\mu}_2 \left| \hat{\mathbf{H}} + [\mathbf{F}+\mathbf{V_0}, \mathbf{T_2}] \right| 0 \right\rangle = 0 \; . \tag{2.79}$$

The reason for this is the explicit inclusion of the Brillouin condition ($[\mathbf{f}+\mathbf{v_0}]_{ai}=0$) in the Lagrangian. Consequently, the occupied-virtual matrix elements $[\mathbf{f}+\mathbf{v_0}]_{ia}$, which would occur in the external dressing of the internal-internal and external-external blocks $[\hat{\mathbf{f}}+\hat{\mathbf{v}}_\mathbf{0}]_{ij}$ and $[\hat{\mathbf{f}}+\hat{\mathbf{v}}_\mathbf{0}]_{ab}$ in the commutator of the Ω_{μ_2} equation, are zero. The related Fock operator $\mathbf{F}$ in the second term of Ω_{μ_2} is neither externally nor internally dressed (unlike the operator $\hat{\mathbf{F}}$ included in the dressed Hamiltonian $\hat{\mathbf{H}}$ in the first term of Ω_{μ_2} and in Ω_{μ_1}), since only the external dressing is of zeroth-order, while the internal dressing of $\hat{\mathbf{F}}$ is of first-order as discussed in section 1.1.4, and therefore neglected in the second term of the CC2 Ω_{μ_2} equation.
Having $\mathbf{F}+\mathbf{V_0}$ instead of $\mathbf{F}+\hat{\mathbf{V}}_\mathbf{0}$ in the Ω_{μ_2} equation implies that the density matrices are generally different to those of the orbital-unrelaxed case and consist of an undressed part $\mathcal{D}$, and a dressed part $\hat{\mathcal{D}}$. $\mathcal{D}$ originates from the term involving the bare $\mathbf{V_0}$ operator in the Ω_{μ_2} condition of the Lagrangian and transforms to the AO basis via the ordinary LMO and PAO coefficient matrices $\mathbf{L}$ and $\mathbf{P}$, which are concatenated in the combined coefficient matrix $\mathbf{C^{loc}}=(\mathbf{L}|\mathbf{P})$. $\hat{\mathcal{D}}$, on the other hand, originates from the terms in the Lagrangian involving the similarity transformed $\hat{\mathbf{V}}_\mathbf{0}$ (via $\hat{\mathbf{H}}$) and transforms to AO basis via the coefficient matrices $\mathbf{\Lambda^p}$ and $\mathbf{\Lambda^h}$ defined in eq. (1.18). Hence, generally, the orbital-relaxed density matrices in AO basis $\mathcal{D}_{\mathrm{AO}}$ are obtained as

$$\mathcal{D}_{\mu\nu} = C^{\mathrm{loc}}_{\mu p}\mathcal{D}_{pq}C^{\mathrm{loc}}_{\nu q} + \Lambda^{p}_{\mu p}\hat{\mathcal{D}}_{pq}\Lambda^{h}_{\nu q} \; . \tag{2.80}$$

In the orbital-unrelaxed case only the similarity transformed perturbation $\hat{\mathbf{V}}_\mathbf{0}$ occurs and thus the first term in eq. (2.80) is dropped.

The first density matrix $\mathcal{D}^0_{\mathrm{AO}}$, needed for the evaluation of the ground state property

$\langle X \rangle_0^{rel}$ according to eq. (2.39), is calculated via eq. (2.80) with

$$\begin{aligned}
\mathcal{D}^0_{pq} &= 2(\delta_{pi}\delta_{qj} + \delta_{pr}\delta_{qi}t^i_r) + \mathcal{D}^\xi_{pq}(\lambda^0), \quad \text{and} \quad \hat{\mathcal{D}}^0_{pq} = \hat{\mathcal{D}}^\xi_{pq}(\lambda^0), \\
\text{with} \quad \mathcal{D}^\xi_{ij}(\lambda^0) &= -2\tilde{\lambda}^{jk,0}_{rs'} S_{r'r} t^{ik}_{r's} S_{s's}, \\
\mathcal{D}^\xi_{rs}(\lambda^0) &= 2\tilde{\lambda}^{kl,0}_{st'} S_{t't} t^{kl}_{rt}, \\
\mathcal{D}^\xi_{ri}(\lambda^0) &= \mathcal{D}^\xi_{ir}(\lambda^0) = 0, \\
\hat{\mathcal{D}}^\xi_{ir}(\lambda^0) &= \tilde{\lambda}^{i,0}_r, \\
\hat{\mathcal{D}}^\xi_{ri}(\lambda^0) &= \tilde{\lambda}^{k,0}_{s'} S_{s's} \tilde{t}^{ik}_{rs}, \\
\hat{\mathcal{D}}^\xi_{rs}(\lambda^0) &= \hat{\mathcal{D}}^\xi_{ij}(\lambda^0) = 0.
\end{aligned} \tag{2.81}$$

In contrast, for the orbital-unrelaxed case, all submatrices of $\mathcal{D}^\xi_{pq}(\lambda^0)$ are added to the corresponding submatrices of $\hat{\mathcal{D}}^\xi_{pq}(\lambda^0)$, and the first term in eq. (2.80) is dropped (cf. eqs. (30) and (26) in Ref. 25).

The density $\mathcal{D}^f$ for properties of singlet excited states, cf. eq. (2.63), accordingly is calculated as

$$\begin{aligned}
\mathcal{D}^f_{pq} &= \mathcal{D}^\xi_{pq}(\lambda^f) + \mathcal{D}^\eta_{pq}, \quad \text{and} \quad \hat{\mathcal{D}}^f_{pq} = \hat{\mathcal{D}}^\xi_{pq}(\lambda^f) + \hat{\mathcal{D}}^\eta_{pq}, \\
\text{with} \quad \mathcal{D}^\eta_{ij} &= -2S_{rr'}\tilde{L}^{ik}_{r's'} S_{s's} R^{jk}_{rs} \ , \\
\mathcal{D}^\eta_{rs} &= 2\tilde{L}^{ij}_{st} S_{tt'} R^{ij}_{rt'} \ , \\
\mathcal{D}^\eta_{ir} &= \mathcal{D}^\eta_{ri} = 0 \ , \\
\hat{\mathcal{D}}^\eta_{ij} &= -\tilde{L}^i_{r'} S_{r'r} R^j_r \ , \\
\hat{\mathcal{D}}^\eta_{rs} &= \tilde{L}^i_s R^i_r, \\
\hat{\mathcal{D}}^\eta_{ir} &= 0 \ , \\
\hat{\mathcal{D}}^\eta_{ri} &= \tilde{L}^j_{s'} S_{s's} \tilde{R}^{ji}_{sr},
\end{aligned} \tag{2.82}$$

and $\tilde{R}^{ij}_{rs} = 2R^{ij}_{rs} - R^{ji}_{rs}$. $\mathcal{D}^\xi(\lambda^f)$ and $\hat{\mathcal{D}}^\xi(\lambda^f)$ are defined according to eq. (2.81). $\mathcal{D}^f_{\text{AO}}$ again is obtained via eq. (2.80). The sum of the $\mathcal{D}^\eta$ and the $\hat{\mathcal{D}}^\eta$ matrix is not identical to the corresponding density matrix for the orbital-unrelaxed case (cf. eqs. (35) and (27) in Ref. 25). In particular, there are no terms involving the ground state doubles amplitudes in the $\hat{\mathcal{D}}^\eta_{ri}$ block in the orbital-relaxed case, due to the absence of the second term in the $A_{\mu_2\nu_1}$ block of the CC2 Jacobian, which was specified in Ref. 25 in the orbital-unrelaxed

context as

$$A_{\mu_2\nu_1} = \langle \tilde{\mu}_2 | [\hat{\mathbf{H}}, \tau_{\nu_1}] + [[\hat{\mathbf{V}}_{\mathbf{0}}, \tau_{\nu_1}], \mathbf{T_2}] | 0 \rangle \ . \tag{2.83}$$

This is also caused by the presence of the bare rather than the similarity transformed $\mathbf{V_0}$ operator in the second term of the Ω_{μ_2} equation.

For properties of triplet excited states the density matrices $\mathcal{D}^f$, $\hat{\mathcal{D}}^f$, $\mathcal{D}^\xi(\lambda^f)$, and $\hat{\mathcal{D}}^\xi(\lambda^f)$ are identically defined as for the singlet states, but $\mathcal{D}^\eta$ and $\hat{\mathcal{D}}^\eta$ comprise the plus and minus combinations of the left and right doubles eigenvectors, $\overset{(+)}{R}$, $\overset{(-)}{R}$, $\overset{(+)}{\tilde{L}}$ and $\overset{(-)}{\tilde{L}}$,

$$\begin{aligned}
\mathcal{D}^\eta_{ij} &= -S_{rr'}S_{ss'}(\overset{(+)}{\tilde{L}}{}^{ik}_{r's'}\overset{(+)}{R}{}^{jk}_{rs} + 2\overset{(-)}{\tilde{L}}{}^{ik}_{r's'}\overset{(-)}{R}{}^{jk}_{rs}) \ , \\
\mathcal{D}^\eta_{rs} &= S_{tt'}(\overset{(+)}{\tilde{L}}{}^{ij}_{st'}\overset{(+)}{R}{}^{ij}_{rt} + 2\overset{(-)}{\tilde{L}}{}^{ij}_{st'}\overset{(-)}{R}{}^{ij}_{rt}) \ , \\
\mathcal{D}^\eta_{ir} &= \mathcal{D}^\eta_{ri} = 0 \ , \\
\hat{\mathcal{D}}^\eta_{ij} &= -\tilde{L}^i_{r'}S_{r'r}R^j_r \ , \\
\hat{\mathcal{D}}^\eta_{rs} &= \tilde{L}^i_s R^i_r \ , \\
\hat{\mathcal{D}}^\eta_{ir} &= 0 \ , \\
\hat{\mathcal{D}}^\eta_{ri} &= \tilde{L}^j_{s'}S_{ss'}\bar{R}^{ji}_{sr},
\end{aligned} \tag{2.84}$$

with $\bar{R}^{ij}_{rs} = 2(\overset{(+)}{R}{}^{ij}_{rs} + \overset{(-)}{R}{}^{ij}_{rs})$. $\mathcal{D}^f_{\mathrm{AO}}$ again is obtained via eq. (2.80). As for singlet excited states the sum of the $\mathcal{D}^\eta$ and the $\hat{\mathcal{D}}^\eta$ matrix is not identical to the corresponding density matrix for the orbital-unrelaxed case, cf. eq. (43) in Ref. 28; the terms involving the ground state doubles amplitudes in the $\hat{\mathcal{D}}^\eta_{ri}$ block are absent, as above.

2.6 Test calculations

Orbital-relaxed first-order properties for the ground state and excited states have been implemented into the `MOLPRO` program package.[61] Most of the relevant routines are parallelized based on a shared file approach, i.e., the scratch files containing the amplitudes, integrals, etc. reside on two file systems, which are common to all parallel threads. Input/output (I/O) is organized such, that both file systems are used. A shared file approach can cause a bottleneck beyond 8-16 cores, depending on the efficiency of the input/output (I/O) subsystem.[28]

The correctness of the code was verified by comparing the results using untruncated pair lists and full domains to the corresponding canonical results obtained with the TURBOMOLE program,[19,21,22,62] and to numerical results obtained from finite differences. The accuracy of the local approximations introduced by restricted pair lists and domains is analysed by comparing local and canonical results for the same test set of molecules and excited states as used previously for excitation energies and orbital-unrelaxed properties.[26–28] The cc-pVDZ and aug-cc-pVDZ AO basis sets[63] are employed together with the related fitting basis sets optimized for DF-MP2.[64] In calculations employing the aug-cc-pVDZ basis the contributions of the most diffuse functions of each angular momentum are discarded in the Pipek-Mezey localization procedure (`cpldel=1` option in MOLPRO).[32] This is generally advisable to achieve a better localization of the LMOs for basis sets with diffuse functions.
If not explicitly stated otherwise, three Laplace quadrature points (LP) were used for the presented calculations. The effect of increasing the number of LPs will be discussed in section 2.6.3.

2.6.1 Approximate Lagrangians for LT-DF-LCC2

As discussed in detail in Ref. 54 for the LT-LMP2 method, the Lagrangians in eqs. (2.10) and (2.40) are not the proper energy Lagrangians, if the Laplace transformation is employed. They are just approximations to the proper Lagrangians, because the application of Laplace transformation for truncated doubles quantities implies a fitting of those to the untruncated canonical ones. Nevertheless, they are used, because the proper LT-DF-LCC2 Lagrangians are impractical due to the appearence of the untruncated doubles quantities (cf. eq. (27) in Ref. 54 and the related discussion).
Yet the errors introduced by the use of these approximate Lagrangians turned out to be small for the LT-LMP2 method and the properties were even slightly closer to the canonical reference than the ones calculated with the standard LMP2 method.
Here, the effect of these approximate Lagrangians on the CC2 orbital-relaxed ground state dipole moments is explored. For the ground state properties the Laplace transformation is used to partition the $\tilde{\lambda}^{\mathbf{0}}$ equation system, eq. (2.6). Table 2.1 lists the z-component of the CC2 ground state dipole moment, calculated in the cc-pVDZ basis using standard domains (`iext`=0) and extended domains (`iext`=1, cf. section 2.6.2), for several molecules. Results for the analytical canonical method and the analytical local methods without (DF-LCC2[24,25]) and with Laplace transform (LT-DF-LCC2) are compared. Moreover, the corresponding numerical results from finite difference calculations

Table 2.1: The z-component (in a.u.) of the orbital-relaxed ground state dipole moment vector is shown for several molecules. Analytical canonical results are shown together with analytical and numerical local results obtained with the DF-LCC2 and the LT-DF-LCC2 method. [from Ref. 29]

		iext=0				iext=1			
	can.	DF-LCC2		LT-DF-LCC2		DF-LCC2		LT-DF-LCC2	
	an.	an.	num.	an.	num.	an.	num.	an.	num.
DMABN	2.895	2.875	2.875	2.875	2.875	2.891	2.891	2.890	2.891
HPA	0.345	0.360	0.360	0.358	0.360	0.347	0.347	0.347	0.347
Propanamide	-1.305	-1.311	-1.311	-1.310	-1.311	-1.305	-1.305	-1.305	-1.305
trans-urocanic acid	1.923	1.934	1.934	1.934	1.934	1.921	1.921	1.922	1.921

with the local methods are included. As can be seen, analytical and numerical results differ only slightly (by up to 0.002 a.u.) for LT-DF-LCC2, whereas they are identical for DF-LCC2. A similar effect is observed also for excited states. Due to the small deviations, one can conclude that the use of the approximate Lagrangians, eqs. (2.10) and (2.40), in the LT-DF-LCC2 method is uncritical for the calculation of first-order properties.

For geometry optimizations the effect of the approximate Lagrangians is expected to be larger, thus it will be discussed in detail in chapter 3.

2.6.2 Pair approximations and domains

As discussed in section 1.1.3 for the ground state and in section 1.2.3 for excited states local approximations are introduced via pair lists and domains.

For the ground state the truncation of the LMO pair list depends solely on the respective LMO interorbital distance R_{g}. For excited states, on the other hand, adaptive pair lists are employed in the LT-DF-LCC2 method, as explained in detail in section IIC of Ref. 26: a set of important LMOs is determined for each individual state (specified by threshold $\kappa_e = 0.999$) and state-specific pair lists are determined from the list of these important orbitals. Such a pair list, corresponding to a certain excited state, comprises all pairs of important LMOs related to that state, and all other pairs up to a certain LMO interorbital distance R_{ex}. Moreover, all pairs from the ground state list are also included.

In order to find reliable values for R_{g} and R_{ex} various calculations with different pair truncations were performed employing the cc-pVDZ basis set for some molecules and states from the test set. Table 2.2 compiles the norm of the canonical ground state

dipole moment vector, and for the two lowest singlet and triplet excited states the norm of the canonical dipole moment difference vector (excited state minus ground state dipole moment), all without and with orbital relaxation. Furthermore, the relative error of the corresponding local calculation is given as the ratio of the norm of the difference vector (canonical minus local) and the norm of the canonical vector. The ratios of the lengths of truncated and full pair lists are also given in table 2.2.

In previous work devoted to orbital-unrelaxed first-order properties pair list specifications of $R_g/R_{ex} = 10/5$ bohr were usually employed. In table 2.2 the orbital-unrelaxed and relaxed results for pair lists determined by $R_g/R_{ex} = 10/5$, 5/3, and 15/10 bohr are compared.

R_g affects the excited state properties through the ground state amplitudes t_{μ_2} and the multipliers $\tilde{\lambda}^f_{\mu_2}$, which are restricted to the ground state pair list and domains. The left and right eigenvectors $\tilde{L}_{\mu_2}$ and R_{μ_2} are restricted to the excited state pair lists and domains, which also contain the ground state pair lists and domains.

As is evident from table 2.2, the errors become clearly smaller when going from R_g/R_{ex}=5/3 to longer pair lists. Yet already 10/5 provides sufficiently accurate results, whereas the combination 15/10 shows no substantial further improvement, but already produces very long pair lists, which increase the computational cost. Note that the results for the state S_2 of *trans*-urocanic acid with different R_g/R_{ex} differ due to the different ground-state pair lists, while the excited state pair list is full in all three cases. The relatively large deviations observed for the S_1 state of the β-Dipeptide will be discussed in detail in section 2.6.4.

Overall, the effect of the pair list truncation is very similar for the orbital-relaxed and unrelaxed properties, and the default settings already used previously of R_g/R_{ex} =10/5 bohr appear to be a good choice, which will be employed in all further calculations of the present work.

The domains for the ground state truncating the pair-specific virtual space are built using the Boughton Pulay (BP) procedure with a criterion of 0.98.[34] The excited state domains are obtained in an adaptive procedure as explained in detail in section IIC of Ref. 26. The orbital domains are determined by specifying an ordered list of important centers for each important LMO. The ground state domains then are augmented with further centers from this list until a threshold of 0.98 is reached by the least-squares optimization procedure introduced in section IIC of Ref. 26.

As discussed earlier, such domains are appropriate for the calculation of excitation energies, but for orbital-unrelaxed properties it was observed that augmenting these domains

Table 2.2: Norms (in a.u.) of the canonical ground state dipole vector $|\mu^0|$ and the canonical dipole difference vectors of the excited states $|\mu^f|$ without orbital relaxation are shown in column $|\mu^{can}|$. The corresponding orbital-relaxed quantities are labeled by the index *rel*. The results for the local calculations with the pair lists criterion combinations R_g/R_{ex}=5/3, 10/5 and 15/10 are given as the ratio of the norm of the difference vector (canonical minus local) relative to the canonical value $|\delta\mu|/|\mu^{can}|$ in %. The last three columns contain the percentage of included pairs. [from Ref. 29]

	State	$\lvert\mu^{can}\rvert$	$\lvert\delta\mu\rvert/\lvert\mu^{can}\rvert$			$\lvert\mu^{can}_{rel}\rvert$	$\lvert\delta\mu_{rel}\rvert/\lvert\mu^{can}_{rel}\rvert$			included pairs		
			5/3	10/5	15/10		5/3	10/5	15/10	5/3	10/5	15/10
β -Dipeptide	S_0	0.423	3.1	0.6	0.5	0.415	2.3	0.3	0.3	57	85	98
	S_1	0.388	23.9	23.7	23.5	0.262	30.3	29.9	29.9	76	87	100
	S_2	0.760	3.1	3.6	3.9	0.607	3.5	3.2	3.1	71	85	98
	T_1	0.436	12.1	11.8	11.6	0.328	13.3	13.0	13.0	78	92	100
	T_2	0.366	9.3	9.1	8.2	0.355	8.4	7.8	7.4	74	86	99
HPA	S_0	0.734	3.2	1.1	0.6	0.756	2.7	0.7	0.4	57	82	98
	S_1	0.242	3.9	1.9	2.5	0.203	1.4	2.7	3.6	77	87	100
	S_2	0.624	7.8	6.2	5.4	0.507	8.3	6.0	5.4	77	86	99
	T_1	0.109	13.4	4.2	5.0	0.091	9.3	3.6	4.9	77	91	100
	T_2	0.332	5.3	1.7	1.3	0.293	2.9	1.2	0.6	74	86	100
trans-urocanic	S_0	1.904	0.6	0.2	0.1	1.935	0.8	0.1	<0.1	66	92	100
acid	S_1	2.310	2.0	0.4	0.4	1.990	1.4	0.8	0.8	92	100	100
	S_2	2.261	0.7	1.4	1.6	2.104	2.2	2.0	2.0	100	100	100
	T_1	0.385	0.9	0.6	0.4	0.340	6.6	0.7	0.3	99	100	100
	T_2	0.312	18.6	3.1	2.1	0.326	12.9	1.5	0.6	90	97	100

Table 2.3: Norms (in a.u.) of the canonical ground state dipole vector $|\mu^0|$ and the canonical dipole difference vectors of the excited states $|\mu^f|$ without orbital relaxation are shown in column $|\mu^{can}|$. The corresponding orbital-relaxed quantities are labeled by the index *rel*. The results for the local calculations using the default domains (`iext`=0) and the domains, which are exended by the nearest neighbours (`iext`=1), are given as the ratio of the norm of the difference vector (canonical minus local) relative to the canonical value $|\delta\mu|/|\mu^{can}|$ in %. The last two columns contain the ratio (local vs. canonical) of the number of unique elements of the doubles quantities for the calculations in %. [from Ref. 29]

	State	$\lvert\mu^{can}\rvert$	$\lvert\delta\mu\rvert/\lvert\mu^{can}\rvert$		$\lvert\mu^{can}_{rel}\rvert$	$\lvert\delta\mu_{rel}\rvert/\lvert\mu^{can}_{rel}\rvert$		Doubles ratio	
			iext=0	iext=1		iext=0	iext=1	iext=0	iext=1
β -Dipeptide	S_0	0.423	3.8	0.6	0.415	2.6	0.3	7	31
	S_1	0.388	26.7	23.7	0.262	34.0	29.9	22	41
	S_2	0.760	5.3	3.6	0.607	5.7	3.2	11	36
	T_1	0.436	13.4	11.8	0.328	14.9	13.0	25	47
	T_2	0.366	26.6	9.1	0.355	23.2	7.8	17	39
HPA	S_0	0.734	5.8	1.1	0.756	2.8	0.7	7	32
	S_1	0.242	2.5	1.9	0.203	3.1	2.7	25	46
	S_2	0.624	8.1	6.2	0.507	7.6	6.0	21	44
	T_1	0.109	13.9	4.2	0.091	10.3	3.6	23	47
	T_2	0.332	4.2	1.7	0.293	2.0	1.2	23	44
trans-urocanic	S_0	1.904	1.6	0.2	1.935	0.6	0.1	15	55
acid	S_1	2.310	2.7	0.4	1.990	2.3	0.8	32	70
	S_2	2.261	1.1	1.4	2.104	2.1	2.0	50	76
	T_1	0.385	6.0	0.6	0.340	0.8	0.7	41	71
	T_2	0.312	21.7	3.1	0.326	12.2	1.5	52	75

by further centers leads to significantly improved accuracy. Such extended domains can be constructed by e.g. adding further centers to the BP ground state domain, which are separated by not more than one bond from the closest atom in the original BP domain (`iext=1` option in `MOLPRO`).
In order to investigate this aspect also for orbital-relaxed properties calculations with default (`iext=0`) and augmented (`iext=1`) domains were performed for some molecules of the test set in the cc-pVDZ basis. Table 2.3 compiles the norm of the canonical dipole moment vector μ^0 for the ground state, and the canonical dipole moment difference vector μ^f (excited state minus ground state dipole moment) for the two lowest lying singlet and triplet excited states of these molecules, along with the relative errors of the local method employing `iext=0` and `iext=1`, respectively. Furthermore, the ratio (local to canonical) of the number of unique elements of the doubles vector of the ground state amplitudes and excited state eigenvectors is shown.
Again the behaviour of the orbital-unrelaxed and relaxed properties is very similar. For some of the states the `iext=0` and `iext=1` results are very similar, but there are some cases like the T_2 state of the *trans*-urocanic acid molecule, where the domain extension leads to a drastic improvement of the accuracy. It is therefore recommended to use extended domains also in calculations of orbital-relaxed properties, although it will be computationally more expensive, as indicated by the higher doubles ratios. For all remaining calculations presented in this contribution the `iext=1` option was employed.

2.6.3 Number of Laplace quadrature points

For orbital-unrelaxed properties it was demonstrated earlier, that three Laplace quadrature points (LP) provide sufficient accuracy.[26,28] In the course of this work this is also verified for orbital-relaxed properties by comparing for some test molecules and states calculations performed with three and five LPs. Results with and without orbital relaxation are compiled in table 2.4 for the cc-pVDZ basis set. It turned out that the effect of the increased number of LPs is typically between one and two orders of magnitude smaller than the error introduced by the local approximation, very similar as for orbital-unrelaxed properties. Due to the small differences in accuracy and the higher computational cost for calculations with an increased number of LPs, three LPs are considered to be adequate for calculations including orbital relaxation.

Table 2.4: Norms (in a.u.) of the canonical dipole difference vectors $|\mu^f|$ of the excited states relative to the ground state without orbital relaxation are shown in column $|\mu^{can}|$, and including orbital relaxation in column $|\mu^{can}_{rel}|$. The results for the local calculations with three and five LPs are given as the ratio of the norm of the difference vector (canonical minus local) relative to the canonical value $|\delta\mu|/|\mu^{can}|$ in %.

	State	$\lvert\mu^{can}\rvert$	$\lvert\delta\mu\rvert/\lvert\mu^{can}\rvert$		$\lvert\mu^{can}_{rel}\rvert$	$\lvert\delta\mu_{rel}\rvert/\lvert\mu^{can}_{rel}\rvert$	
			3LP	5LP		3LP	5LP
HPA	S_1	0.242	1.9	2.2	0.203	2.7	2.6
	S_2	0.624	6.2	6.5	0.507	6.0	6.2
	T_1	0.109	4.2	3.8	0.091	3.6	2.9
	T_2	0.332	1.7	1.5	0.293	1.2	1.0
N-acetylglycine	S_1	0.741	3.4	3.4	0.591	2.0	1.8
	S_2	0.594	1.2	1.1	0.477	1.3	1.1
	T_1	0.793	2.7	2.8	0.671	1.2	1.2
	T_2	0.659	1.2	1.1	0.563	1.0	0.8
Propanamide	S_1	0.789	5.1	5.1	0.641	5.1	5.0
	S_2	2.646	1.7	1.6	2.336	1.7	1.7
	T_1	0.836	4.0	4.0	0.716	3.6	3.6
	T_2	0.794	2.4	2.4	0.756	1.9	2.0
trans-urocanic	S_1	2.310	0.4	0.5	1.990	0.8	0.6
acid	S_2	2.261	1.4	1.1	2.104	2.0	1.2
	T_1	0.385	0.6	0.6	0.340	0.7	0.8
	T_2	0.312	3.1	2.4	0.326	1.5	0.2

2.6.4 Accuracy of the local approximations

As already mentioned above, the accuracy of the local approximations was checked by comparing local and canonical calculations for a set of test molecules and excited singlet and triplet states already used in previous work.[26–28] The orbital-unrelaxed dipole moments differ slightly from the ones published in Ref. 27 and 28 because of the lower convergence threshold for the ground state in gradient calculations.
Table 2.5 compiles the norms of the orbital-unrelaxed and relaxed canonical reference dipole moments for the ground state and the two lowest singlet and triplet states of these molecules, along with deviations of the local calculations from the canonical values. These deviations are again calculated as the ratio of the norm of the difference vector between local and canonical dipole moment, and the norm of the canonical dipole moment, respectively.

Table 2.5: Column $|\mu^{can}|$ shows the norms (in a.u.) of the orbital-unrelaxed canonical ground state dipole vector $|\mu^0|$ and for the individual excited states the corresponding difference vectors $|\mu^f|$ (with respect to $|\mu^0|$). Similarly, column $|\mu^{can}_{rel}|$ contains the related orbital-relaxed values. The results of the local calculations are given as the ratio of the norm of the difference vector (canonical minus local) relative to the canonical norm, $|\delta\mu|/|\mu^{can}|$ in %. For the excited states also the canonical excitation energy ω_{can} and the character of the excitation are listed. [from Ref. 29]

		cc-pVDZ						aug-cc-pVDZ					
				orbital-unrelaxed		orbital-relaxed				orbital-unrelaxed		orbital-relaxed	
	State	ω_{can}	Char.	$\lvert\mu^{can}\rvert$	$\frac{\lvert\delta\mu\rvert}{\lvert\mu^{can}\rvert}$	$\lvert\mu^{can}_{rel}\rvert$	$\frac{\lvert\delta\mu_{rel}\rvert}{\lvert\mu^{can}_{rel}\rvert}$	ω_{can}	Char.	$\lvert\mu^{can}\rvert$	$\frac{\lvert\delta\mu\rvert}{\lvert\mu^{can}\rvert}$	$\lvert\mu^{can}_{rel}\rvert$	$\frac{\lvert\delta\mu_{rel}\rvert}{\lvert\mu^{can}_{rel}\rvert}$
β -Dipeptide	S_0			0.423	0.6	0.415	0.3			0.436	0.6	0.427	1.2
	S_1	4.861	$n \to \pi^*$	0.388	23.7	0.262	29.9	4.715	$n \to \pi^*$	0.372	23.4	0.249	34.2
	S_2	5.825	$n \to \pi^*$	0.760	3.6	0.607	3.2	4.982	$n \to Ry$	1.557	22.9	1.336	25.7
	T_1	4.496	$n \to \pi^*$	0.436	11.8	0.328	13.0	4.418	$n \to \pi^*$	0.444	11.6	0.326	15.6
	T_2	5.387	$\pi \to \pi^*$	0.366	9.1	0.355	7.8	4.935	$n \to Ry$	1.475	18.7	1.289	20.5
Dipeptide	S_0			1.304	0.1	1.330	0.2			1.339	0.2	1.365	0.1
	S_1	5.871	$n \to \pi^*$	0.735	2.8	0.587	1.6	5.743	$n \to \pi^*$	0.963	7.6	0.799	9.3
	S_2	6.106	$n \to \pi^*$	0.740	4.2	0.602	3.0	5.864	$n \to Ry$	0.984	4.9	0.749	6.3
	T_1	5.504	$n \to \pi^*$	0.789	2.3	0.668	1.0	5.440	$n \to \pi^*$	0.963	3.7	0.830	4.3
	T_2	5.763	$n \to \pi^*$	0.794	2.2	0.681	1.4	5.669	$n \to \pi^*$	0.954	3.6	0.829	3.9
DMABN	S_0			2.904	<0.1	2.895	0.2			3.039	<0.1	3.042	0.1
	S_1	4.525	$\pi \to \pi^*$	0.935	1.2	0.793	1.3	4.323	$\pi \to \pi^*$	1.003	0.5	0.844	0.8
	S_2	4.891	$\pi \to \pi^*$	2.072	0.3	1.793	0.5	4.495	$\pi \to Ry$	2.806	1.9	2.838	1.8
	T_1	3.716	$\pi \to \pi^*$	0.807	0.2	0.710	0.8	3.648	$\pi \to \pi^*$	0.892	0.4	0.789	0.7
	T_2	4.184	$\pi \to \pi^*$	1.181	1.1	1.058	1.0	4.011	$\pi \to \pi^*$	1.213	0.3	1.078	0.4
Guanine	S_0			2.512	0.1	2.563	0.1			2.542	0.1	2.601	0.1
	S_1	5.316	$\pi \to \pi^*$	0.340	3.2	0.258	1.9	4.743	$\pi \to Ry$	4.374	10.4	4.210	10.4
	S_2	5.660	$n \to \pi^*$	1.390	1.7	1.090	1.4	5.022	$\pi \to \pi^*$	0.628	0.7	0.541	2.4
	T_1	4.506	$\pi \to \pi^*$	0.658	1.2	0.595	0.1	4.310	$\pi \to \pi^*$	0.515	12.2	0.448	12.9

Continued on next page

Table 2.5 – continued from previous page

			cc-pVDZ						aug-cc-pVDZ				
				orbital-unrelaxed		orbital-relaxed				orbital-unrelaxed		orbital-relaxed	
	State	ω_{can}	Char.	$\lvert\mu^{can}\rvert$	$\frac{\lvert\delta\mu\rvert}{\lvert\mu^{can}\rvert}$	$\lvert\mu^{can}_{rel}\rvert$	$\frac{\lvert\delta\mu_{rel}\rvert}{\lvert\mu^{can}_{rel}\rvert}$	ω_{can}	Char.	$\lvert\mu^{can}\rvert$	$\frac{\lvert\delta\mu\rvert}{\lvert\mu^{can}\rvert}$	$\lvert\mu^{can}_{rel}\rvert$	$\frac{\lvert\delta\mu_{rel}\rvert}{\lvert\mu^{can}_{rel}\rvert}$
	T_2	4.566	$\pi \to \pi^*$	0.372	2.3	0.341	3.0	4.400	$\pi \to \pi^*$	0.274	3.9	0.241	2.3
HPA	S_0			0.734	1.1	0.756	0.7			0.726	0.6	0.748	0.9
	S_1	4.984	$\pi \to \pi^*$	0.242	1.9	0.203	2.7	4.816	$\pi \to \pi^*$	0.203	4.0	0.160	4.9
	S_2	6.149	$n \to \pi^*$	0.624	6.2	0.507	6.0	5.216	$\pi \to Ry$	4.510	3.5	4.460	3.6
	T_1	4.254	$\pi \to \pi^*$	0.109	4.2	0.091	3.6	4.189	$\pi \to \pi^*$	0.106	1.7	0.086	2.1
	T_2	4.582	$\pi \to \pi^*$	0.332	1.7	0.293	1.2	4.433	$\pi \to \pi^*$	0.285	1.8	0.246	1.6
p-cresol	S_0			0.521	1.1	0.528	0.8			0.519	0.4	0.533	0.3
	S_1	4.982	$\pi \to \pi^*$	0.256	1.8	0.218	3.8	4.795	$\pi \to \pi^*$	0.253	1.7	0.210	2.4
	S_2	6.326	$\pi \to \pi^*$	0.832	1.1	0.741	1.4	5.145	$\pi \to Ry$	4.280	4.6	4.209	4.6
	T_1	4.228	$\pi \to \pi^*$	0.165	3.4	0.146	1.9	4.156	$\pi \to \pi^*$	0.194	2.9	0.173	2.5
	T_2	4.588	$\pi \to \pi^*$	0.305	1.9	0.269	0.8	4.421	$\pi \to \pi^*$	0.273	1.6	0.239	1.2
N-acetylglycine	S_0			1.070	0.1	1.085	0.1			1.035	0.2	1.050	0.2
	S_1	5.862	$n \to \pi^*$	0.741	3.4	0.591	2.0	5.732	$n \to \pi^*$	0.948	6.9	0.784	8.1
	S_2	6.252	$n \to \pi^*$	0.594	1.2	0.477	1.3	5.989	$n \to Ry$	2.218	12.6	1.974	13.9
	T_1	5.489	$n \to \pi^*$	0.793	2.7	0.671	1.2	5.421	$n \to \pi^*$	0.962	3.9	0.828	4.4
	T_2	5.883	$n \to \pi^*$	0.659	1.2	0.563	1.0	5.779	$n \to \pi^*$	0.667	1.6	0.567	1.8
Phenylalanine	S_0			1.755	0.3	1.790	0.1			1.787	0.1	1.831	0.2
	S_1	5.260	$\pi \to \pi^*$	0.015	36.7	0.013	30.8	5.152	$\pi \to \pi^*$	0.053	11.2	0.050	8.2
	S_2	5.827	$n \to Ry$	0.571	12.6	0.459	13.0	5.693	$n \to Ry$	0.623	6.1	0.503	6.4
	T_1	4.304	$\pi \to \pi^*$	0.016	19.7	0.017	9.8	4.273	$\pi \to \pi^*$	0.021	8.5	0.020	11.9
	T_2	5.089	$\pi \to \pi^*$	0.027	14.4	0.025	7.7	4.976	$\pi \to \pi^*$	0.068	3.9	0.065	4.1
1-phenylpyrrole	S_0			0.697	0.1	0.688	0.1			0.689	0.3	0.683	0.3
	S_1	5.073	$\pi \to \pi^*$	0.883	0.6	0.803	0.3	4.921	$\pi \to \pi^*$	1.100	0.5	1.002	0.5
	S_2	5.555	$\pi \to \pi^*$	2.381	0.1	2.186	0.2	5.309	$\pi \to \pi^*$	2.236	0.5	2.061	0.4

Continued on next page

Table 2.5 – continued from previous page

			cc-pVDZ					aug-cc-pVDZ				
				orbital-unrelaxed		orbital-relaxed				orbital-unrelaxed		orbital-relaxed	
	State	ω_{can}	Char.	$\lvert\mu^{can}\rvert$	$\frac{\lvert\delta\mu\rvert}{\lvert\mu^{can}\rvert}$	$\lvert\mu^{can}_{rel}\rvert$	$\frac{\lvert\delta\mu_{rel}\rvert}{\lvert\mu^{can}_{rel}\rvert}$	ω_{can}	Char.	$\lvert\mu^{can}\rvert$	$\frac{\lvert\delta\mu\rvert}{\lvert\mu^{can}\rvert}$	$\lvert\mu^{can}_{rel}\rvert$	$\frac{\lvert\delta\mu_{rel}\rvert}{\lvert\mu^{can}_{rel}\rvert}$
	T_1	4.181	$\pi \rightarrow \pi^*$	0.343	0.4	0.313	0.2	4.127	$\pi \rightarrow \pi^*$	0.416	0.9	0.378	0.2
	T_2	4.492	$\pi \rightarrow \pi^*$	1.490	2.1	1.426	1.7	4.391	$\pi \rightarrow \pi^*$	1.479	5.6	1.408	4.3
Propanamide	S_0			1.312	0.2	1.358	<0.1			1.373	<0.1	1.423	0.2
	S_1	5.926	$n \rightarrow \pi^*$	0.789	5.1	0.641	5.1	5.667	$n \rightarrow \pi^*$	1.026	9.4	0.861	10.9
	S_2	7.491	$n \rightarrow Ry$	2.646	1.7	2.336	1.7	5.755	$n \rightarrow Ry$	3.713	2.2	3.439	2.3
	T_1	5.555	$n \rightarrow \pi^*$	0.836	4.0	0.716	3.6	5.368	$n \rightarrow \pi^*$	1.033	5.9	0.901	6.5
	T_2	6.134	$\pi \rightarrow \pi^*$	0.794	2.4	0.756	1.9	5.719	$n \rightarrow Ry$	3.550	7.2	3.283	7.6
Tyrosine	S_0			1.320	0.4	1.357	0.3			1.409	0.5	1.456	0.3
	S_1	4.995	$\pi \rightarrow \pi^*$	0.222	2.6	0.183	2.0	4.834	$\pi \rightarrow \pi^*$	0.192	2.8	0.151	3.1
	S_2	5.824	$n \rightarrow Ry$	0.570	11.8	0.456	12.2	5.292	$\pi \rightarrow Ry$	4.157	13.6	4.118	13.4
	T_1	4.243	$\pi \rightarrow \pi^*$	0.101	9.7	0.080	7.0	4.176	$\pi \rightarrow \pi^*$	0.130	2.0	0.108	2.2
	T_2	4.621	$\pi \rightarrow \pi^*$	0.352	2.5	0.312	1.3	4.481	$\pi \rightarrow \pi^*$	0.304	1.1	0.267	1.1
trans-urocanic	S_0			1.904	0.2	1.935	0.1			2.030	0.3	2.077	0.1
acid	S_1	4.987	$n \rightarrow \pi^*$	2.310	0.4	1.990	0.8	4.863	$n \rightarrow \pi^*$	2.285	1.0	1.949	0.9
	S_2	5.207	$\pi \rightarrow \pi^*$	2.261	1.4	2.104	2.0	4.931	$\pi \rightarrow \pi^*$	2.202	2.3	2.061	2.7
	T_1	3.377	$\pi \rightarrow \pi^*$	0.385	0.6	0.340	0.7	3.308	$\pi \rightarrow \pi^*$	0.466	0.9	0.416	0.2
	T_2	5.050	$\pi \rightarrow \pi^*$	0.312	3.1	0.326	1.5	4.671	$n \rightarrow \pi^*$	2.232	1.1	1.955	0.8

As already discussed earlier by Köhn and Hättig, the difference between orbital-relaxed and unrelaxed canonical dipole moments is for excited states generally larger than for the ground state.[22] For the ground state a large part of the orbital relaxation is already provided by the singles $\mathbf{T_1}$ and the orbital relaxation effects in the test set are in the range of 1-3 %. Yet for excited states the orbital relaxation effects can clearly become larger than for the ground state. E.g., for the S_1 state of the Dipeptide molecule in the cc-pVDZ basis the norm of the unrelaxed dipole moment amounts to $|\mu| = 0.735$ a.u., which decreases to $|\mu_{rel}| = 0.587$ a.u. when orbital relaxation effects are taken into account.

The results for the singlet and triplet excited states are visualized in figure 2.1. The norms (in a.u.) of the orbital-unrelaxed (green) and orbital-relaxed (blue) canonical dipole moment difference vectors $|\mu^f|$ are shown together with the absolute deviations of the local method, i.e. the norms of the difference vector (canonical minus local) for the orbital-unrelaxed (yellow) and orbital-relaxed (orange) dipole moments. It can be seen, that there are no significant differences in accuracy between the orbital-relaxed and orbital-unrelaxed results. The new orbital relaxation code does not introduce additional deviations for the properties.

The relative deviation of the local ground state dipole moments is for both basis sets in most of the cases smaller than 1 %. For singlet and triplet excited states the relative deviations are substantially larger, but usually clearly below 10 %. For phenylalanine the relative deviations are larger, because the absolute values are tiny.

For the majority of the excited states calculated in the cc-pVDZ basis the deviations of the local from the canonical results are smaller when orbital relaxation is taken into account. In the aug-cc-pVDZ basis, on the other hand, the deviations appear to be slightly larger for the orbital-relaxed results.

For the S_1 ($n \rightarrow \pi^*$) state of the β-Dipeptide a particularly large deviation between the local and the canonical calculation was observed (more than 20 % for the cc-pVDZ basis; for the aug-cc-pVDZ basis even more). On the other hand, the structurally very similar Dipeptide did not exhibit such deviations. Plots of the density difference between excited and ground state, as shown in figure 2.2, do not reveal any significant discrepancies between the canonical and the local case. For comparison, the density difference of the S_2 ($n \rightarrow \pi^*$) state, for which canonical and local dipole moment vectors are in much better agreement, is also shown. Extending the pair lists or increasing the number of Laplace quadrature points in the β-Dipeptide calculation does not improve the results. On the other hand, the canonical result is retrieved to good accuracy with an

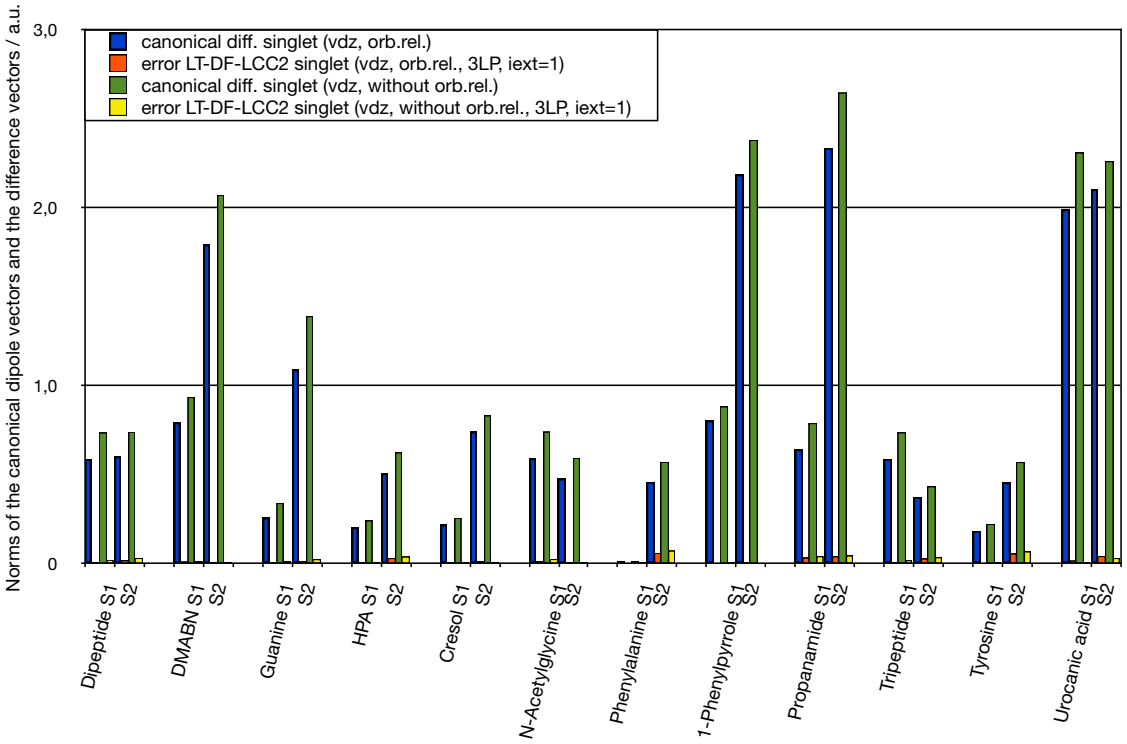

(a) Singlet excited states.

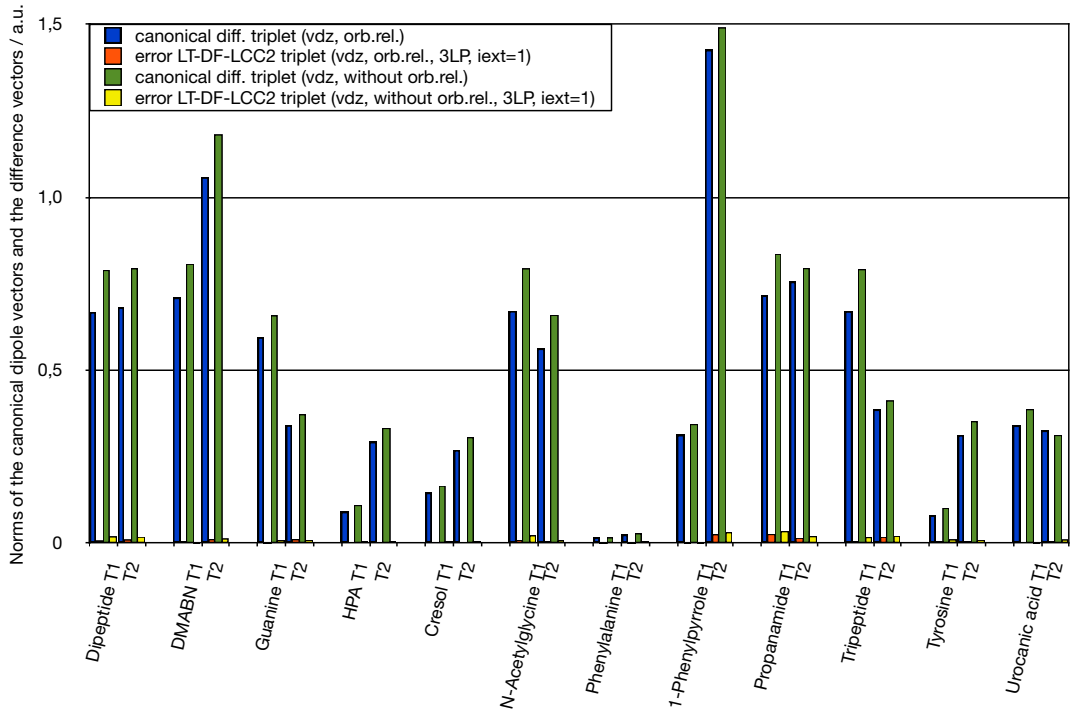

(b) Triplet excited states.

Figure 2.1: The norms (in a.u.) of the orbital-unrelaxed (green) and orbital-relaxed (blue) canonical dipole moment difference vectors $|\mu^f|$ are shown. Moreover, the norm of the difference vector (canonical minus local) is shown for the orbital-unrelaxed (yellow) and orbital-relaxed (orange) dipole moments.

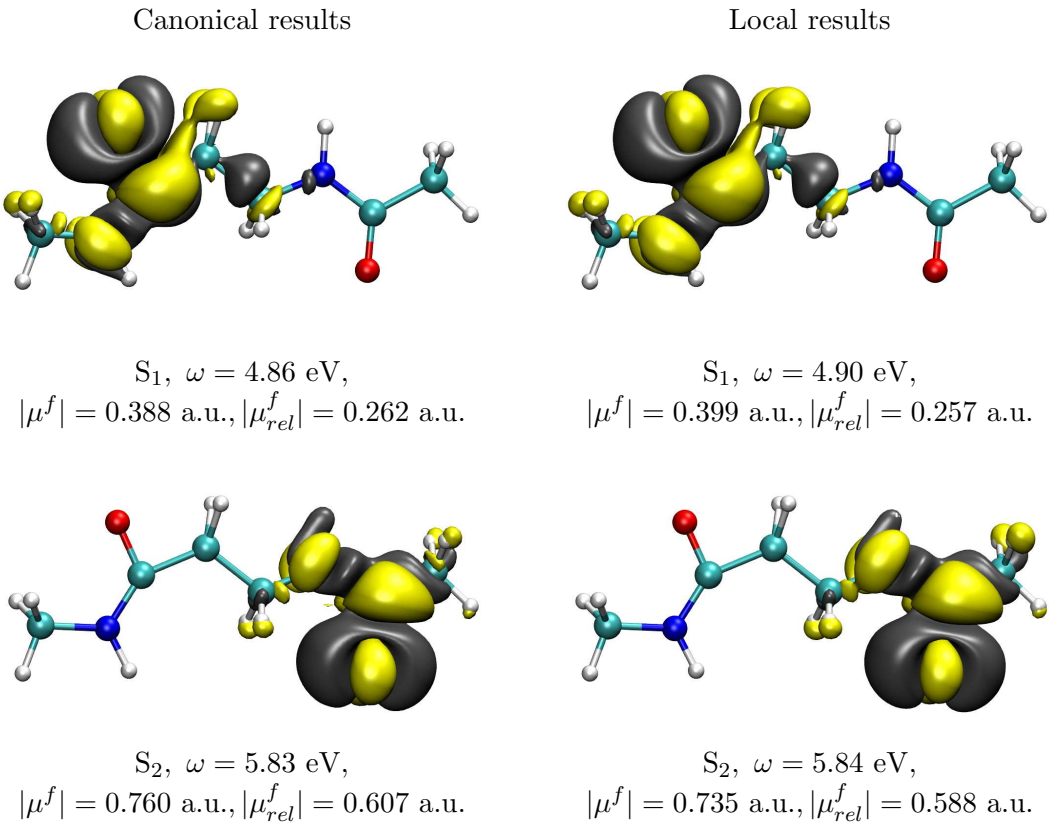

Figure 2.2: Canonical and local orbital-relaxed density differences between the two lowest singlet excited states and the ground state of the β-Dipeptide molecule (cc-pVDZ basis set). The yellow and grey iso-surfaces represent a value of $+0.002$ and -0.002, respectively. [from Ref. 29]

increased domain threshold. By augmenting the domains stepwise by individual atoms the discrepancy between canonical and local calculation can finally be traced to the two H-atoms on the C-atom in α position to the carbonyl group, where the excitation to the S_1 state is located. With the default threshold, these two H-atoms, which are in `cis`-postion to the O-atom of the carbonyl group, are not included in the domain related to the LMOs of the carbonyl group. Including these two atoms reduces the deviation from the canonical result for the dipole moment difference vector to 5.0 %, and to 6.8 % with, and without orbital relaxation. Neither for the S_2 state of β-Dipeptide, nor for the S_1 and S_2 states of Dipeptide such H-atoms in `cis`-postion to the O-atom of the carbonyl group relevant for the particular excitations do occur. Furthermore, omitting these H-atoms in the relevant domains of the S_1 state calculation, but employing a bigger basis set on the C and O atoms of the carbonyl group also leads to a deviation of less than 10 % between the local and respective canonical result. Based on these observations basis set superposition error (BSSE) effects in the canonical calculation may be a possible explanation for the discrepancy between the local and the canonical result. The local method might provide a more balanced description of, e.g., the dipoles of the S1 state vs. that of the S2 state.

2.6.5 Efficiency of the code

As an illustrative example for the efficiency and applicability of the new code results from calculations on the D21L6 (3-(5-(5-(4-(bis(4-(hexyloxy)phenyl)amino)phenyl)thiophene-2-yl)thiophene-2-yl)-2-cyanoacrylic acid) molecule are presented. This molecule, which is displayed in figure 2.3, is an organic sensitizer for solar-cell applications.[65]
The D21L6 molecule was already used as an example in earlier work[28,61] and comprises 98 atoms, 262 correlated electrons, and 948 basis functions in the cc-pVDZ AO basis. The norms of the orbital-unrelaxed and relaxed dipole moments of the ground state and the two lowest singlet and triplet excited states are given in table 2.6. For the D21L6 molecule substantial savings are achieved by the local method: the ratios of the lengths of truncated *vs.* full pair lists are about 30% for the ground state, and between 48 and 64% for the calculated excited states. The ratios local *vs.* canonical of the number of unique elements of the doubles vector is less than 1% for the ground state amplitudes, and between less than 6% (state T_1), and about 19% (states S_3 and S_4) for the excited state eigenvectors. The maximum ratio is quite large, because the lists and domains of the states S_3 and S_4 are unified during the Davidson process, for all other states the ratio lies below 10%.

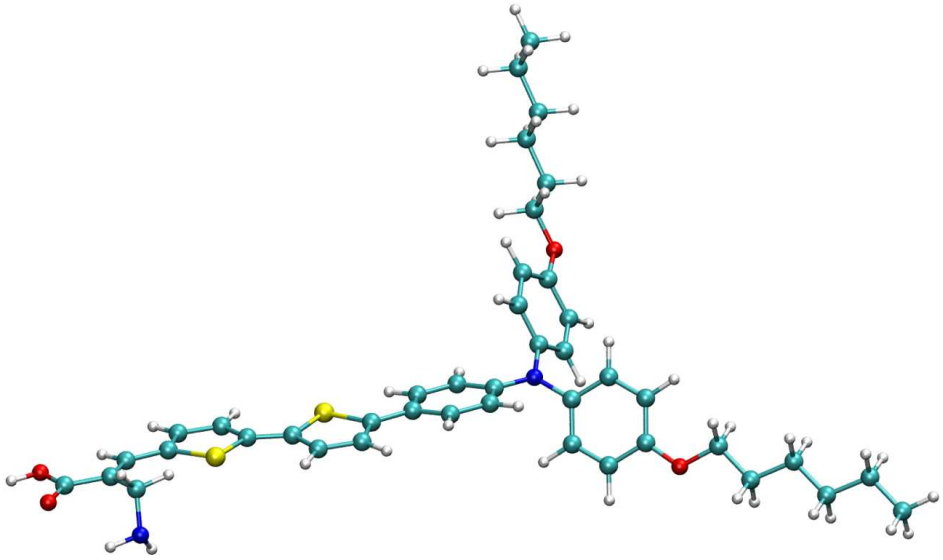

Figure 2.3: D21L6, an organic sensitizer for solar-cell applications.

The experimentally observed absorption maximum in the visible region at 2.71 eV with a high molar extinction coefficient, which was assigned to a $\pi \rightarrow \pi^*$ CT transition[65] corresponds to the $S_0 \rightarrow S_1$ transition, cf. the results in table 2.6. The calculated excitation energy of the S_1 state of 2.79 eV (2.74 eV in Ref. 61 due to the different convergence threshold, c.f. section 2.6.4) is in excellent agreement with the experimental value, probably due to fortuitous cancellation of errors given the relatively modest AO basis that has been used. Also the calculated transition strength of 1.35 a.u. is sizable and thus hints at a high extinction coefficient, as seen in the experiment. The CT character of the S_1 state is indicated by the large increase in the dipole moment along the direction of the residue carrying the thiophene groups, on going from the S_0 to the S_1 state (cf. table 2.6 and figure 2.4). The S_2 state also has some CT character, whereas the two lowest triplet states show no charge transfer,[28] as is also indicated by the much smaller dipole moment changes.

The calculation was run in parallel mode on seven AMD Opteron 6180 SE 2.50 GHz cores. The timings for finding the left and right eigenvectors of the Jacobian and for the calculation of orbital un-relaxed properties were discussed in detail earlier,[26,28] here the emphasis is on the additional time needed for the orbital relaxation. The detailed timings for the most time-consuming steps are listed in table 2.6.
Altogether for each excited state the calculation of orbital-relaxed properties (without calculation of the left eigenvector) takes about 10-11 hours, 40% of this time is needed

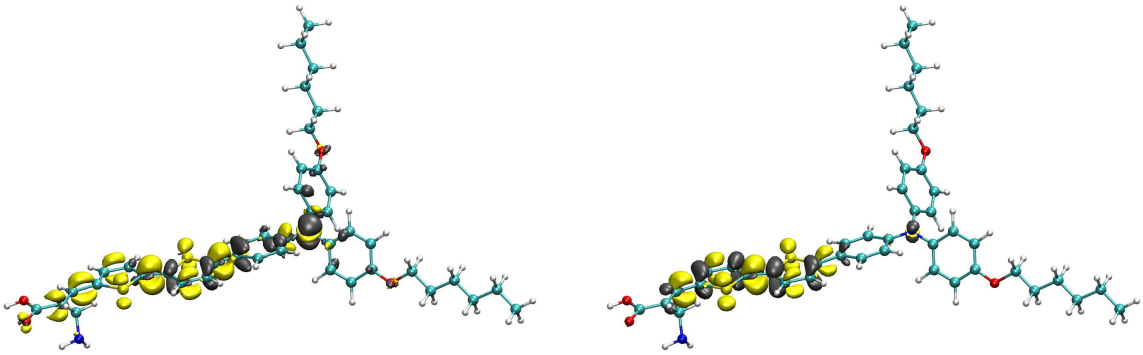

$S_1, \omega = 2.7$ eV,
$|\mu^f| = 7.15$ a.u., $|\mu^f_{rel}| = 7.06$ a.u.

$T_1, \omega = 2.0$ eV,
$|\mu^f| = 1.64$ a.u., $|\mu^f_{rel}| = 1.63$ a.u.

Figure 2.4: Orbital-relaxed density differences between the lowest singlet and triplet excited states and the ground state of the D21L6 molecule. The yellow and grey iso-surfaces represent a value of +0.002 and −0.002, respectively. [from Ref. 29]

for the parts, which also have to be calculated for unrelaxed properties, the rest is needed for the additional routines for the orbital relaxation. The largest fraction of the CPU and elapsed time is required for the calculation of the intermediates for the linear *z-vector equations*, i.e. $B_{\mu i}$, $B_{\mu r}$, $B_{r\mu}$ (eqs. (2.28), (2.29), (2.37) for the ground state, eqs. (2.57), (2.58), (2.59) for singlet excited states and eqs. (2.75), (2.76), (2.77) for triplet excited states). For the ground state this step takes about 1.5 hours, while for the excited states about 5-6 hours are needed per state (except for the states S_3 and S_4 with larger unified lists and domains, where about 8 hours are required). Solving the linear *z-vector equations*, on the other hand, takes less than half an hour per state (almost entirely for the Z-CPHF equations, while the Z-CPL equations take virtually no time). About 30% of the time for the intermediates $B_{\mu i}$, $B_{\mu r}$, $B_{r\mu}$ is needed for the terms including $g(d)$ (cf. eq. (2.30)) and about the same fraction for the calculation of $d^{f(LR)}$ (cf. eqs. (2.62) and (2.78)). The contractions with half transformed integrals require about 15% of the time. For the states S_3 and S_4 the calculation of $d^{f(LR)}$ is much more time-consuming, thus the time ratios differ.

Using the settings described above a calculation involving the four lowest singlet and triplet excited states on a system of this size can be performed within about four weeks. The effect of the local approximations is quite evident in this case, because the triplet states are calculated within about 1.5 weeks, while the singlet calculation takes about 2.5 weeks, mainly due to the larger unified lists and domains for the states S_3 and S_4.

Table 2.6: Results and timings for the few lowest singlet and triplet states of D21L6: Column $|\mu|$ shows the norms (in a.u.) of the orbital-unrelaxed local ground state dipole vector $|\mu^0|$ and for the individual excited states the corresponding difference vectors $|\mu^f|$ (with respect to $|\mu^0|$). Similarly, column $|\mu_{rel}|$ contains the related orbital-relaxed values. For the excited states also the local excitation energy ω and the character of the excitation are listed. The timings (in minutes) were obtained on 7 CPUs, AMD Opteron 6180 SE 2.50 GHz. [from Ref. 29]

State	ω	Char.	$\|\mu\|$	$\|\mu_{rel}\|$	$t(\tilde{\lambda})^a$	$t(\mathcal{D}^f)^b$	$t(d^{f(LR)})^c$	$t(B)^d$	$t(HT)^e$	$t(g)^f$	$t(z)^g$
S_0			2.670	2.711	227			113	9	73	31
S_1	2.787	CT	7.151	7.058	275	6	62	309	67	110	31
S_2	3.634	CT	5.142	4.918	269	5	59	302	66	106	32
S_3	3.735^h	$\pi \rightarrow \pi^*$	0.152^h	0.319^h	253	13	237	478	63	105	31
S_4	3.933^h	CT	5.535^h	5.332^h	276	13	237	492	72	108	31
T_1	2.041	$\pi \rightarrow \pi^*$	1.638	1.625	237	8	81	319	58	111	25
T_2	2.726	$\pi \rightarrow \pi^*$	2.307	2.260	235	8	88	322	58	108	30
T_3	3.438^h	$\pi \rightarrow \pi^*$	1.510^h	1.472^h	229	9	114	354	58	111	29
T_4	3.554^h	$\pi \rightarrow \pi^*$	0.293^h	0.313^h	241	10	135	372	64	106	31

a) Elapsed time for calculation of the Lagrange multipliers $\tilde{\lambda}$ for this state.
b) Elapsed time for calculation of the density $\mathcal{D}^f$ (cf. eqs. (2.80-2.84).
c) Elapsed time for calculation of $d^{f(LR)}$ (cf. eqs. (2.62) and (2.78)).
d) Elapsed time for calculation of $B_{\mu i}$, $B_{\mu r}$, $B_{r\mu}$ (cf. eqs. (2.37-2.29), eqs. (2.57-2.59), eqs. (2.75-2.77)).
e) Elapsed time for the terms of $B_{\mu i}$, $B_{\mu r}$, $B_{r\mu}$ including contractions with half transformed integrals.
f) Elapsed time for the terms of $B_{\mu i}$, $B_{\mu r}$, $B_{r\mu}$ including $g(d)$.
g) Elapsed time for solving the linear *z-vector equations*.
h) These results have to be taken with a grain of salt, because only a total of four states was calculated.

The largest amount of the time is needed for solving the left and right eigenvalue equation of the Jacobian, while the Lagrange multipliers and densities for the properties are calculated within about half a day per state.

2.7 Conclusions

Formalism, implementation, test calculations, and an application example for orbital-relaxed first-oder properties of excited states in the context of the local CC2 response method LT-DF-LCC2 were presented. The new method extends the scope for calculations of CC2 excited state properties including orbital relaxation to extended molecular systems. The utilization of Laplace transformation enables multistate calculations and

state-specific local approximations. It is demonstrated, that the deviations of the local results from the canonical reference are very similar for orbital-relaxed and orbital-unrelaxed properties. For our benchmark set of test molecules and excited states these deviations are usually clearly smaller than 10 %, though there are some exceptions, which were discussed.
As an illustrative application example the lowest four singlet and triplet excited states of the molecule D21L6, an organic sensitizer for solar-cell applications, were calculated. The lowest excited singlet state corresponds to a CT transition with a large change in the dipole moment and sizable transition strength, in agreement with the experiment, while the lowest triplet states show no CT character. The calculation of the singlet states of D21L6 is slower than the triplet calculation, because the pair lists and domains are unified for the states S_3 and S_4. Thus, this example clearly demonstrates the effect of the local approximations. For systems of this size, i.e. about hundred atoms, the calculation of excitation energies, orbital-unrelaxed and orbital-relaxed dipole moments of the four lowest singlet and triplet excited states can be performed within about four weeks on a standard workstation.

The next step is the implementation of analytic gradients with respect to nuclear displacements for excited states in the framework of the local CC2 response method LT-DF-LCC2. The orbital-relaxed Lagrangians, which were derived in this chapter, will be the starting points for that.

Chapter 3

Analytic energy gradients

The content of this chapter has been submitted for publication (Ref 66), and parts of the following text are identical to the submitted manuscript. The manuscript was revised concerning the context given in this thesis, i.e. basic principles, which were discussed in the preceding chapters, are shortened or omitted, while some aspects are discussed more detailed.
The application example in section 3.6.2 was evaluated in collaboration with Thomas Merz.

3.1 Introduction

Equilibrium and transition structures of molecules, which are stationary points on potential energy hypersurfaces (PES), are of great interest in chemistry and physics. Knowledge about the PES of the electronically ground and excited states is the basis for understanding or predicting photophysical processes. For locating stationary points on the PES the gradient of the energy with respect to nuclear displacements has to be calculated.
Gradients can be calculated numerically or analytically, but numerical calculations are only applicable to small molecules. The pioneering work of Pulay for SCF calculations[67–69] was followed by the development of analytic ground state gradients for a variety of *ab initio* methods, amongst others configuration interaction (CI),[70,71] multiconfigurational SCF (MCSCF),[72,73] Møller-Plesset (MP) perturbation theory[74,75] and Coupled Cluster theory (CC).[76] Also gradients for local ground state methods have been presented, e.g. for MP2[59,77] and quadratic CI.[78] Ground state methods are well-established nowadays, while theoretical studies of electronically excited states at a reliable level of

ab initio theory are still very challenging.
As discussed in section 1.2 excited states can be treated based on the CC ansatz using the framework provided by linear response theory, i.e. time-dependent CC (TD-CC),[9,37–39] or using the equation-of-motion approach (EOM-CC).[45–49] Analytic energy gradients for excited states have been developed in the context of both, EOM-CC[79–81] and TD-CC.[38,82] They compete against analytic gradients within the time-dependent density functional theory (TD-DFT),[83–85] which are computationally cheaper, but often unreliable. If charge transfer states, Rydberg states or excitations of extended π systems are involved, TD-DFT methods often fail qualitatively.[12–14]
For the CC2 model analytic energy gradients have been developed for the ground state[86–88] and for excited states.[22] The work by Köhn and Hättig employs the density fitting approximation in order to reduce the computational cost for ground and excited state calculations.[22,88] For a further reduction of the computational cost local correlation methods have been proposed and excitation energies, transition moments and first-order properties with and without explicit orbital relaxation were implemented into the MOLPRO[58] program package earlier.[24–29] This code enables calculations for extended molecular systems consisting of hundred or more atoms. The work on orbital-relaxation is now continued and analytic energy gradients with respect to nuclear displacements are presented for the ground state and excited states based on the local CC2 methods with and without the use of Laplace transform (DF-LCC2 and LT-DF-LCC2, cf. section 1.2.3).
Contrary to LT-DF-LCC2, where an approximated energy Lagrangian is used, the DF-LCC2 method is based on the proper energy Lagrangian.[29,54] For first-order properties it has been shown in chapter 2 that the use of the approximated Lagrangian in the LT-DF-LCC2 method does not cause any problems. For geometry optimizations the effects of the approximation are expected to be larger, thus this aspect will be explored explicitly.

This chapter is organized as follows: First the working equations for the implementation of the gradients are derived for the ground state and for singlet and triplet excited states in the sections 3.2, 3.3, and 3.4, respectively. In section 3.5 a hybrid method for the investigation of the effect of the approximate Lagrangians in the LT-DF-LCC2 method is introduced. The accuracy of the local approximations is explored in section 3.6, and as an illustrative application example, excited state geometry optimizations of two molecules consisting of more than fifty atoms are carried out, which are of relevance

for a photocatalytic decarboxylation reaction of present interest. Finally, section 3.7 summarizes the chapter.

3.2 The electronic ground state

As in the preceding chapter the formalism is derived for an orthonormal basis of localized occupied and canonical virtual molecular orbitals (MO). The transformation to the basis of nonorthogonal PAOs is performed *a posteriori*.

3.2.1 The Lagrangian

The gradient for the local CC2 ground state energy, i.e. HF plus correlation energy, contains terms from the underlying HF calculation, which are obtained starting from the Lagrangian for the HF energy E_0^{HF},

$$\mathcal{L}_0^{\mathrm{HF}} = E_0^{\mathrm{HF}} - 2f_{ij}\left((\mathbf{C}^\dagger \mathbf{S}^{\mathrm{AO}}\mathbf{C})_{ij} - \delta_{ij}\right) \ . \tag{3.1}$$

The HF energy is calculated as

$$E_0^{\mathrm{HF}} = 2h_{ii} + 2(ii|jj) - (ij|ji) \ . \tag{3.2}$$

The second term of the Lagrangian contains the orthonormality condition for the coefficients ($(\mathbf{C}^\dagger \mathbf{S}^{\mathrm{AO}}\mathbf{C})_{ij} = \delta_{ij}$) with the Fock matrix elements f_{ij} as corresponding Lagrange multipliers. The terms resulting from the derivative of $\mathcal{L}_0^{\mathrm{HF}}$ with respect to nuclear displacements are added a posteriori to the CC2 correlation contributions to obtain the gradient for the entire local CC2 ground state energy.

As already discussed in the context of orbital-relaxed properties (cf. section 2.2.1) the local orbital-relaxed CC2 Lagrangian for the ground state correlation energy E_0^{CC2} is defined as

$$\mathcal{L}_0^{\mathrm{CC2}} \ = \ E_0^{\mathrm{CC2}} + \tilde{\lambda}_{\mu_i}^0 \Omega_{\mu_i} + z_{ij}^{loc,0} r_{ij} + z_{ai}^0 f_{ai} + x_{pq}^0 \left[\mathbf{C}^\dagger \mathbf{S}^{\mathrm{AO}}\mathbf{C} - \mathbf{1}\right]_{pq} \ . \tag{3.3}$$

It includes the conditions for the amplitudes ($\Omega_{\mu_i} = 0$), the localization conditions ($r_{ij} = 0$), the Brillouin condition ($f_{ai} = 0$), and the orthonormality condition ($\mathbf{C}^\dagger \mathbf{S}^{\mathrm{AO}}\mathbf{C} = \mathbf{1}$). The related multipliers are $\tilde{\lambda}_{\mu_i}^0$, $z_{ij}^{loc,0}$, z_{ai}^0, and x_{pq}^0, respectively. By choosing the Pipek-

Mezey localization[32] the corresponding criteria r_{ij} are defined according to eq. (2.11). The Lagrangian is required to be stationary with respect to all parameters. Differentiation of $\mathcal{L}_0^{\mathrm{CC2}}$ with respect to the CC amplitudes $\mathbf{t}$ yields the equations for the multipliers $\tilde{\lambda}^{\mathbf{0}}$, cf. eq. (2.6). Differentiation of $\mathcal{L}_0^{\mathrm{CC2}}$ with respect to the orbital variations O_{pq} yields the orbital *z-vector equations*, from which the multipliers $\mathbf{z^0}$, $\mathbf{z^{loc,0}}$, and $\mathbf{x^0}$ are obtained as discussed in detail in section 2.2.2. The derivative of the Lagrangian with respect to the orbital variations was partitioned into four contributions,

$$\left(\frac{\partial \mathcal{L}_0^{\mathrm{CC2}}}{\partial O_{pq}}\right)_{\mathbf{V}_0=0} = [\mathbf{B^0} + \tilde{\mathbf{B}}(\mathbf{z^0}) + \mathbf{b}(\mathbf{z^{loc,0}}) + 2\mathbf{x^0}]_{pq} \ , \tag{3.4}$$

with

$$\begin{aligned}
[\mathbf{B^0}]_{pq} &= \left(\frac{\partial}{\partial O_{pq}}(E_0^{\mathrm{CC2}} + \tilde{\lambda}^0_{\mu_i}\Omega_{\mu_i})\right)_{\mathbf{V}_0=0} \ , \\
[\tilde{\mathbf{B}}(\mathbf{z^0})]_{pq} &= \left(\frac{\partial}{\partial O_{pq}} z^0_{ai} f_{ai}\right)_{\mathbf{V}_0=0} \ , \\
[\mathbf{b}(\mathbf{z^{loc,0}})]_{pi} &= \left(\frac{\partial}{\partial O_{pi}} z^{loc,0}_{kl} r_{kl}\right)_{\mathbf{V}_0=0} \ .
\end{aligned} \tag{3.5}$$

These quantities will also occur in the final gradient equations. They are calculated according to the working equations given in section 2.2.2, i.e. eqs. (2.17), (2.28), (2.29) and (2.37).

3.2.2 Derivation of the gradient

The full LCC2 ground state gradient $\mathcal{L}_0^q$ is obtained by differentiating the Lagrangian $\mathcal{L}_0$, containing both the HF and CC2 contributions, with respect to the nuclear displacements q,

$$\mathcal{L}_0^q = \left(\frac{\partial \mathcal{L}_0}{\partial q}\right)_{q=0} = \left(\frac{\partial (\mathcal{L}_0^{\mathrm{HF}} + \mathcal{L}_0^{\mathrm{CC2}})}{\partial q}\right)_{q=0} \ . \tag{3.6}$$

Employing the definitions of the undressed and dressed fock matrices,

$$\begin{aligned}
f_{\mu\nu} &= h_{\mu\nu} + 2L_{\rho k}L_{\sigma k}[(\mu\nu|\rho\sigma) - 0.5(\mu\sigma|\rho\nu)] \ , \\
\hat{f}_{\mu\nu} &= h_{\mu\nu} + 2\Lambda^p_{\rho k}\Lambda^h_{\sigma k}[(\mu\nu|\rho\sigma) - 0.5(\mu\sigma|\rho\nu)] \ ,
\end{aligned} \tag{3.7}$$

the gradient $\mathcal{L}_0^q$ can be written in terms of the AO derivative integrals $h_{\mu\nu}^q$, $(\mu\nu|\rho\sigma)^q$ and $S_{\mu\nu}^q$. Due to the density fitting (DF) approximation the derivative four-index integrals $(\mu\nu|\rho\sigma)^q$ are decomposed according to

$$(\mu\nu|\rho\sigma)^q = (\mu\nu|P)^q c_{\rho\sigma}^P + c_{\mu\nu}^P (P|\rho\sigma)^q - c_{\mu\nu}^P J_{PQ}^q c_{\rho\sigma}^Q \ , \tag{3.8}$$

with the derivatives of the three-index integrals $(\mu\nu|P)$ and of the Coulomb matrix of the auxiliary fitting functions J_{PQ}.
The derivation of the working equation for the gradient is demonstrated for the exemplary term $\tilde{\lambda}_r^{i,0}\hat{f}_{ri}$, which originates from the general expression $\tilde{\lambda}_{\mu_1}^0\langle\tilde{\mu}_1|\hat{F}|0\rangle$ in the amplitude condition, and was also used as an example in section 2.2.3. Using eq. (3.7) for $\hat{f}_{ri}$ the derivative of this term with respect to a nuclear displacement q is

$$\begin{aligned}\left(\frac{\partial\tilde{\lambda}_r^i\hat{f}_{ri}}{\partial q}\right)_{q=0} =& \tilde{\lambda}_r^i\Lambda_{\mu r}^p\Lambda_{\nu i}^h\left\{h_{\mu\nu}^q + 2\Lambda_{\rho k}^p\Lambda_{\sigma k}^h\left[(\mu\nu|P)^q c_{\rho\sigma}^P + c_{\mu\nu}^P(P|\rho\sigma)^q - J_{PQ}^q c_{\mu\nu}^P c_{\rho\sigma}^Q\right.\right. \\ & \left.\left. -0.5\left((\mu\sigma|P)^q c_{\rho\nu}^P + c_{\mu\sigma}^P(P|\rho\nu)^q - J_{PQ}^q c_{\mu\sigma}^P c_{\rho\nu}^Q\right)\right]\right\} \ . \end{aligned} \tag{3.9}$$

Sorting all terms resulting from the derivative of the Lagrangian $\mathcal{L}_0$ with respect to the nuclear displacement according to the derivative AO integrals yields the working equation for the gradient in LMO/PAO basis,

$$\begin{aligned}\mathcal{L}_0^q \;=\;& h_{\mu\nu}^q\mathcal{D}_{\mu\nu}^0 + S_{\mu\nu}^q\left\{\left(\frac{\partial r_{ij}}{\partial S_{\mu\nu}^{\mathrm{AO}}}\right)z_{ij}^{loc} + X_{\mu\nu}^0\right\} \\ & +(\mu\nu|P)^q\left\{(\mathcal{D}_{\mu\nu}^0 - \frac{1}{2}d_{\mu\nu}^{\mathrm{HF}})^{\mathrm{HF}}b^P + {}^{\mathcal{D}^0}b^P d_{\mu\nu}^{\mathrm{HF}} - 2(\mathcal{D}_{\mu\rho}^0 - \frac{1}{2}d_{\mu\rho}^{\mathrm{HF}})c_{i\rho}^P L_{\nu i}\right. \\ & \quad +L_{\mu i}P_{\nu r}[2V_{ir}^P + \bar{V}_{ir}^P + 4b^P t_r^i + 2b^P X(\lambda^0 T)_{ir} + 2^{\lambda^0}b^P t_r^i + 2^{X(\lambda^0 T)}b^P t_r^i \\ & \quad\quad -2\bar{c}_{ji}^P t_r^j - \bar{c}_{ji}^P X(\lambda^0 T)_{jr} - {}^{X(\lambda^0 T)}\bar{c}_{ki}^P t_r^k] \\ & \quad + \Lambda_{\mu r}^p\Lambda_{\nu i}^h[2\hat{\bar{V}}_{ir}^P + 2b^P\tilde{\lambda}_r^{i,0}] + L_{\mu i}\Lambda_{\nu j}^h[-\tilde{\lambda}_r^{j,0}S_{rr'}V_{ir'}^P - {}^{\lambda^0 t}\bar{c}_{ji}^P] \\ & \quad \left.+\Lambda_{\mu r}^p P_{\nu s}[\tilde{\lambda}_r^{i,0}V_{is}^P - \hat{c}_{kj}^P t_s^k\tilde{\lambda}_r^{j,0}]\right\} \\ & -J_{PQ}^q\left\{c_{ir}^P[V_{ir}^Q + \bar{V}_{ir}^Q + 2b^Q t_r^i + 2b^Q X(\lambda^0 T)_{ir} + 2^{\lambda^0}b^Q t_r^i - t_r^j\bar{c}_{ji}^Q - {}^{X(\lambda^0 T)}\bar{c}_{ji}^Q t_r^j]\right. \\ & \quad \left.+\hat{c}_{ri}^P\hat{\bar{V}}_{ir}^Q - \hat{c}_{ji}^P\,{}^{\lambda^0 t}\bar{c}_{ij}^Q + {}^{\mathcal{D}^0}b^P\,{}^{\mathrm{HF}}b^Q - (\mathcal{D}_{\mu\nu}^0 - \frac{1}{2}d_{\mu\nu}^{\mathrm{HF}})c_{\mu i}^P c_{i\nu}^Q\right\} \ , \end{aligned} \tag{3.10}$$

with the densitiy $\mathcal{D}^{\mathbf{0}}$ as defined in eqs. (2.80) and (2.81) in section 2.5, and the HF

density $d^{\mathrm{HF}}_{\mu\nu} = 2L_{\mu i}L_{\nu i}$. Other intermediates are

$$\begin{aligned}
V^Q_{ir} &= \tilde{t}^{ij}_{rs} c^{js}_Q \ , & \hat{\bar{V}}^Q_{ir} &= \tilde{\lambda}^{ij,0}_{rs} \hat{c}^{sj}_Q \ , \\
\bar{V}^Q_{ir} &= \tilde{t}^{ij}_{rs} (\tilde{\lambda}^{j,0}_t \hat{c}^P_{ts} - S_{ss'} \tilde{\lambda}^{k,0}_{s'} \hat{c}^P_{jk}) \ , & X(\lambda^0 T)_{ir} &= \tilde{\lambda}^{j,0}_s S_{ss'} \tilde{t}^{ji}_{s'r} \ , \\
{}^{\mathrm{HF}}b^Q &= c^Q_{\mu\nu} d^{\mathrm{HF}}_{\mu\nu} \ , & {}^{\mathcal{D}^0}b^Q &= c^Q_{\mu\nu} (\mathcal{D}^0_{\mu\nu} - \frac{1}{2} d^{\mathrm{HF}}_{\mu\nu}) \ , \\
b^Q &= c^Q_{ir} t^i_r \ , & \bar{c}^Q_{ij} &= c^Q_{ir} t^j_r \ , \\
{}^{\lambda^0}b^Q &= \hat{c}^Q_{ri} \tilde{\lambda}^{i,0}_r \ , & {}^{\lambda^0}\bar{c}^Q_{ij} &= \hat{c}^Q_{rj} \tilde{\lambda}^{i,0}_r \ , \\
{}^{X(\lambda^0 T)}b^Q &= c^Q_{ir} X(\lambda^0 T)_{ir} \ , & {}^{X(\lambda^0 T)}\bar{c}^Q_{ij} &= c^Q_{ir} X(\lambda^0 T)_{jr} \ , \\
{}^{\lambda^0 T}\bar{c}^Q_{ij} &= \tilde{\lambda}^{i,0}_s \hat{c}^Q_{sr} t^j_r \ . & & \qquad (3.11)
\end{aligned}$$

The terms, which are contracted with the derivative AO overlap integrals $S^q_{\mu\nu}$, are discussed in detail in the following paragraph.

Derivatives with respect to the AO overlap matrix

The derivative AO overlap integrals $S^q_{\mu\nu}$ are for the gradient $\mathcal{L}^q_0$ contracted with the derivatives of the localization criterion r_{ij}, which were defined in Ref. 59 as

$$\left(\frac{\partial r_{ij}}{\partial S^{\mathrm{AO}}_{\mu\nu}}\right) = (1 - \mathcal{P}_{ij}) \sum_A \left[2L_{\mu i}L_{\nu i}S^A_{ij} + S^A_{ii}(L_{\mu i}L_{\nu j} + L_{\mu j}L_{\nu i})\right] \delta_{\mu\in A} \ , \qquad (3.12)$$

including S^A_{ij} as defined in eq. (2.12), and $\delta_{\mu\in A}$ which restricts the index μ to AOs on atom A. Moreover, the derivative AO overlap integrals are contracted with the intermediate quantity $\mathbf{X^0}$. $\mathbf{X^0}$ comprises the terms originating from the orthonormality condition in $\mathcal{L}^{\mathrm{HF}}_0$, from the orthonormality condition in $\mathcal{L}^{\mathrm{CC2}}_0$ and from the dependency of the transformation matrix $\mathbf{Q} = \mathbf{C}^{\mathbf{v}\dagger}\mathbf{S}^{\mathbf{AO}}$ on the AO overlap matrix. The terms of the latter are in the following collected in $\mathbf{X}^{\mathbf{Q,0}}$,

$$\begin{aligned}
X^{Q,0}_{\mu\nu} &= \left(\frac{\partial \mathcal{L}_0}{\partial \tilde{\lambda}^{ij,0}_{ab}}\right)\left(\frac{\partial \tilde{\lambda}^{ij,0}_{ab}}{\partial S^{\mathrm{AO}}_{\mu\nu}}\right) + \left(\frac{\partial \mathcal{L}_0}{\partial t^{ij}_{ab}}\right)\left(\frac{\partial t^{ij}_{ab}}{\partial S^{\mathrm{AO}}_{\mu\nu}}\right) \ , \\
X^0_{\mu\nu} &= C_{\mu p}(-2\epsilon_i \delta_{ij} + x^0_{pq} + X^{Q,0}_{pq}) C^\dagger_{q\nu} \ . \qquad (3.13)
\end{aligned}$$

$C^\dagger_{q\nu}$ is the short-hand notation for $[\mathbf{C}^\dagger]_{q\nu}$. As explained in section 2.2.2 only the derivatives of the Lagrangian with respect to the doubles amplitudes and multipliers have to be calculated. Contrary to the singles, which remain completely unrestricted, the doubles residuals vanish only within the pair domains in local basis, but not in canonical basis.

The working equations for $\mathbf{X^{Q,0}}$ are obtained by applying first the relation $Q_{ar} = C^{v\dagger}_{a\mu} S^{\mathrm{AO}}_{\mu\nu} \delta_{\nu r}$, as shown in the following for the first term (cf. derivation of the LMP2 gradient, Appendix C in Ref. 59),

$$\begin{aligned}
\left(\frac{\partial \mathcal{L}_0}{\partial \tilde{\lambda}^{ij,0}_{ab}}\right)\left(\frac{\partial \tilde{\lambda}^{ij,0}_{ab}}{\partial S^{\mathrm{AO}}_{\mu\nu}}\right) &= \left(\frac{\partial \mathcal{L}_0}{\partial \tilde{\lambda}^{ij,0}_{ab}}\right)\left(\frac{\partial (Q_{ar}\tilde{\lambda}^{ij,0}_{rs} Q^{\dagger}_{sb})}{\partial S^{\mathrm{AO}}_{\mu\nu}}\right) \\
&= \left(\frac{\partial \mathcal{L}_0}{\partial \tilde{\lambda}^{ij,0}_{ab}}\right)\left(C^{v\dagger}_{a\mu}\delta_{\nu r}\tilde{\lambda}^{ij,0}_{rs} Q^{\dagger}_{sb} + Q_{ar}\tilde{\lambda}^{ij,0}_{rs}\delta_{s\mu} C^{v}_{\nu b}\right) \\
&= C^{v}_{\mu a}\left(\frac{\partial \mathcal{L}_0}{\partial \tilde{\lambda}^{ij,0}_{ab}}\right) Q_{bs}\tilde{\lambda}^{ji,0}_{s\nu} + \tilde{\lambda}^{ji,0}_{\mu r} Q^{\dagger}_{ra}\left(\frac{\partial \mathcal{L}_0}{\partial \tilde{\lambda}^{ij,0}_{ab}}\right) C^{v\dagger}_{b\nu} \,, \qquad (3.14)
\end{aligned}$$

and then the relation $\mathbf{1} = \mathbf{L}\mathbf{L}^{\dagger}\mathbf{S}^{\mathrm{AO}} + \mathbf{C^v}\mathbf{C^{v\dagger}}\mathbf{S}^{\mathrm{AO}}$, yielding

$$\begin{aligned}
&C^{v}_{\mu a}\left(\frac{\partial \mathcal{L}_0}{\partial \tilde{\lambda}^{ij,0}_{ab}}\right) Q_{bs}\tilde{\lambda}^{ji,0}_{sr}\delta_{r\rho} S^{\mathrm{AO}}_{\rho\sigma}(L_{\sigma k}L^{\dagger}_{k\nu} + C^{v}_{\sigma c}C^{v\dagger}_{c\nu}) \\
&\quad + (L_{\mu k}L^{\dagger}_{k\sigma} + C^{v}_{\mu c}C^{v\dagger}_{c\sigma}) S^{\mathrm{AO}}_{\sigma\rho}\delta_{\rho s}\tilde{\lambda}^{ji,0}_{sr} Q^{\dagger}_{ra}\left(\frac{\partial \mathcal{L}_0}{\partial \tilde{\lambda}^{ij,0}_{ab}}\right) C^{v\dagger}_{b\nu} \\
&= C^{v}_{\mu a}\left(\frac{\partial \mathcal{L}_0}{\partial \tilde{\lambda}^{ij,0}_{ab}}\right) Q_{bs}\tilde{\lambda}^{ji,0}_{sr}\delta_{r\rho} S^{\mathrm{AO}}_{\rho\sigma} L_{\sigma k}L^{\dagger}_{k\nu} + C^{v}_{\mu a}\left(\frac{\partial \mathcal{L}_0}{\partial \tilde{\lambda}^{ij,0}_{ab}}\right)\tilde{\lambda}^{ji,0}_{bc} C^{v\dagger}_{c\nu} \\
&\quad + L_{\mu k}L^{\dagger}_{k\sigma} S^{\mathrm{AO}}_{\sigma\rho}\delta_{\rho s}\tilde{\lambda}^{ji,0}_{sr} Q^{\dagger}_{ra}\left(\frac{\partial \mathcal{L}_0}{\partial \tilde{\lambda}^{ij,0}_{ab}}\right) C^{v\dagger}_{b\nu} + C^{v}_{\mu c}\tilde{\lambda}^{ji,0}_{ca}\left(\frac{\partial \mathcal{L}_0}{\partial \tilde{\lambda}^{ij,0}_{ab}}\right) C^{v\dagger}_{b\nu} \,. \qquad (3.15)
\end{aligned}$$

Analogous terms are obtained for the derivative with respect to the amplitudes. Eq. (2.34) implicitly defines the relation

$$t^{ji}_{rt} Q^{\dagger}_{tb}\left(\frac{\partial (E^{\mathrm{CC2}}_0 + \tilde{\lambda}^0_{\mu_i}\Omega_{\mu_i})}{\partial t^{ij}_{ab}}\right) + \tilde{\lambda}^{ji,0}_{rt} Q^{\dagger}_{tb}\left(\frac{\partial (E^{\mathrm{CC2}}_0 + \tilde{\lambda}^0_{\mu_i}\Omega_{\mu_i})}{\partial \tilde{\lambda}^{ij,0}_{ab}}\right) = \frac{1}{2} B^0_{r\nu} C^{v}_{\nu a} \,, \qquad (3.16)$$

with the intermediate $B^0_{r\nu}$, which is already known from the calculation of the Lagrange multipliers. The derivatives of $(E^{\mathrm{CC2}}_0 + \tilde{\lambda}^0_{\mu_i}\Omega_{\mu_i})$ with respect to the amplitudes t^{ij}_{ab} and multipliers $\tilde{\lambda}^{ij,0}_{ab}$ are equivalent to the derivatives of $\mathcal{L}_0$, because in $\mathcal{L}_0$ only these terms depend on t^{ij}_{ab} and $\tilde{\lambda}^{ij,0}_{ab}$. Thus eq. (3.16) can be used together with the result of eq.

(3.15) to express $X^{Q,0}_{\mu\nu}$ as

$$\begin{aligned}
X^{Q,0}_{\mu\nu} &= C^{v}_{\mu a}\left[\left(\frac{\partial\mathcal{L}_0}{\partial\tilde{\lambda}^{ij,0}_{ab}}\right)Q_{bs}\tilde{\lambda}^{ji,0}_{sr}+\left(\frac{\partial\mathcal{L}_0}{\partial t^{ij}_{ab}}\right)Q_{bs}t^{ji}_{sr}\right]\delta_{r\rho}S^{\mathrm{AO}}_{\rho\sigma}L_{\sigma k}L^{\dagger}_{k\nu}\\
&\quad+C^{v}_{\mu a}\left[\left(\frac{\partial\mathcal{L}_0}{\partial\tilde{\lambda}^{ij,0}_{ab}}\right)Q_{br}\tilde{\lambda}^{ji,0}_{rs}+\left(\frac{\partial\mathcal{L}_0}{\partial t^{ij}_{ab}}\right)Q_{br}t^{ji}_{rs}\right]Q^{\dagger}_{sc}C^{v\dagger}_{c\nu}\\
&\quad+L_{\mu k}L^{\dagger}_{k\sigma}S^{\mathrm{AO}}_{\sigma\rho}\delta_{\rho s}\left[\tilde{\lambda}^{ji,0}_{sr}Q^{\dagger}_{ra}\left(\frac{\partial\mathcal{L}_0}{\partial\tilde{\lambda}^{ij,0}_{ab}}\right)+t^{ji}_{sr}Q^{\dagger}_{ra}\left(\frac{\partial\mathcal{L}_0}{\partial t^{ij}_{ab}}\right)\right]C^{v\dagger}_{b\nu}\\
&\quad+C^{v}_{\mu c}Q_{cr}\left[\tilde{\lambda}^{ji,0}_{rs}Q^{\dagger}_{sa}\left(\frac{\partial\mathcal{L}_0}{\partial\tilde{\lambda}^{ij,0}_{ab}}\right)+t^{ji}_{rs}Q^{\dagger}_{sa}\left(\frac{\partial\mathcal{L}_0}{\partial t^{ij}_{ab}}\right)\right]C^{v\dagger}_{b\nu}\\
&= \frac{1}{2}\Big\{C^{v}_{\mu a}[C^{v\dagger}_{a\rho}(B^{0}_{r\rho})^{\dagger}\delta_{r\sigma}S^{\mathrm{AO}}_{\sigma\kappa}L_{\kappa i}]L^{\dagger}_{i\nu}+C^{v}_{\mu a}[C^{v\dagger}_{a\sigma}(B^{0}_{r\sigma})^{\dagger}Q^{\dagger}_{rb}]C^{v\dagger}_{b\nu}\\
&\qquad+L_{\mu i}[L^{\dagger}_{i\sigma}S^{\mathrm{AO}}_{\sigma\rho}\delta_{\rho r}B^{0}_{r\kappa}C^{v}_{\kappa a}]C^{v\dagger}_{a\nu}+C^{v}_{\mu a}[Q_{ar}B^{0}_{r\sigma}C^{v}_{\sigma b}]C^{v\dagger}_{b\nu}\Big\}\\
&= \frac{1}{2}\Big\{C^{v}_{\mu a}X^{Q,0}_{ai}L^{\dagger}_{i\nu}+C^{v}_{\mu a}X^{Q,0}_{ab}C^{v\dagger}_{b\nu}+L_{\mu i}X^{Q,0}_{ia}C^{v\dagger}_{a\nu}\Big\}\ . \qquad (3.17)
\end{aligned}$$

Since $\mathbf{X}^{\mathbf{0}}_{\mathrm{AO}}$ is traced with the symmetric derivative overlap matrix in the expression for the gradient, cf. eq. (3.10), only the symmetric part of $\mathbf{X}^{\mathbf{0}}_{\mathrm{AO}}$ can contribute. Thus for the mixed external and internal part only the upper triangular off-diagonal blocks, i.e. the external-internal part, needs to be considered (with a factor of two) while the internal-external part can be dropped (see also appendix C in Ref. 59). The multipliers x^0_{pq} are already symmetrized by definition, cf. eq. (2.21),

$$x^{0}_{pq}=-\frac{1}{4}(1+\mathcal{P}_{pq})[\mathbf{B^0}+\tilde{\mathbf{B}}(\mathbf{z^0})+\mathbf{b}(\mathbf{z^{loc,0}})]_{pq}\ , \qquad (3.18)$$

thus one obtains

$$\begin{aligned}
X^{0}_{ai} &= x^{0}_{ai}+X^{Q,0}_{ai}+(x^{0}_{ia}+X^{Q,0}_{ia})^{\dagger}=2x^{0}_{ai}+X^{Q,0}_{ai}+(X^{Q,0}_{ia})^{\dagger}\ ,\\
X^{0}_{ia} &= 0\ . \qquad (3.19)
\end{aligned}$$

Moreover, it can be seen in eq. (3.17), that there is no internal-internal contribution to $\mathbf{X^Q}$ and the external-external contribution is already symmetric, thus X^0_{ab} and X^0_{ij} are

$$\begin{aligned}
X^{0}_{ab} &= x^{0}_{ab}+X^{Q,0}_{ab}\ ,\\
X^{0}_{ij} &= x^{0}_{ij}-2\epsilon_i\delta_{ij}\ . \qquad (3.20)
\end{aligned}$$

Finally, employing eq. (3.17) for $X^{Q,0}_{pq}$, eq. (3.18) for x^0_{pq}, and eqs. (2.16) and (2.22) defining the quantities $\tilde{\mathbf{B}}(\mathbf{z^0})$ and $\mathbf{B^0}$, which are needed for x^0_{pq}, as

$$\begin{aligned}
&\tilde{\mathbf{B}}(\mathbf{z^0}) = \mathbf{f}\bar{\mathbf{z}}^\mathbf{0} + \mathbf{g}(\bar{\mathbf{z}}^\mathbf{0})\mathbf{d}^{\mathrm{HF}} \ , \\
&[\mathbf{B^0}]_{pq} = C_{\mu p}B^0_{\mu i} + C_{\mu p}B^0_{\mu r}Q_{ra} + C_{\mu p}S^{\mathrm{AO}}_{\mu\rho}\delta_{\rho r}B^0_{r\nu}C^v_{\nu a} \ ,
\end{aligned} \tag{3.21}$$

the working equations for $X^0_{\mu\nu} = C_{\mu p}X^0_{pq}C_{\nu q}$ are

$$\begin{aligned}
X^0_{ab} &= \frac{1}{2}C^{v\dagger}_{a\mu}(-B^0_{\mu r} + (B^0_{r\mu})^\dagger)Q^\dagger_{rb} \ , \\
X^0_{ij} &= -\frac{1}{4}L^\dagger_{i\mu}B^0_{\mu j} - \frac{1}{4}(B^0_{\mu i})^\dagger L_{\mu j} - g(\bar{z}^0)_{ij} - \frac{1}{2}b(z^{loc,0})_{ij} - 2\epsilon_i\delta_{ij} \ , \\
X^0_{ai} &= -Q_{ar}(B^0_{\mu r})^\dagger L_{\mu i} - [\mathbf{z^0 f}]_{ai} \ , \\
X^0_{ia} &= 0 \ ,
\end{aligned} \tag{3.22}$$

with

$$\begin{aligned}
\left[\mathbf{b}(\mathbf{z^{loc,0}})\right]_{pi} &= \sum_{k>l}\left(\frac{\partial r_{kl}}{\partial O_{pi}}\right)_{\mathbf{v}_0=0} z^{loc,0}_{kl} \ , \\
\left(\frac{\partial r_{kl}}{\partial O_{pi}}\right)_{\mathbf{v}_0=0} &= \sum_A \left[2(S^A_{pk}\delta_{ik} - S^A_{pl}\delta_{il})S^A_{kl} + (S^A_{kk} - S^A_{ll})(S^A_{pl}\delta_{ik} + S^A_{pk}\delta_{il})\right] \ , \\
g(\bar{z}^0)_{pq} &= ((pq|mn) - 0.5(pn|mq))\bar{z}^0_{mn} \ , \\
\bar{\mathbf{z}}^\mathbf{0} &= \mathbf{z^0} + \mathbf{z^{0\dagger}} \ .
\end{aligned} \tag{3.23}$$

The working equations for $B^0_{\mu i}$, $B^0_{\mu r}$ and $B^0_{r\mu}$ are given in eqs. (2.28), (2.29) and (2.37), respectively.

In the final expressions for X^0_{ab} the symmetry of this quantity is no longer obvious due to the cancellation of terms between x^0_{ab} and $X^{\mathrm{Q},0}_{ab}$. Nevertheless, the symmetry is still there, as it must be, since this quantity is obtained as the sum of two symmetric matrices. To obtain the expression for X^0_{ab} the symmetry relation $B^0_{ab} = B^0_{ba}$ was employed, which is not obvious, but can be proved indirectly, cf. appendix B.

3.3 Singlet excited states

3.3.1 The Lagrangian

As discussed in section 2.3.1 the local orbital-relaxed CC2 Lagrangian $\mathcal{L}_{f'}$ for the energy of a singlet excited state f is the sum of the Lagrangian $\mathcal{L}_0$ for the ground state energy and the Lagrangian $\mathcal{L}_f$ for the excitation energy,

$$\begin{aligned}\mathcal{L}_{f'} &= \mathcal{L}_0 + \mathcal{L}_f \ , \\ \mathcal{L}_f &= \tilde{L}^f \mathbf{A} R^f + \tilde{\lambda}^f_{\mu_i} \Omega_{\mu_i} - \omega_f [\tilde{L}^f \mathbf{M} R^f - \mathbf{1}] \\ &\quad + z^{loc,f}_{ij} r_{ij} + z^f_{ai} f_{ai} + x^f_{pq} \left[\mathbf{C}^\dagger \mathbf{S}^{\mathrm{AO}} \mathbf{C} - \mathbf{1}\right]_{pq} . \end{aligned} \tag{3.24}$$

To obtain the excitation energy $\omega_f = \tilde{L}^f \mathbf{A} R^f$, with the contravariant left eigenvector $\tilde{L}^f$ and the covariant right eigenvector R^f, the left and right eigenvalue equations for the Jacobian $\mathbf{A}$,

$$\mathbf{A} R^f = \omega_f \mathbf{M} R^f \qquad \text{and} \qquad \tilde{L}^f \mathbf{A} = \omega_f \tilde{L}^f \mathbf{M} \ , \tag{3.25}$$

have to be solved ($\mathbf{M}$ is the metric of contra- and covariant CSFs). The CC2 Jacobian for singlet excited states takes according to eq. (1.22) the form

$$A_{\mu_i \nu_j} = \begin{pmatrix} \langle \tilde{\mu}_1 | [\hat{\mathbf{H}}, \tau_{\nu_1}] + [[\hat{\mathbf{H}}, \tau_{\nu_1}], \mathbf{T_2}]) | 0 \rangle & \langle \tilde{\mu}_1 | [\hat{\mathbf{H}}, \tau_{\nu_2}] | 0 \rangle \\ \langle \tilde{\mu}_2 | [\hat{\mathbf{H}}, \tau_{\nu_1}] | 0 \rangle & \langle \tilde{\mu}_2 | [\mathbf{F}, \tau_{\nu_2}] | 0 \rangle \end{pmatrix} . \tag{3.26}$$

The second term of $\mathcal{L}_f$ in eq. (3.24) is the condition for the ground state amplitudes with the corresponding Lagrange multipliers $\tilde{\lambda}$. The third term enforces the orthogonality of left and right eigenvector. The remaining terms represent the localization, Brillouin and orbital-orthogonality conditions, with the corresponding multipliers $\mathbf{z^{loc,f}}$, $\mathbf{z^f}$ and $\mathbf{x^f}$, respectively. For conciseness the state index f is omitted for $\tilde{L}$, R, and ω in the following.

Differentiation of the Lagrangian $\mathcal{L}_f$ with respect to the amplitudes $\mathbf{t}$ yields the equation for the multipliers $\tilde{\lambda}^{\mathbf{f}}$, cf. eq. (2.55). As discussed in the context of orbital-relaxed properties in section 2.3.2 and analogously to the ground state, stationarity of $\mathcal{L}_f$ with respect to orbital variations O_{pq} yields the linear *z-vector equations*,

$$0 \ = \ (1 - \mathcal{P}_{pq})[\mathbf{B^f} + \tilde{\mathbf{B}}(\mathbf{z^f}) + \mathbf{b}(\mathbf{z^{loc,f}})]_{pq}, \tag{3.27}$$

and a set of equations for the multipliers $\mathbf{x^f}$,

$$x^f_{pq} = -\frac{1}{4}(1 + \mathcal{P}_{pq})[\mathbf{B^f} + \tilde{\mathbf{B}}(\mathbf{z^f}) + \mathbf{b}(\mathbf{z^{loc,f}})]_{pq} \ . \tag{3.28}$$

The *z-vector equations* decouple into the Z-CPL equations determining $\mathbf{z^{loc,f}}$, and the Z-CPHF equations determining $\mathbf{z^f}$. Apart from a different right hand side these equations are equivalent to those of the ground state. The quantities $\tilde{\mathbf{B}}(\mathbf{z^f})$ and $\mathbf{b}(\mathbf{z^{loc,f}})$ occuring in these equations are defined according to eq. (3.5), and $\mathbf{B^f}$ according to eq. (2.49) as

$$\begin{aligned}[\mathbf{B^f}]_{pq} &= \left(\frac{\partial}{\partial O_{pq}}(\tilde{L}\mathbf{A}R + \tilde{\lambda}^f_{\mu i}\Omega_{\mu i} - \omega(\tilde{L}\mathbf{M}R - \mathbf{1}))\right)_{\mathbf{V}_0=0} \\ &= C_{\mu p}B^f_{\mu i} + C_{\mu p}B^f_{\mu r}Q_{ra} + C_{\mu p}S^{\mathrm{AO}}_{\mu\rho}\delta_{\rho r}B^f_{r\nu}C^v_{\nu a} \ . \end{aligned} \tag{3.29}$$

The working equations for $\mathbf{B^f}$ can be found in section 2.3.2, eqs. (2.57) - (2.59).

3.3.2 Derivation of the gradient

The gradient $\mathcal{L}^q_{f'}$ for the geometry optimization of the excited state f is obtained as the derivative of the Lagrangian $\mathcal{L}_{f'}$ with respect to nuclear displacements employing eq. (3.7) for the Fock matrix elements and eq. (3.8) for the four-index integrals. It is the sum of the ground state gradient $\mathcal{L}^q_0$ as defined in eq.(3.10), and the gradient for the difference between ground and excited state $\mathcal{L}^q_f$,

$$\mathcal{L}^q_{f'} = \mathcal{L}^q_0 + \mathcal{L}^q_f \ . \tag{3.30}$$

To reveal the difference between singlet and triplet excited states $\mathcal{L}^q_f$ is splitted into a part ${}^{13}\mathcal{L}^q_f$, which collects the terms, that are the same for singlet and triplet states, and a part ${}^{1}\mathcal{L}^q_f$, which collects the terms appearing only for singlet states. Sorting the terms according to the AO derivative integrals yields the working equations for ${}^{13}\mathcal{L}^q_f$ and ${}^{1}\mathcal{L}^q_f$

in LMO/PAO basis,

$$
\begin{aligned}
\mathcal{L}_f^q &= {}^{13}\mathcal{L}_f^q + {}^{1}\mathcal{L}_f^q \ , \\
{}^{13}\mathcal{L}_f^q &= h_{\mu\nu}^q \mathcal{D}_{\mu\nu}^f + S_{\mu\nu}^q \left\{ \left(\frac{\partial r_{ij}}{\partial S_{\mu\nu}^{\mathrm{AO}}} \right) z_{ij}^{loc} + X_{\mu\nu}^f \right\} \\
&\quad + (\mu\nu|P)^q \Big\{ \mathcal{D}_{\mu\nu}^f {}^{\mathrm{HF}}b^P + {}^{\mathcal{D}^f}b^P \ d_{\mu\nu}^{\mathrm{HF}} - 2 \ \mathcal{D}_{\mu\rho}^f c_{i\rho}^P L_{\nu i} \\
&\qquad + L_{\mu i} P_{\nu r} [2({}^{\lambda^f L}b^P + {}^{\lambda^f}b^P + {}^{LR}b^P + {}^{d}b^P) t_r^i + 2 b^P d_{ir}^{\lambda^f L} - {}^{Lt}\bar{c}_{ji}^P R_r^j \\
&\qquad\qquad - ({}^{d}\bar{c}_{ji}^P + {}^{\lambda^f L}\bar{c}_{ji}^P) t_r^j - \bar{c}_{ji}^P d_{jr}^{\lambda^f L} \\
&\qquad\qquad + \bar{V}_{ir}^P + {}^{LR}\bar{V}_{ir}^P - V_{is}^P S_{ss'} \tilde{L}_{s'}^k R_r^k + V_{jr}^P d_{ij}^L] \\
&\qquad + \Lambda_{\mu r}^p \Lambda_{\nu i}^h [2 \hat{\bar{V}}_{ir}^P + {}^{L}W_{ir}^P + 2 b^P \tilde{\lambda}_r^{i,f}] \\
&\qquad + L_{\mu i} \Lambda_{\nu j}^h [- {}^{LR}\bar{c}_{ji}^P - {}^{\lambda^f t}\bar{c}_{ji}^P + 2 b^P d_{ij}^L - \bar{c}_{ki}^P d_{kj}^L \\
&\qquad\qquad - V_{ir}^P S_{rr'} \tilde{\lambda}_{r'}^{j,f} - {}^{R}V_{ir}^P S_{rr'} \tilde{L}_{r'}^j - {}^{L}V_{jr}^P S_{rr'} R_{r'}^i] \\
&\qquad + \Lambda_{\mu r}^p P_{\nu s} [\tilde{\lambda}_r^{i,f} V_{is}^P + \tilde{L}_r^{i\,R} V_{is}^P + {}^{L}V_{ir}^P R_s^i - \hat{c}_{ik}^P \tilde{L}_r^k R_s^i - \hat{c}_{ik}^P \tilde{\lambda}_r^{k,f} t_s^i \\
&\qquad\qquad + 2 b^P d_{rs}^L - {}^{R}\bar{c}_{kj}^P t_s^k \tilde{L}_r^j] \Big\} \\
&\quad - J_{PQ}^q \Big\{ c_{ir}^P [\bar{V}_{ir}^Q + {}^{LR}\bar{V}_{ir}^Q + 2({}^{\lambda^f}b^Q + {}^{\lambda^f L}b^Q + {}^{LR}b^Q) t_r^i - {}^{Lt}\bar{c}_{ji}^Q R_r^j \\
&\qquad - ({}^{d}\bar{c}_{ji}^Q + {}^{\lambda^f L}\bar{c}_{ji}^Q) t_r^j] \\
&\qquad + \hat{c}_{ri}^P [\hat{\bar{V}}_{ir}^Q + {}^{L}W_{ir}^Q] + \hat{c}_{ij}^P [- {}^{LR}\bar{c}_{ji}^Q - {}^{\lambda^f t}\bar{c}_{ji}^Q + 2 b^Q d_{ij}^L] \\
&\qquad + {}^{\mathcal{D}^f}b^P \ {}^{\mathrm{HF}}b^Q - \mathcal{D}_{\mu\nu}^f c_{\mu i}^P c_{i\nu}^Q \Big\} \ , \\
{}^{1}\mathcal{L}_f^q &= (\mu\nu|P)^q \left\{ L_{\mu i} P_{\nu r} [2({}^{L}b^P + {}^{X(LT)}b^P) R_r^i + 2 {}^{R}b^P X(LT)_{ir} - {}^{X(LT)}\bar{c}_{ji}^P R_r^j \right. \\
&\qquad\qquad \left. - {}^{R}\bar{c}_{ji}^P X(LT)_{jr}] + \Lambda_{\mu r}^p \Lambda_{\nu i}^h 2 {}^{R}b^P \tilde{L}_r^i \right\} \\
&\quad - J_{PQ}^q \Big\{ c_{ir}^P [2({}^{L}b^Q + {}^{X(LT)}b^Q) R_r^i - {}^{X(LT)}\bar{c}_{ji}^Q R_r^j] \Big\} \ ,
\end{aligned}
\tag{3.31}
$$

with the intermediates

$$
\begin{aligned}
X(LT)_{ir} &= \tilde{L}^j_s S_{ss'} \tilde{t}^{ji}_{s'r} \ , & d^{\lambda^f L}_{ir} &= \tilde{\lambda}^{j,f}_s S_{ss'} \tilde{t}^{ji}_{s'r} + \tilde{L}^j_s S_{ss'} \tilde{R}^{ji}_{s'r} \\
d^L_{ij} &= -\tilde{L}^j_s S_{ss'} R^i_{s'} \ , & d^L_{rs} &= \tilde{L}^k_r R^k_s \ , \\
{}^R b^Q &= c^Q_{ir} R^i_r \ , & {}^R \bar{c}^Q_{ij} &= c^Q_{ir} R^j_r \ , \\
{}^{X(LT)} b^Q &= c^Q_{ir} X(LT)_{ir} \ , & {}^{X(LT)} \bar{c}^Q_{ij} &= c^Q_{ir} X(LT)_{jr} \ , \\
{}^{\lambda^f L} b^Q &= c^Q_{ir} d^{\lambda^f L}_{ir} \ , & {}^{\lambda^f L} \bar{c}^Q_{ij} &= c^Q_{ir} d^{\lambda^f L}_{jr} \ , \\
{}^d b^Q &= \hat{c}^Q_{ij} d^L_{ij} \ , & {}^d \bar{c}^Q_{ij} &= \hat{c}^Q_{ik} d^L_{jk} \ , \\
{}^{LR} b^Q &= \hat{c}^Q_{rs} d^L_{rs} \ , & {}^{LR} \bar{c}^Q_{ij} &= \tilde{L}^i_s \hat{c}^Q_{sr} R^j_r \ , \\
{}^L b^Q &= \hat{c}^Q_{ri} \tilde{L}^i_r \ , & {}^{Lt} \bar{c}^Q_{ij} &= \tilde{L}^i_s \hat{c}^Q_{sr} t^j_r \ , \\
{}^{\lambda^f} b^Q &= \hat{c}^Q_{ri} \tilde{\lambda}^{i,f}_r \ , & {}^{\lambda^f t} \bar{c}^Q_{ij} &= \tilde{\lambda}^{i,f}_s \hat{c}^Q_{sr} t^j_r \ , \\
{}^{\mathcal{D}^f} b^Q &= c^Q_{\mu\nu} \mathcal{D}^f_{\mu\nu} \ , & & \\
{}^R V^Q_{ir} &= \tilde{R}^{ij}_{rs} c^Q_{js} \ , & {}^L V^Q_{ir} &= 2\tilde{L}^{ij}_{rs} \hat{c}^Q_{sj} \ , \\
\hat{\bar{V}}^Q_{ir} &= \tilde{\lambda}^{ij,f}_{rs} \hat{c}^Q_{sj} \ , & \bar{V}^Q_{ir} &= \tilde{t}^{ij}_{rs} (\hat{\bar{B}}^Q_{js} + \hat{\bar{B}}'^Q_{js}) \ , \\
\hat{\bar{B}}^Q_{ir} &= \lambda^{i,f}_s \hat{c}^Q_{sr} - S_{rr'} \lambda^{k,f}_{r'} \hat{c}^Q_{ik} \ , & \hat{\bar{B}}'^Q_{ir} &= d^L_{ki} c^Q_{kr} - S_{rr'} d^L_{r's} c^Q_{is} \ , \\
{}^L W^Q_{ir} &= 2\tilde{L}^{ij}_{rs} (R^j_t \hat{c}^Q_{st} - S_{ss'} R^k_{s'} \hat{c}^Q_{kj}) \ , & {}^{LR} \bar{V}^Q_{ir} &= \tilde{R}^{ij}_{rs} (\tilde{L}^j_t \hat{c}^Q_{ts} - S_{ss'} \tilde{L}^k_{s'} \hat{c}^Q_{jk}) \ .
\end{aligned} \tag{3.32}
$$

The excited state density $\mathcal{D}^f_{\mu\nu}$, which occurs in the gradient ${}^{13}\mathcal{L}^q_f$, was discussed in section 2.5, cf. eqs. (2.80) - (2.82). The terms, which are contracted with the derivative AO overlap integrals $S^q_{\mu\nu}$, are discussed in detail in the following paragraph.

Derivatives with respect to the AO overlap matrix

The derivative AO overlap integrals $S^q_{\mu\nu}$ are for the gradient $\mathcal{L}^q_f$ contracted with the derivatives of the localization criterion r_{ij} as defined in eq. (3.12), and with the intermediate quantity $\mathbf{X^f}$. Analogously to the ground state the quantity $\mathbf{X^f}$ collects the terms originating from the orthogonality condition in $\mathcal{L}_f$ and from the dependency of the transformation matrix $\mathbf{Q}$ on the AO overlap matrix,

$$
\begin{aligned}
X^{Q,f}_{\mu\nu} &= \left(\frac{\partial \mathcal{L}_f}{\partial \tilde{\lambda}^{ij,f}_{ab}}\right)\left(\frac{\partial \tilde{\lambda}^{ij,f}_{ab}}{\partial S^{\mathrm{AO}}_{\mu\nu}}\right) + \left(\frac{\partial \mathcal{L}_f}{\partial t^{ij}_{ab}}\right)\left(\frac{\partial t^{ij}_{ab}}{\partial S^{\mathrm{AO}}_{\mu\nu}}\right) \\
&\quad + \left(\frac{\partial \mathcal{L}_f}{\partial \tilde{L}^{ij}_{ab}}\right)\left(\frac{\partial \tilde{L}^{ij}_{ab}}{\partial S^{\mathrm{AO}}_{\mu\nu}}\right) + \left(\frac{\partial \mathcal{L}_f}{\partial R^{ij}_{ab}}\right)\left(\frac{\partial R^{ij}_{ab}}{\partial S^{\mathrm{AO}}_{\mu\nu}}\right) \ , \\
X^f_{\mu\nu} &= C_{\mu p}(x^f_{pq} + X^{Q,f}_{pq}) C^\dagger_{q\nu} \ .
\end{aligned} \tag{3.33}
$$

Following the strategy, which was demonstrated in the preceding section for the ground state, the working equations for $\mathbf{X^f}$ are finally obtained as

$$\begin{aligned}
X^f_{\mu\nu} &= C_{\mu p} X^f_{pq} C_{\nu q} \ , \\
X^f_{ab} &= \frac{1}{2} C^{v\dagger}_{a\mu}(-B^f_{\mu r} + (B^f_{r\mu})^\dagger) Q^\dagger_{rb} \ , \\
X^f_{ij} &= -\frac{1}{4} L^\dagger_{i\mu} B^f_{\mu j} - \frac{1}{4}(B^f_{\mu i})^\dagger L_{\mu j} - g(\bar{z}^f)_{ij} - \frac{1}{2} b(z^{loc,f})_{ij} \ , \\
X^f_{ai} &= -Q_{ar}(B^f_{\mu r})^\dagger L_{\mu i} - [\mathbf{z^f f}]_{ai} \ , \\
X^f_{ia} &= 0 \ .
\end{aligned} \tag{3.34}$$

$\mathbf{b}(\mathbf{z^{loc,f}})$ is defined according to eq. (3.23), and the working equations for $B^f_{r\mu}$, $B^f_{\mu i}$ and $B^f_{\mu r}$ are given in section 2.3.2, eqs. (2.57) - (2.59), respectively.

3.4 Triplet excited states

3.4.1 The Lagrangian

The general formulation of the Lagrangian for an excited state f given in eq. (3.24) holds also for triplet excited states. The triplet operators and corresponding CSFs were introduced in section 1.2.2. They lead to the Jacobian $\mathbf{A}$ for triplet excited states,

$$A_{\mu_i \nu_j} = \begin{pmatrix} \langle \tilde{\mu}_1 | [\hat{\mathbf{H}}, \tau_{\nu_1}] + [[\hat{\mathbf{H}}, \tau_{\nu_1}], \mathbf{T_2}]) | 0 \rangle & \langle \tilde{\mu}_1 | [\hat{\mathbf{H}}, \overset{(+)}{\tau}_{\nu_2}] | 0 \rangle & \langle \tilde{\mu}_1 | [\hat{\mathbf{H}}, \overset{(-)}{\tau}_{\nu_2}] | 0 \rangle \\ \langle \overset{(+)}{\tilde{\mu}}_2 | [\hat{\mathbf{H}}, \tau_{\nu_1}] | 0 \rangle & \langle \overset{(+)}{\tilde{\mu}}_2 | [\mathbf{F}, \overset{(+)}{\tau}_{\nu_2}] | 0 \rangle & 0 \\ \langle \overset{(-)}{\tilde{\mu}}_2 | [\hat{\mathbf{H}}, \tau_{\nu_1}] | 0 \rangle & 0 & \langle \overset{(-)}{\tilde{\mu}}_2 | [\mathbf{F}, \overset{(-)}{\tau}_{\nu_2}] | 0 \rangle \end{pmatrix} . \tag{3.35}$$

Solving the left and right eigenvalue equations for this Jacobian yields the excitation energies and left and right eigenvectors for triplet excited states. The cluster operator $\mathbf{T}$ refers to the ground state and therefore always contains singlet excitation operators.

3.4.2 Derivation of the gradient

Analogously to the singlet excited state gradient, $\mathcal{L}^q_{f'}$ for the excited triplet state f is the sum of the ground state gradient $\mathcal{L}^q_0$ and the gradient for the triplet excitation energy

$\mathcal{L}_f^q$,

$$\begin{aligned} \mathcal{L}_{f'}^q &= \mathcal{L}_0^q + \mathcal{L}_f^q \\ &= \mathcal{L}_0^q + {}^{13}\mathcal{L}_f^q + {}^{3}\mathcal{L}_f^q \ . \end{aligned} \tag{3.36}$$

For the sake of compactness the difference $\mathcal{L}_f^q$ is splitted into ${}^{13}\mathcal{L}_f^q$, which was introduced above (cf. eq. (3.31)) and collects all terms appearing in both the singlet and the triplet case, and a second part ${}^{3}\mathcal{L}_f^q$ comprising triplet specific terms. The latter is calculated as

$$\begin{aligned} {}^{3}\mathcal{L}_f^q &= (\mu\nu|P)^q \left\{ L_{\mu i} P_{\nu r} [- {}^{X'(LT)}\bar{c}_{ji}^{P} R_r^j - {}^{R}\bar{c}_{ji}^{P} X'(LT)_{jr}] \right\} \\ &\quad - J_{PQ}^q \left\{ - c_{ir}^{P} \ {}^{X'(LT)}\bar{c}_{ji}^{Q} R_r^j \right\} \ . \end{aligned} \tag{3.37}$$

The density $\mathcal{D}^f$ in AO basis appearing in ${}^{13}\mathcal{L}_f^q$ is for triplet states calculated as discussed in section 2.5, eqs. (2.80), (2.81) and (2.84). Other intermediates occuring in ${}^{13}\mathcal{L}_f^q$ or ${}^{3}\mathcal{L}_f^q$, which are defined differently compared to the corresponding singlet state intermediates, are

$$\begin{aligned} \bar{R}_{rs}^{ij} &= 2(\overset{(+)}{R}{}_{rs}^{ij} + \overset{(-)}{R}{}_{rs}^{ij}) \ , & \bar{L}_{rs}^{ij} &= 2(\overset{(+)}{\tilde{L}}{}_{rs}^{ij} + \overset{(-)}{\tilde{L}}{}_{rs}^{ij}) \ , \\ {}^{R}V_{ir}^{Q} &= \bar{R}_{rs}^{ij} c_{js}^{Q} \ , & {}^{L}V_{ir}^{Q} &= \frac{1}{2} \bar{L}_{rs}^{ij} \hat{c}_{sj}^{Q} \ , \\ {}^{LR}\bar{V}_{ir}^{Q} &= \bar{R}_{sr}^{ji} (\tilde{L}_t^j \hat{c}_{ts}^{Q} - S_{ss'} \tilde{L}_{s'}^k \hat{c}_{jk}^{Q}) \ , & {}^{L}W_{ir}^{Q} &= \frac{1}{2} \bar{L}_{sr}^{ji} (R_t^j \hat{c}_{st}^{Q} - S_{ss'} R_{s'}^k \hat{c}_{kj}^{Q}) \ , \\ X'(LT)_{ir} &= - \tilde{L}_s^j S_{ss'} t_{s'r}^{ij} \ , & {}^{X'(LT)}\bar{c}_{ij}^{Q} &= c_{ir}^{Q} X'(LT)_{jr} \ , \\ d_{ir}^{\lambda^f L} &= \tilde{\lambda}_s^{j,f} S_{ss'} \tilde{t}_{s'r}^{ji} + \tilde{L}_s^j S_{ss'} \bar{R}_{s'r}^{ji} \ . \end{aligned} \tag{3.38}$$

The quantity $X_{\mu\nu}^f$ is for triplet excited states obtained analogously to the corresponding quantity for singlet excited states, cf. eq. (3.33), but for triplet states the plus and minus combinations of the left and right doubles eigenvectors, $\overset{(+)}{R}$, $\overset{(-)}{R}$, $\overset{(+)}{\tilde{L}}$ and $\overset{(-)}{\tilde{L}}$, have

to be taken into account for $X_{\mu\nu}^{Q,f}$,

$$\begin{aligned} X_{\mu\nu}^{Q,f} &= \left(\frac{\partial \mathcal{L}_f}{\partial \tilde{\lambda}_{ab}^{ij,f}}\right)\left(\frac{\partial \tilde{\lambda}_{ab}^{ij,f}}{\partial S_{\mu\nu}^{\mathrm{AO}}}\right) + \left(\frac{\partial \mathcal{L}_f}{\partial t_{ab}^{ij}}\right)\left(\frac{\partial t_{ab}^{ij}}{\partial S_{\mu\nu}^{\mathrm{AO}}}\right) \\ &+ \left(\frac{\partial \mathcal{L}_f}{\partial \overset{(+)}{\tilde{L}}{}_{ab}^{ij}}\right)\left(\frac{\partial \overset{(+)}{\tilde{L}}{}_{ab}^{ij}}{\partial S_{\mu\nu}^{\mathrm{AO}}}\right) + \left(\frac{\partial \mathcal{L}_f}{\partial \overset{(-)}{\tilde{L}}{}_{ab}^{ij}}\right)\left(\frac{\partial \overset{(-)}{\tilde{L}}{}_{ab}^{ij}}{\partial S_{\mu\nu}^{\mathrm{AO}}}\right) \\ &+ \left(\frac{\partial \mathcal{L}_f}{\partial \overset{(+)}{R}{}_{ab}^{ij}}\right)\left(\frac{\partial \overset{(+)}{R}{}_{ab}^{ij}}{\partial S_{\mu\nu}^{\mathrm{AO}}}\right) + \left(\frac{\partial \mathcal{L}_f}{\partial \overset{(-)}{R}{}_{ab}^{ij}}\right)\left(\frac{\partial \overset{(-)}{R}{}_{ab}^{ij}}{\partial S_{\mu\nu}^{\mathrm{AO}}}\right) . \end{aligned} \tag{3.39}$$

The resulting working equations are formally the same as for singlet states, i.e. eq. (3.34), with the corresponding triplet quantities $B_{r\mu}^{f}$, $B_{\mu i}^{f}$ and $B_{\mu r}^{f}$. The working equations for them can be found in section 2.4.2, eqs. (2.75) - (2.77).

3.5 Hybrid method (LT-)DF-LCC2

So far no distinction has been made, whether Laplace transform was used for solving the eigenvalue equations or not. The derived equations are valid for both the DF-LCC2 and the LT-DF-LCC2 method. The details of the two methods were discussed in section 1.2.3 as well as in several publications.[24–29]

In the case of DF-LCC2 the Lagrangians $\mathcal{L}_0$ and $\mathcal{L}_f$ are the proper energy Lagrangians. But as discussed in detail in Ref. 54 for the LT-LMP2 method, they are only approximations to the exact energy Lagrangians, if Laplace transformation is employed, because the application of Laplace transformation for truncated doubles quantities implies a fitting of those to the untruncated canonical ones. Nevertheless, these approximate Lagrangians are used for the calculation of properties and gradients, because the proper LT-DF-LCC2 Lagrangians are impractical due to the appearence of the untruncated doubles quantities (cf. eq. (27) in Ref. 54 and the related discussion).

Yet the errors introduced by the use of these approximate Lagrangians turned out to be negligible for the calculation of excitation energies and first-order properties (cf. section 2.6.1). For geometry optimizations the effect of the approximate Lagrangians might be more problematic.

Besides the DF-LCC2 and the LT-DF-LCC2 methods, also a hybrid method was implemented for the investigation of this aspect, which will in the following be called

(LT-)DF-LCC2. The basic idea is to combine the exact energy Lagrangian of the DF-LCC2 method with the local approximations obtained from the LT-DF-LCC2 method, which are in many cases more appropriate than the pair lists and domains of the DF-LCC2 method. The first step of an (LT-)DF-LCC2 calculation is the Davidson diagonalization for the right eigenvalue problem employing the LT-DF-LCC2 code. The converged LT-DF-LCC2 eigenvectors are used as starting guess for a DF-LCC2 calculation without LT. In the DF-LCC2 method the local approximations are not state-specific, thus the pair list and domains, which are obtained from the initial LT-DF-LCC2 step for the state of interest, are used for each of the excited states in the DF-LCC2 part.
The methods DF-LCC2 and (LT-)DF-LCC2 have only been implemented for singlet excited states.

3.6 Test calculations

The energy gradients for the ground state and for excited states have been implemented into the `MOLPRO` program package[61] and most of the relevant routines were parallelized based on a shared file approach, i.e., the scratch files containing the amplitudes, integrals, etc. reside on two file systems, which are common to all parallel threads. Input/output is organized such, that both file systems are concurrently used.
The underlying HF reference was computed employing the density fitting approximation.[89] In all LT-DF-LCC2 calculations three Laplace quadrature points were used, exemplary calculations with five points showed no significant improvement of the results. The cc-pVDZ AO basis set[63] was employed together with the related fitting basis set optimized for DF-MP2.[64]
The geometry optimizations were performed using the quadratic steepest descent algorithm[90–92] in combination with the model Hessian proposed by Lindh.[93]
The correctness of the code was verified by comparing the results calculated with untruncated pair lists and full domains to the corresponding canonical results obtained with the RI-CC2 gradient code of the `TURBOMOLE` program.[19,21,22,62]

3.6.1 Accuracy of the local methods

The error of the local approximations introduced by restricted pair lists and domains as discussed in the sections 1.1.3 and 1.2.3 is analysed by comparing local and canonical results.

In all presented calculations the ground state LMO pair list contains all pairs of LMOs with a respective LMO interorbital distance up to 10 bohr. The ground state domains truncating the pair-specific virtual space are built using the Boughton Pulay (BP) procedure with a criterion of 0.98.[34] The final orbital domains are obtained by augmenting the BP domains by further centers separated by not more than one bond from the closest atom in the original BP domain (`iext=1` option in `MOLPRO`).

In LT-DF-LCC2 calculations adaptive pair lists are employed for excited state quantities. They are obtained as explained in detail in section 1.2.3, i.e. a set of important LMOs (specified by a threshold $\kappa_e = 0.999$) is determined by analysis of the actual approximation to the eigenvector for each individual state. The excited state pair lists contain all pairs of these important LMOs, all other pairs with an interorbital distance up to 5 bohr, and all pairs of the ground state list. The excited state domains are obtained in an adaptive procedure, which is also based on analysis of the actual approximation to the eigenvector. The state-specific orbital domains are determined by specifying an ordered list of important centers for each important LMO. The ground state domains then are augmented with further centers from this list until a threshold of 0.98 is reached by the least-squares optimization procedure introduced in section IIC of Ref. 26.

In DF-LCC2 calculations the local approximations are not adaptive and state-specific. They are *a priori* obtained from analysis of the CIS wavefunction of the studied state as explained in detail in section 1.2.3. The important orbitals, which determine the pair list, are obtained from the CIS coefficients (specified by a threshold $\kappa_e = 0.995$) and the domains are constructed applying the Boughton Pulay (BP) procedure with a criterion of 0.98 to modified orbitals (eq. (24) in Ref 24), which describe for a given excited state the entire excitation from the respective LMO based on the CIS coefficients. The final excited state pair lists and domains are obtained analogously to the LT-DF-LCC2 case, i.e. by adopting the ground state pair list and augmenting the ground state orbital domains.

In the hybrid method (LT-)DF-LCC2 the local approximations are obtained by an initial LT-DF-LCC2 step, yet the geometry optimization is carried out by the DF-LCC2 method with the doubles quantities of all states being restricted to the LT-DF-LCC2 lists and domains of that state, for which the geometry optimization is carried out.

The local approximations including the number of redundant functions in each pair domain, are kept fixed during the optimization process in order to avoid discontinuities on the potential energy surface.

During a geometry optimization the energetical order of the excited states may change.

Table 3.1: Canonical adiabatic excitation energies (in eV) are listed in column ω. For the local methods the deviations of the energies $\Delta\omega$ (local-canonical, in eV), the rms deviation σ_{rms} in atomic positions (in Å) and the number of iterations of the geometry optimization N_{it} are shown.

			DF-LCC2			(LT-)DF-LCC2			LT-DF-LCC2		
	State	ω	$\Delta\omega$	σ_{rms}	N_{it}	$\Delta\omega$	σ_{rms}	N_{it}	$\Delta\omega$	σ_{rms}	N_{it}
DMABN	S_0			0.003	4					0.003	4
	S_1	4.251	0.011	0.003	6	0.000	0.003	6	-0.004	0.003	8
	S_2	4.640	-0.001	0.004	6	-0.007	0.004	6	-0.010	0.003	6
HPA	S_0			0.039	14					0.039	14
	T_1	3.777							-0.001	0.033	27
	T_2	4.287							-0.001	0.020	15
p-cresol	S_0			0.002	3					0.002	3
	S_1	4.708	0.010	0.002	5	-0.004	0.002	5	-0.011	0.002	5
	S_2	6.024	0.000	0.003	7	-0.002	0.003	7	-0.008	0.003	10
	T_1	3.755							-0.007	0.003	9
	T_2	4.283							-0.003	0.002	7
1-phenylpyrrole	S_0			0.008	12					0.011	12
	S_1	4.732	0.015	0.005	16	0.006	0.006	16	0.007	0.007	13
	T_1	3.736							0.000	0.008	16
Tyrosine	S_0			0.035	19					0.032	18
	S_1	4.717	0.018	0.038	17	0.002	0.041	16	-0.003	0.036	19
	T_1	3.823							0.000	0.040	25
	T_2	4.324							0.002	0.060	21
trans-urocanic	S_0			0.008	4					0.008	4
acid	S_1	3.862	0.018	0.004	8	0.011	0.004	8	0.004	0.006	7
	S_2	4.803	0.018	0.006	6	0.006	0.006	6	0.007	0.007	6
	T_1	2.795							-0.002	0.004	7
	T_2	3.734							-0.007	0.004	7

The character of the eigenvectors is analysed in each iteration of the Davidson process by calculating the overlap with the vectors from the preceding iteration. This enables following a particular state during the geometry optimization, even if the order of the states changes. This default behaviour of the implementation was turned off to compare the results with the canonical results obtained with `TURBOMOLE`, which is lacking this option. In this case the program always optimizes, e.g., the second lowest state, even if the state, which was the second lowest for the starting geometry, is no longer the second lowest for subsequent geometries.

Figure 3.1 shows schematic potential energy curves of the ground state S_0 and the excited state S_1 of a molecule. The difference between the energies of the ground and

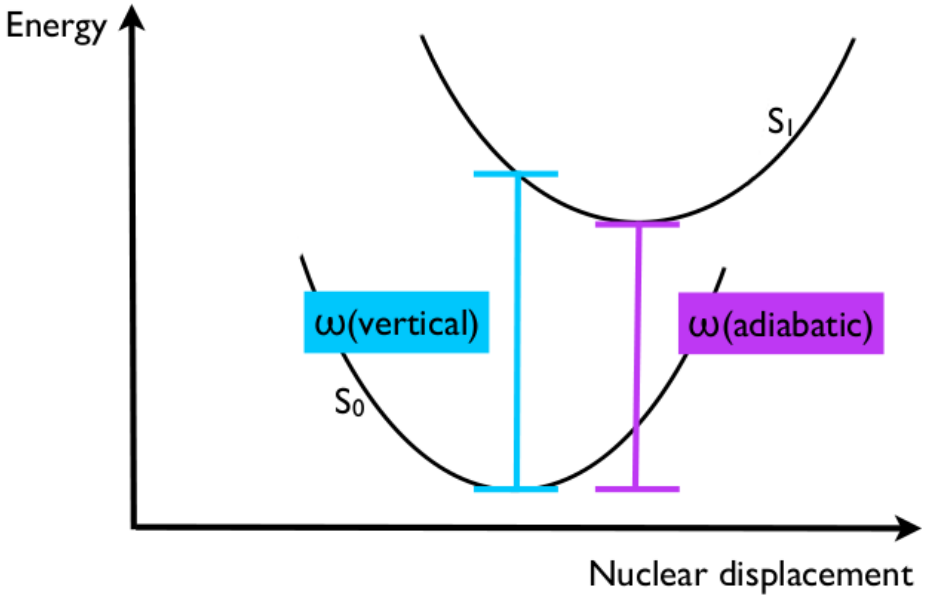

Figure 3.1: Schematic potential energy curves for the ground state S_0 and the excited state S_1 reveal the difference between the *vertical* excitation energy in the minimum structure of the ground state (turquoise) and the *adiabatic* excitation energy (purple), i.e. the difference between the minimum excited state energy and the minimum ground state energy.

the excited state in the minimum structure of the ground state is in the following called *vertical* excitation energy. The difference between the minimum excited state energy and the minimum ground state energy is called *adiabatic* excitation energy.
Table 3.1 compiles canonical adiabatic excitation energies of several molecules and states and the deviations of the local results. Moreover, for the local methods the root-mean-square (rms) deviation σ_{rms} in atomic positions R_i from the canonical reference is listed, which is calculated as

$$\sigma_{\text{rms}} = \sqrt{|\sum_{i}^{N}(R_i^{loc} - R_i^{can})^2|/N} \ , \tag{3.40}$$

where N denotes the number of atoms in the molecule. For measuring bond lengths and angles, as well as for calculating σ_{rms} and the preceding alignment of the structures the VMD program was used.[94]
All excited state geometry optimizations were started from the respective optimized ground state geometry, while all ground state geometry optimizations were started from

the respective geometries used originally in Ref. 51.

Excitation energies and σ_{rms} do not show a noticable difference in accuracy between the individual local methods. Moreover, also the convergence behaviour of the geometry optimization is very similar for all three methods, as can be seen in table 3.1. This implies that the approximate Lagrangians cause no problems in geometry optimizations using the LT-DF-LCC2 method. Thus, there is no need to use the DF-LCC2 method or the hybrid (LT-)DF-LCC2 method, which are computationally much more expensive, because the eigenvalue problem can not be reduced to an effective singles problem as it is done in the LT-DF-LCC2 method. For example, the local calculations for the state S_1 of DMABN were run in parallel mode on seven Intel Xeon X5560 2.80 GHz cores. The (LT-)DF-LCC2 and DF-LCC2 optimizations ran three to four times longer than the LT-DF-LCC2 calculation. The difference does not arise from the convergence behaviour of the optimization: with a total of 8 iterations the LT-DF-LCC2 optimization in this case even needed 2 iterations more for convergence than the DF-LCC2 and the (LT-)DF-LCC2 calculations.

The deviations of the adiabatic excitation energies are not larger than those of the vertical excitation energies calculated in the ground state equilibrium geometry, which were studied in detail earlier.[26,28] Generally they lie clearly below 0.05 eV as can be seen in figure 3.2, where the deviations of the adiabatic and vertical excitation energies ($\Delta\omega = \omega_{loc} - \omega_{can}$) are plotted for the molecules and states in table 3.1. The deviations are substantially smaller than the expected accuracy of the canonical CC2 response method itself, which is about 0.3 eV, cf. tables IV and V in Ref. 95. Furthermore, σ_{rms} lies in all of the cases clearly below 0.1 Å.

To understand the larger σ_{rms} for HPA and tyrosine, their structures have to be considered. As can be seen in figure 3.3 HPA and tyrosine consist of an aromatic ring and a side chain. Thus a deviation in one of the angles at the connection of the two parts can cause a larger σ_{rms}. For example, in the optimized ground state geometry of HPA the maximum deviation from local to canonical dihedral angles, which describe the position of the side chain relative to the aromatic ring, is 2.6°. This leads to a bad alignment for one half of the structure and a relatively high σ_{rms}, although each of the two parts of the structure considered separatly is very similar to the canonical one. Hence, also the deviations of the local bond lengths and angles from the canonical ones should be considered explicitly.

For the same molecules and states as in table 3.1 the maximum deviations of the bond lenghts, bond angles, and dihedral angles are listed in table 3.2. For bond lengths the

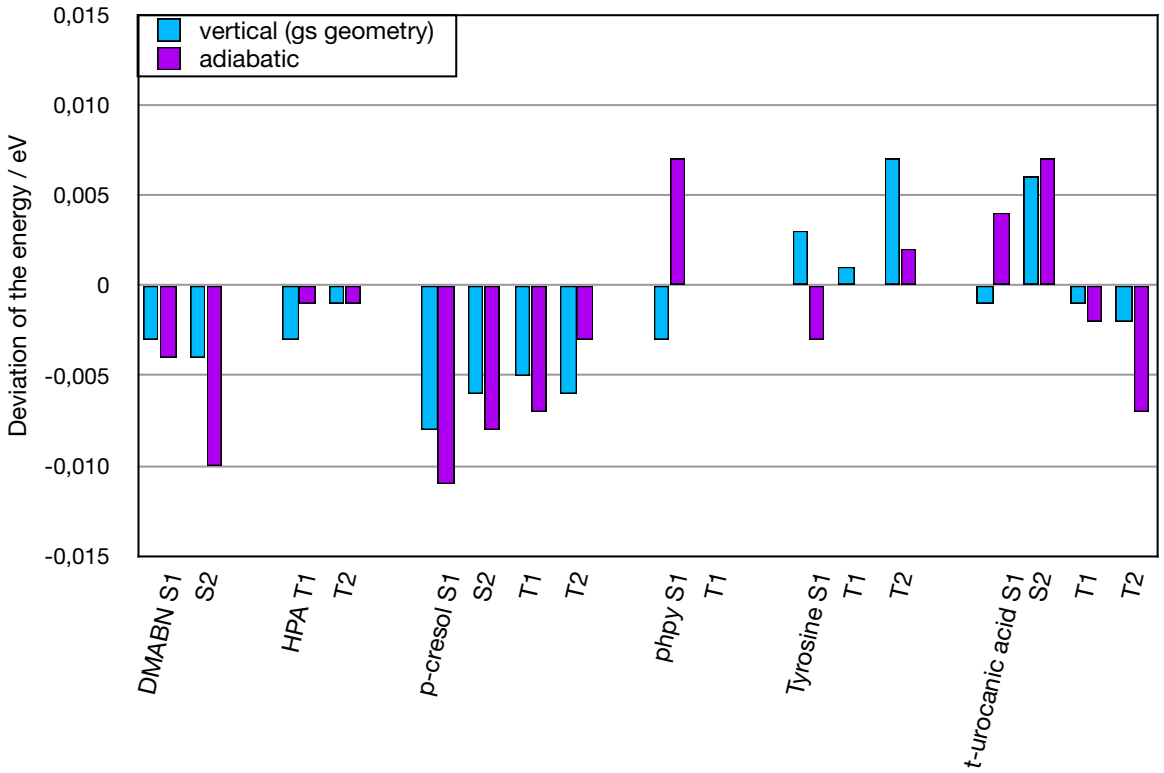

Figure 3.2: The deviation of the local adiabatic (purple) and vertical (turquoise) excitation energies (local-canonical, in eV) are shown.

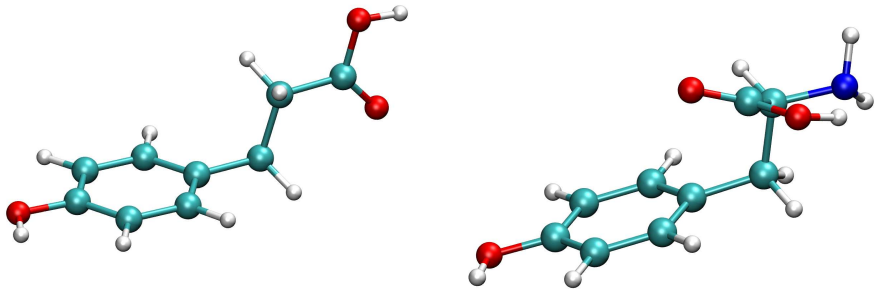

Figure 3.3: Ground state structures of HPA (left) and tyrosine (right).

Table 3.2: The maximum deviations of the local bond lengths r (in Å), bond angles α and dihedral angles τ (in °) are shown (absolute values).

		DF-LCC2			(LT-)DF-LCC2			LT-DF-LCC2		
	State	Δr	$\Delta\alpha$	$\Delta\tau$	Δr	$\Delta\alpha$	$\Delta\tau$	Δr	$\Delta\alpha$	$\Delta\tau$
DMABN	S_0	<0.01	0.10	0.01				<0.01	0.10	0.01
	S_1	<0.01	0.09	<0.01	<0.01	0.09	<0.01	<0.01	0.09	<0.01
	S_2	0.01	0.17	0.02	0.01	0.16	0.02	0.01	0.19	0.02
HPA	S_0	0.01	0.19	2.61				0.01	0.18	2.58
	T_1							0.01	0.22	2.64
	T_2							0.01	0.28	1.06
p-cresol	S_0	0.01	0.07	<0.01				0.01	0.06	<0.01
	S_1	0.01	0.13	<0.01	0.01	0.11	<0.01	0.01	0.08	<0.01
	S_2	<0.01	0.11	<0.01	<0.01	0.10	<0.01	<0.01	0.09	<0.01
	T_1							0.01	0.09	<0.01
	T_2							<0.01	0.06	<0.01
1-phenylpyrrole	S_0	<0.01	0.06	0.70				<0.01	0.06	0.94
	S_1	0.01	0.17	0.45	0.01	0.11	0.31	0.01	0.18	0.76
	T_1							0.01	0.10	0.49
Tyrosine	S_0	0.01	0.33	2.18				0.01	0.33	1.98
	S_1	0.01	2.43	2.11	0.01	2.46	2.30	0.01	2.45	2.03
	T_1							0.01	0.32	2.50
	T_2							0.01	0.63	2.90
trans-urocanic	S_0	<0.01	0.35	<0.01				<0.01	0.35	<0.01
acid	S_1	0.01	0.37	<0.01	<0.01	0.16	<0.01	<0.01	0.22	<0.01
	S_2	<0.01	0.32	<0.01	<0.01	0.38	<0.01	<0.01	0.45	<0.01
	T_1							0.01	0.17	<0.01
	T_2							0.01	0.11	0.01

maximum deviation is 0.01 Å. The deviations of the bond angles are in most of the cases clearly smaller than 1°, the observed maximum deviation is 2.5°. For dihedral angles deviations up to 2.9° are observed, but in most of the cases they are clearly smaller. Again, there are no significant differences between the three implemented local methods.

3.6.2 Efficiency of the code

As an illustrative example for the efficiency and applicability of the new code results from calculations on the molecules **1** and **2** are presented, which are shown in figure 3.4. Molecule **2** is obtained from **1** via protonation of the phthalimide moiety. Molecule **1** comprises 55 atoms, 162 correlated electrons, and 554 basis functions in cc-pVDZ basis, molecule **2** 56 atoms, 162 correlated electrons, and 559 basis functions. Similar but smaller molecules were recently in the focus of experimental and theoretical studies in the context of the synthesis of 9,10-Dihydrophenanthrenes via photocatalytic decarboxylation.[96] In that context canonical CC2 calculations indicated, that the cationic biradical intermediate in the first step of the decarboxylation reaction is formed starting from a molecule, which is equivalent to **1**, rather by protonation of the molecule and subsequent intramolecular electron transfer (IET) than by an initial IET and a subsequent protonation of the phthalimide anion-radical.
Analogously to the reaction in Ref. 96 the two possible reaction pathways depicted in figure 3.4 are discussed for the formation of the cationic biradical intermediate **4** starting from molecule **1**. On the one hand molecule **4** could be obtained via **3**, i.e. by an initial IET and subsequent protonation of the phthalimide moiety. On the other hand the protonation of the phthalimide moiety followed by an IET could yield **4** via molecule **2**.

Low lying charge transfer (CT) states indicate an IET, thus in a first step the lowest lying excited states of **1** and **2** at their corresponding relaxed electronic ground state geometries were calculated. The resulting excitation energies and orbital-relaxed dipole moment changes are compiled in table 3.3. For the protonated molecule **2** there are several low lying singlet and triplet CT states featuring large changes of the dipole moment, whereas for the unprotonated molecule **1** each of the lowest excited states results from a local excitation, with the exception of the S_3 state. This picture is analogous to that obtained in the previous study on the smaller system,[96] where only for the protonated molecule (corresponding to **2**) low lying CT states could be observed in the canonical

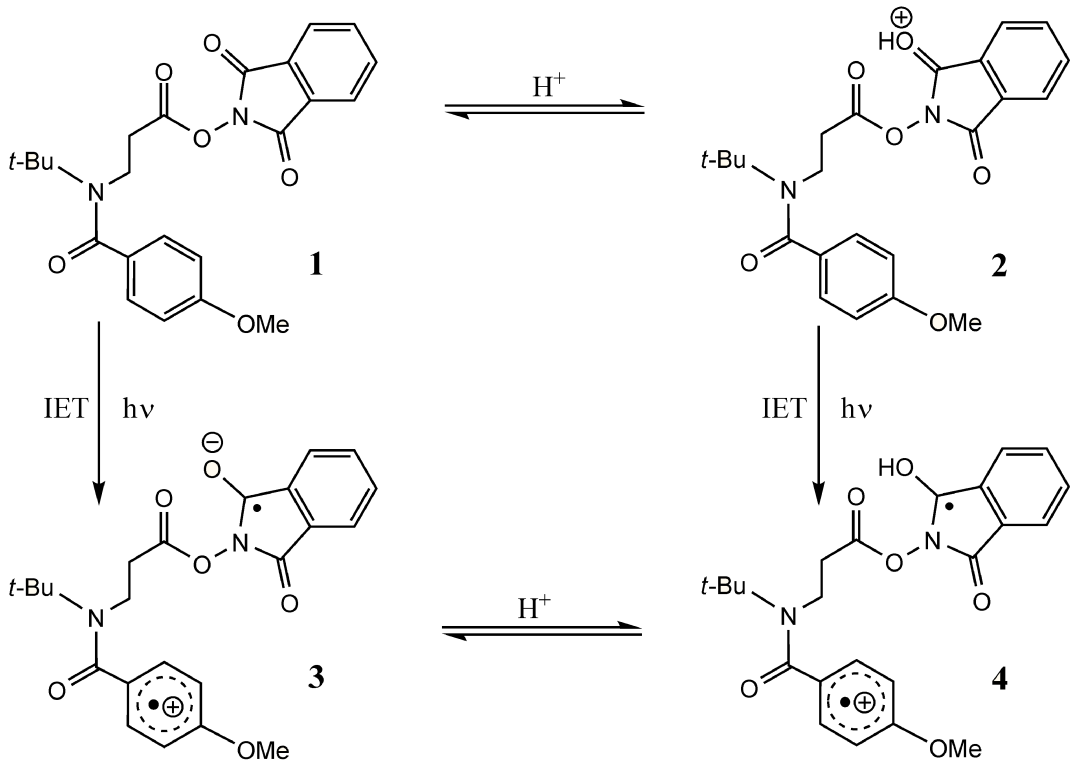

Figure 3.4: Two possible pathways for the reaction of molecule **1** to molecule **4**, both including a protonation step and an IET, cf. Scheme 4 in Ref. 96. An initial IET leads to intermediate **3**, an initial protonation step to intermediate **2**.

Table 3.3: Vertical excitation energies ω (in eV) and the norm of the dipole moment vector describing the change from the ground state to the excited state $|\mu^f|$ (in a.u.) are shown for the lowest excited states of the molecules **1** and **2** at their relaxed ground state geometry. Moreover, the ratio (local vs. canonical) of the number of unique elements of the doubles quantities is listed in %.

	molecule **1**				molecule **2**			
State	character	ω	$\|\mu^f\|$	doubles ratio	character	ω	$\|\mu^f\|$	doubles ratio
S_1	$n \rightarrow \pi^*$	4.13	1.29	9.6	CT	2.38	6.49	20.5
S_2	$n \rightarrow \pi^*$	4.48	1.04	11.1	CT	2.99	5.90	20.3
S_3	CT	4.57	9.16	22.1	CT	3.29	5.55	22.3
S_4^a	$\pi \rightarrow \pi^*$	4.73	0.48	22.1	$\pi \rightarrow \pi^*$	3.41	0.40	16.9
S_5^a	$\pi \rightarrow \pi^*$	4.86	0.07	14.8	CT	3.80	5.39	19.5
T_1	$\pi \rightarrow \pi^*$	3.82	0.16	10.9	CT	2.38	6.47	20.6
T_2	$n \rightarrow \pi^*$	3.87	1.21	10.9	$\pi \rightarrow \pi^*$	2.91	2.24	19.9
T_3	$\pi \rightarrow \pi^*$	3.99	0.13	7.6	CT	2.98	4.55	19.9
T_4^a	$\pi \rightarrow \pi^*$	4.30	1.40	16.0	CT	3.27	5.13	22.7
T_5^a	$\pi \rightarrow \pi^*$	4.51	0.93	8.4	$n \rightarrow \pi^*$	3.67	2.36	18.4

a) These results have to be taken with a grain of salt, because only a total of five states was calculated.

CC2 calculations. Moreover, the excitation energies of **2** are clearly lower than those of **1**, with the latter lying above the range accessible for the sensitizer used in the experiments ([Ir(dtb-bpy)(ppy)$_2$]PF$_6$).[97] Figure 3.5 shows the orbital-relaxed density differences to the ground state for the states S_1, T_1 and S_3 of molecule **1** and for the states S_1 and T_1 of molecule **2**. The CT character of the states S_1 and T_1 of molecule **2** shifting electron density from the phenyl to the phthalimide moiety is clearly visible. On the other hand, the S_1 and T_1 states of **1** are localized on the phthalimide moiety. The S_3 state of **1** (with a relatively high excitation energy of 4.57eV) also has CT character, but is shifting charge from the carbonyl group rather than the phenyl ring to the phthalimide moiety. These results indicate, that the cationic biradical intermediate **4** is formed by an initial protonation of **1** with a subsequent IET, which is in line with the conclusion drawn for the similar system in Ref. 96.

In a second step, geometry optimizations for the lowest excited states of the molecules **1** and **2** were carried out. The changes of the molecular geometries during the optimizations of the S_1 state are shown in figure 3.6. For the S_1 state of molecule **1** no substantial geometry changes are observed relative to the ground state structure. For the S_1 state of molecule **2** the geometry does not converge and approaches a conical

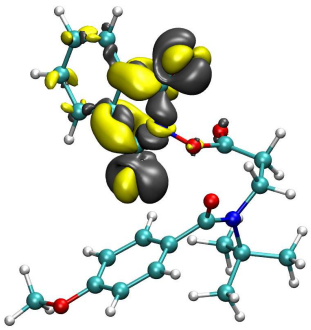

1 S_1, ω=4.13eV

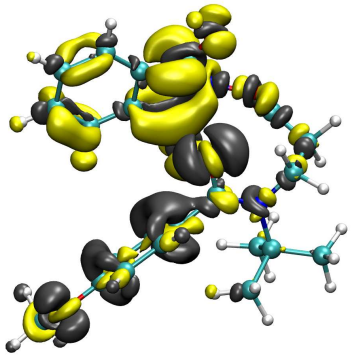

2 S_1, ω=2.38eV

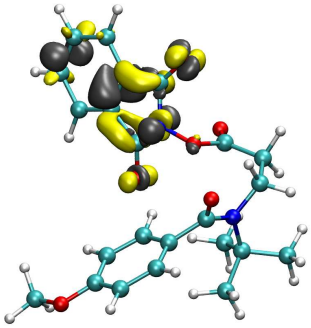

1 T_1, ω=3.82eV

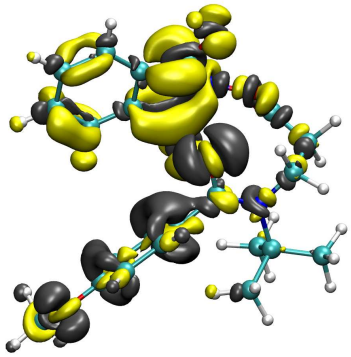

2 T_1, ω=2.38eV

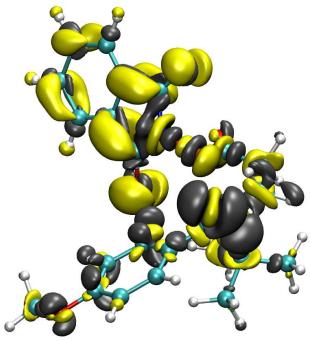

1 S_3, ω=4.57eV

Figure 3.5: Orbital-relaxed density differences between some of the lowest excited states and the ground state of the molecules **1** and **2** at the relaxed ground state geometry. The yellow and grey iso-surfaces represent a value of +0.003 and −0.003, respectively.

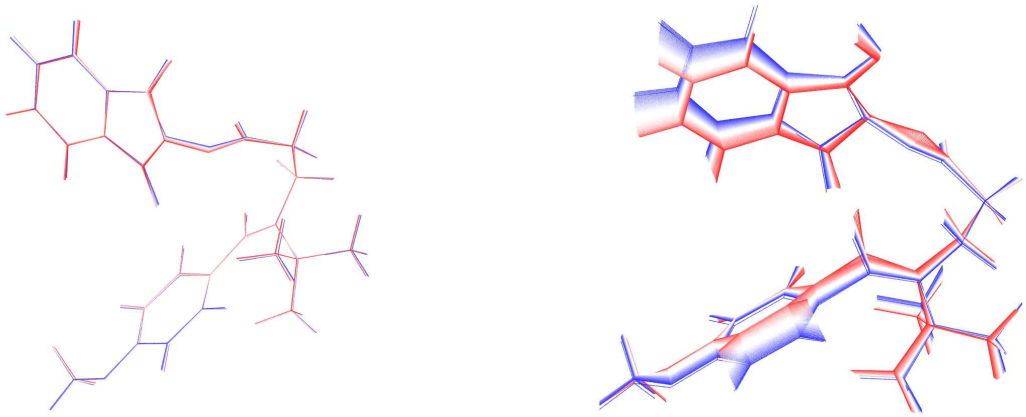

1 ω=4.13eV, ω=2.76eV **2** ω=2.38eV, ω=0.06eV

Figure 3.6: Change of the geometry of the molecules **1** and **2** during the optimization of state S_1 starting from the ground state geometry (red) and the corresponding excitation energies at the beginning and at the end of the optimization (i.e. for molecule **2** 50 optimization steps without convergence). The optimization steps are indicated by color (from red to blue).

intersection with the ground state. During the first iterations the length of the bond between the nitrogen atom of the phthalimide moiety and the oxygen atom connecting it to the rest of the molecule rapidly increases from 1.36Å to 1.41Å. At the same time, the length of the bond between this oxygen and the carbon atom of the carbonyl group decreases from 1.45Å to 1.40Å, while the angle between the two oxygen atoms increases slightly. The same behaviour is also observed for the lowest triplet state of molecule **2**. These findings are again in agreement with those of the previous study on a similar system[96] and match the proposed mechanism, in which the subsequent step (after formation of **4**) is the elimination of phthalimide and CO_2 from **4**. Moreover, structural changes within the phenyl and phthalimide moieties of molecule **2** indicate the proposed IET. In contrast to the system studied in Ref. 96 there is a carbonyl group next to the phenyl moiety, which seems to play a role in the stabilization of molecule **4**.

The ratios local *vs.* canonical of the number of unique elements in the doubles vector are shown in table 3.3. They lie between 7.6% and 22.7% for the individual excited states of **1** and **2**. These small ratios indicate substantial computational savings due to the local approximations.
The calculations were run in parallel mode, e.g. the optimization of the S_1 state of molecule **1** was run on seven Intel(R) Xeon(R) X5660 2.80GHz cores and the optimiza-

tion of the S_1 state of molecule **2** on seven AMD Opteron 6180 SE 2.50 GHz cores. The optimization of molecule **1** converged within 17 iterations with a threshold of 10^{-6} for the energy and 10^{-3} for the gradient. The right eigenvalue equation was solved for the three lowest lying states, while the left eigenvector, Lagrange multipliers, densities and gradient were calculated only for the ground and the first excited state. The optimization was finished after 12 days. A bit more than one day was needed for the initial step, in which also the local approximations are determined, while one optimization step took about 14.5 hours [1]. For the protonated molecule **2** the initial step took about 1.5 days and one iteration about 18 hours[2] due to the larger domains (cf. the doubles ratios in table 3.3). The optimization did not converge for that case due to the conical intersection with the ground state, as discussed above.

The timings for finding the left and right eigenvectors of the Jacobian and for the calculation of orbital-unrelaxed properties were discussed in detail earlier.[26,28] The Davidson diagonalization starts from the converged vectors of the preceding optimization step, thus in the first optimization steps it converges slower than in later optimization steps, where only little changes in the vectors occur. In the optimization steps 1 and 10 the right eigenvectors for **1** were obtained within 5.3 and 3.5 hours, and for **2** within 8.3 and 2.6 hours, respectively. The left eigenvector is obtained starting from the right eigenvector within several iterations. Thus the effect of the larger domains in **2** is not as distinct as for the right eigenvector and the duration of this step is quite constant during the optimization, i.e. about 1.5 hours.

As discussed in section 2.6.5 most of the time for the calculation of the Lagrange multipliers for the orbital relaxation, i.e. $\mathbf{z}$, $\mathbf{z^{loc}}$ and $\mathbf{x}$, is needed for the intermediates $B_{\mu i}$, $B_{\mu r}$, $B_{r\mu}$ for the linear *z-vector equations*, while solving the linear *z-vector equations* takes only a few minutes (the latter almost entirely for the Z-CPHF equations, while the Z-CPL equations take virtually no time). For **1** and **2** the linear *z-vector equations* are solved within less than 5 minutes, and the intermediates are calculated within a bit less than one hour for **1** and about 75 minutes for **2**.

In the assembly of the final gradient according to eqs. (3.10) and (3.31), the construction of the intermediate quantities for the contractions with the derivative integrals $h^q_{\mu\nu}$, $(\mu\nu|P)^q$, $S^q_{\mu\nu}$ and J^q_{PQ} is the dominating step of the calculation: for the two molecules **1** and **2** the overall times for assembling the gradient (including both ground and excited

[1] Due to further optimization of the gradient routines after submission of this thesis the time for one optimization step was reduced to less than 13 hours, leading to an expected duration of the entire optimization of less than 11 days.

[2] One optimization step takes a bit less than 15 hours using the optimized code.

state parts) were 2.75 and 4.5 hours [3], respectively.

3.7 Conclusions

Based on the work on orbital relaxation, which was presented in the previous chapter, formalism, implementation, and test calculations for gradients with respect to nuclear displacements are reported in the context of the local CC2 response method LT-DF-LCC2. The new method enables geometry optimizations for the ground state and for excited states of extended molecular systems. It is demonstrated, that the Laplace transformation can also be utilized in the context of local CC2 gradients to enable multistate calculations and state-specific local approximations. The accuracy of the method using LT is in the same range as without LT. It was shown, that the deviations of geometries and adiabatic excitation energies from the canonical reference, as well as the convergence behaviour of the geometry optimizations are virtually identical for the (much slower) methods DF-LCC2 and (LT-)DF-LCC2, in which the proper Lagrangian can be used, and the LT-DF-LCC2 method, where the true Lagrangian has to be approximated. Thus, the approximated Lagrangians cause no problems, neither for first-order properties as shown in chapter 2, nor for geometry optimizations.
The deviations of the local adiabatic excitation energies from the canonical ones are in the same range as the deviations of the vertical excitation energies, i.e. clearly smaller than 0.05eV for the molecules and states in our test set. The equilibrium structures are in all of our test cases very similar to the canonical ones. The maximum deviation in bond lengths as observed in our test calculations amounts to 0.01Å, the deviation in bond angles is in most of the cases clearly smaller than 1°. Deviations in dihedral angles are usually somewhat larger, the observed maximum deviation in our test set amounts to 2.9°.
As an illustrative application example geometry optimizations were performed for excited states of molecules, which are of interest for photocatalytic reactions and consist of more than 50 atoms. In agreement with the results for a similar system there is a clear indication, that the first reaction step is the protonation of the phthalimide moiety, which is followed by an intramolecular electron transfer step. For systems of this size the optimization of an excited state geometry is possible within several days to weeks on a standard workstation, depending on the convergence behaviour. One optimization step

[3] Using the optimized code the assembly of the gradient takes about 60 minutes for molecule **1** and 80 minutes for molecule **2**.

for the studied system containing 56 atoms took 14.5 hours using the settings described above, the entire optimization took 12 days.

Chapter 4

Summary

Analytic energy gradients and orbital-relaxed properties for excited states in extended molecular systems were developed based on the local CC2 response method LT-DF-LCC2, and implemented into the MOLPRO program package. The method employs local approximations and the density fitting approximation to reduce the computational cost. Moreover, Laplace transformation is used to partition the occuring eigenvalue equation systems containing the Jacobian in order to enable multistate calculations and state-specific local approximations. Both the gradient for geometry optimizations and the molecular properties at particular geometries help to understand and predict the photophysical behaviour, which plays a crucial role for various applications.

The first step towards analytic energy gradients is the explicit inclusion of orbital relaxation into the Lagrangian for the energy of the respective state as demonstrated in chapter 2. Compared to the orbital-unrelaxed Lagrangian, which was used in previous work on first-order properties, three additional sets of Lagrange multipliers appear for the new conditions, namely the Brillouin, localization and orthonormality condition. These multipliers are determined by the derivative of the Lagrangian with respect to the orbital variations, which leads to the *z-vector equations*. The orbital-relaxed Lagrangian is not only the starting point for gradients with respect to nuclear displacements, but also for orbital-relaxed properties, e.g. the orbital-relaxed dipole moment. The properties are obtained as derivatives of the Lagrangian with respect to the strength of an corresponding perturbation.
Test calculations confirmed, that the number of Laplace quadrature points and the local approximations, which were chosen earlier for orbital-unrelaxed properties, are also appropriate for relaxed properties. It is shown, that with these settings the deviations of

the local dipole moments from the canonical reference are very similar for orbital-relaxed and unrelaxed properties, i.e. for the test set of molecules and excited states they are smaller than 10%. There are some exceptions, which were discussed.
As an illustrative application example the four lowest singlet and triplet excited states of an organic sensitizer for solar-cell applications, which comprises almost 100 atoms and 950 basis functions in the used cc-pVDZ basis, were calculated. In agreement with experiment the lowest singlet excited state was assigned to a charge transfer (CT) transition with a large change in the dipole moment, whereas the lowest triplet states show no CT character. Moreover, this system illustrates the effect of the local approximations on the computational time: the singlet calculation was clearly slower than the triplet calculation, because for the states S_3 and S_4 the pair lists and domains are unified during the Davidson diagonalization and thus considerably larger. The calculation of excitation energies, orbital-unrelaxed and orbital-relaxed dipole moments of the four lowest singlet and triplet excited states of this molecule with almost 100 atoms was performed within about 4 weeks.

In Chapter 3 analytic energy gradients for geometry optimizations were derived. The gradient is obtained as the derivative of the orbital-relaxed Lagrangian for the energy of the particular state with respect to nuclear displacements. In contrast to the formalism for properties, derivative integrals occur for the gradient. The gradients were implemented for the LT-DF-LCC2 method and the DF-LCC2 method without Laplace transformation. Moreover, a hybrid method was implemented, which combines their advantages, i.e. the exact Lagrangians of the DF-LCC2 method and the often more appropriate local approximations of the LT-DF-LCC2 method.
Test calcuations showed, that Laplace transformation can also be utilized for local CC2 gradients to enable multistate calculations and state-specific local approximations, although the Lagrangian is in this case only an approximation to the exact energy Lagrangian. The accuracy of the method using LT is in the same range as in the DF-LCC2 method and in the hybrid method. Moreover, LT-DF-LCC2 is computationally much cheaper, because only an effective singles eigenvalue equation system has to be solved. Thus the LT-DF-LCC2 method is clearly preferable over the DF-LCC2 method and the hybrid method, in which the optimization is carried out without LT. The deviations of the local adiabatic excitation energies from the canonical ones were in the test set clearly smaller than 0.05 eV, which is as large as for vertical excitation energies. The obtained equilibrium structures are very similar to the canonical ones, i.e., in the test

set the maximum deviation of the bond lengths is 0.01 Å, the deviations of the bond angles are usually smaller than 1° (maximum deviation 2.5°), and for dihedral angles deviations up to 2.9° are observed, but in most of the cases they are clearly smaller.
As an illustrative application example excited state geometry optimizations for two molecules were presented, which occur in a photocatalytic decarboxylation reaction that is of interest presently in our group in the context of an application project. Each of the molecules comprises more than fifty atoms. In agreement with the results for a similar system a clear indication was found, that the first reaction step is the protonation of the phthalimide moiety, which is followed by an intramolecular electron transfer. For systems of this size the optimization of an excited state geometry is possible within several days to weeks, depending on the convergence behaviour. For the studied system comprising 56 atoms a single optimization step took 14.5 hours, and in total eleven days until convergence was reached.

A future project based on the presented method could be the development of gradients for the local algebraic diagrammatic approach ADC(2). This variational method has a close relationship to CC2 and is already implemented in the `MOLPRO` program package for the calculation of excitation energies. Moreover, a local CC2 method employing orbital specific virtuals (OSVs) instead of PAOs for the virtual space is presently developed in our group and could be extended to properties and gradients based on the theory and implementation presented in this thesis.

Bibliography

[1] E. Lewars, The concept of the potential energy surface, in *Computational Chemistry*, page 9, Springer US, 2003.

[2] T. Merz and M. Schütz, Description of excited states in photocatalysis with theoretical methods, in *Chemical Photocatalysis*, edited by B. König, page 263, De Gruyter, Berlin, Boston, 2013.

[3] M. Born and R. Oppenheimer, Annalen der Physik **389**, 457 (1927).

[4] N. Turro, V. Ramamurthy, and J. Scaiano, *Modern molecular photochemistry of organic molecules*, University Science Books, 2010.

[5] B. König, editor, *Chemical Photocatalysis*, De Gruyter, Berlin, Boston, 2013.

[6] J. Čížek, J. Chem. Phys. **45**, 4256 (1966).

[7] J. Čížek, Adv. Chem. Phys. **14**, 35 (1969).

[8] J. Čížek and J. Paldus, Int. J. Quantum Chem. **5**, 359 (1971).

[9] O. Christiansen, P. Jørgensen, and C. Hättig, Int. J. Quantum Chem. **68**, 1 (1998).

[10] O. Christiansen, H. Koch, and P. Jørgensen, Chem. Phys. Lett. **243**, 409 (1995).

[11] P. Pulay, S. Saebø, and W. Meyer, J. Chem. Phys. **81**, 1901 (1984).

[12] A. Dreuw and M. Head-Gordon, Chem. Rev. **105**, 4009 (2005).

[13] S. Grimme and M. Parac, ChemPhysChem **3**, 292 (2003).

[14] K. Sadeghian and M. Schütz, J. Am. Chem. Soc. **129**, 4068 (2007).

[15] E. J. Baerends, D. E. Ellis, and P. Ros, Chem. Phys. **2**, 41 (1973).

[16] J. L. Whitten, J. Chem. Phys. **58**, 4496 (1973).

[17] B. I. Dunlap, J. W. D. Connolly, and J. R. Sabin, J. Chem. Phys. **71**, 3396 (1979).

[18] C. Hättig and F. Weigend, J. Chem. Phys. **113**, 5154 (2000).

[19] C. Hättig and A. Köhn, J. Chem. Phys. **117**, 6939 (2002).

[20] K. Hald, C. Hättig, D. Yeager, and P. Jørgensen, Chem. Phys. Lett. **328**, 291 (2000).

[21] C. Hättig, A. Köhn, and K. Hald, J. Chem. Phys. **116**, 5401 (2002).

[22] A. Köhn and C. Hättig, J. Chem. Phys. **119**, 5021 (2003).

[23] N. O. C. Winter and C. Hättig, J. Chem. Phys. **134**, 184101 (2011).

[24] D. Kats, T. Korona, and M. Schütz, J. Chem. Phys. **125**, 104106 (2006).

[25] D. Kats, T. Korona, and M. Schütz, J. Chem. Phys. **127**, 064107 (2007).

[26] D. Kats and M. Schütz, J. Chem. Phys. **131**, 124117 (2009).

[27] D. Kats and M. Schütz, Z. Phys. Chem. **224**, 601 (2010).

[28] K. Freundorfer, D. Kats, T. Korona, and M. Schütz, J. Chem. Phys. **133**, 244110 (2010).

[29] K. Ledermüller, D. Kats, and M. Schütz, J. Chem. Phys. **139**, 084111 (2013).

[30] P. Pulay, Chem. Phys. Lett. **100**, 151 (1983).

[31] S. Saebø and P. Pulay, Annu. Rev. Phys. Chem. **44**, 213 (1993).

[32] J. Pipek and P. G. Mezey, J. Chem. Phys. **90**, 4916 (1989).

[33] S. F. Boys, in *Quantum Theory of Atoms, Molecules, and the Solid State*, edited by P. O. Löwdin, page 253, Academic, New York, 1966.

[34] J. W. Boughton and P. Pulay, J. Comput. Chem. **14**, 736 (1993).

[35] J. Ortiz, J. Chem. Phys. **101**, 6743 (1994).

[36] M. E. Casida, Time-dependent density-functional response theory for molecules, in *Recent Advances in Computational Chemistry*, edited by D. P. Chong, volume 1, page 155, World Scientific, Singapore, 1995.

[37] T. Helgaker and P. Jørgensen, Adv. Quant. Chem. **19**, 183 (1988).

[38] H. Koch and P. Jørgensen, J. Chem. Phys. **93**, 3333 (1990).

[39] T. B. Pedersen and H. Koch, J. Chem. Phys. **106**, 8059 (1997).

[40] D. Kats, D. Usvyat, and M. Schütz, Phys. Rev. A **83**, 062503 (2011).

[41] G. Wälz, D. Kats, D. Usvyat, T. Korona, and M. Schütz, Phys. Rev. A **86**, 052519 (2012).

[42] P. Jørgensen and T. Helgaker, J. Chem. Phys. **89**, 1560 (1988).

[43] T. Helgaker, P. Jørgensen, and N. C. Handy, Theor. Chim. Acta **76**, 227 (1989).

[44] H. Koch, H. J. A. Jensen, P. Jørgensen, and T. Helgaker, J. Chem. Phys. **93**, 3345 (1990).

[45] H. Monkhorst, Int. J. Quantum Chem. Symp. **11**, 421 (1977).

[46] H. Sekino and R. J. Bartlett, Int. J. Quantum Chem. Symp. **18**, 255 (1984).

[47] J. Geertsen, M. Rittby, and R. J. Bartlett, Chem. Phys. Lett. **164**, 57 (1989).

[48] J. F. Stanton and R. J. Bartlett, J. Chem. Phys. **98**, 7029 (1993).

[49] D. C. Comeau and R. J. Bartlett, Chem. Phys. Lett. **207**, 414 (1993).

[50] H. Koch, O. Christiansen, P. Jørgensen, and J. Olsen, Chem. Phys. Lett. **244**, 75 (1995).

[51] T. Korona and H.-J. Werner, J. Chem. Phys. **118**, 3006 (2003).

[52] T. D. Crawford and R. A. King, Chem. Phys. Lett. **366**, 611 (2002).

[53] J. Almlöf, Chem. Phys. Lett. **181**, 319 (1991).

[54] D. Kats, D. Usvyat, and M. Schütz, Phys. Chem. Chem. Phys. **10**, 3430 (2008).

[55] S. A. Kucharski and R. J. Bartlett, Fifth-order many-body perturbation theory and its relationship to various coupled-cluster approaches, volume 18 of *Advances in Quantum Chemistry*, page 281, Academic Press, 1986.

[56] K. Freundorfer, Development of local coupled cluster methods for the calculation of excited triplet states, Master's thesis, Universität Regensburg, 2010.

[57] T. Korona, CCGen, unpublished.

[58] H.-J. Werner et al., Molpro, version 2012.1, a package of ab initio programs, 2012, see http://www.molpro.net.

[59] M. Schütz, H.-J. Werner, R. Lindh, and F. R. Manby, J. Chem. Phys. **121**, 737 (2004).

[60] S. Loibl and M. Schütz, J. Chem. Phys. **137**, 084107 (2012).

[61] H.-J. Werner, P. J. Knowles, G. Knizia, F. R. Manby, and M. Schütz, WIREs Comput Mol Sci **2**, 242 (2012).

[62] R. Ahlrichs, M. Bär, M. Häser, H. Horn, and C. Kömel, Chem. Phys. Lett. **162**, 165 (1989).

[63] T. H. Dunning, Jr., J. Chem. Phys. **90**, 1007 (1989).

[64] F. Weigend, A. Köhn, and C. Hättig, J. Chem. Phys. **116**, 3175 (2002).

[65] J. Yum et al., Angew. Chem. Int. Edit. **48**, 1576 (2009).

[66] K. Ledermüller and M. Schütz, Local CC2 response method based on the Laplace transform: Analytic energy gradients for ground and excited states, submitted for publication.

[67] P. Pulay, Mol. Phys. **17**, 197 (1969).

[68] P. Pulay, Direct use of the gradient for investigating molecular energy surfaces, in *Applications of electronic structure theory*, page 153, Springer, US, 1977.

[69] P. Pulay, G. Fogarasi, F. Pang, and J. E. Boggs, J. Am. Chem. Soc. **101**, 2550 (1979).

[70] B. R. Brooks et al., J. Chem. Phys. **72**, 4652 (1980).

[71] R. Krishnan, H. B. Schlegel, and J. A. Pople, J. Chem. Phys. **72**, 4654 (1980).

[72] S. Kato and K. Morokuma, Chem. Phys. Lett. **65**, 19 (1979).

[73] J. D. Goddard, N. C. Handy, and H. F. Schaefer III, J. Chem. Phys. **71**, 1525 (1979).

[74] J. A. Pople, R. Krishnan, H. B. Schlegel, and J. S. Binkley, Int. J. Quantum Chem. **16**, 225 (1979).

[75] G. Fitzgerald, R. Harrison, W. D. Laidig, and R. J. Bartlett, J. Chem. Phys. **82**, 4379 (1985).

[76] P. Jørgensen and J. Simons, J. Chem. Phys. **79**, 334 (1983).

[77] A. E. Azhary, G. Rauhut, P. Pulay, and H.-J. Werner, J. Chem. Phys. **108**, 5185 (1998).

[78] G. Rauhut and H.-J. Werner, Phys. Chem. Chem. Phys. **3**, 4853 (2001).

[79] J. F. Stanton, J. Chem. Phys. **99**, 8840 (1993).

[80] J. F. Stanton and J. Gauss, J. Chem. Phys. **100**, 4695 (1994).

[81] P. G. Szalay, Int. J. Quantum Chem. **55**, 151 (1995).

[82] M. Kállay and J. Gauss, J. Chem. Phys. **121**, 9257 (2004).

[83] C. V. Caillie and R. D. Amos, Chem. Phys. Lett. **308**, 249 (1999).

[84] C. V. Caillie and R. D. Amos, Chem. Phys. Lett. **317**, 159 (2000).

[85] F. Furche and R. Ahlrichs, J. Chem. Phys. **117**, 7433 (2002).

[86] O. Christiansen, J. F. Stanton, and J. Gauss, J. Chem. Phys. **108**, 3987 (1998).

[87] K. Hald et al., J. Chem. Phys. **118**, 2985 (2003).

[88] C. Hättig, J. Chem. Phys. **118**, 7751 (2003).

[89] R. Polly, H.-J. Werner, F. R. Manby, and P. J. Knowles, Mol. Phys. **102**, 2311 (2004).

[90] F. Eckert and H.-J. Werner, Theor. Chem. Acc. **100**, 21 (1998).

[91] J. Sun and K. Ruedenberg, J. Chem. Phys. **99**, 5257 (1993).

[92] J. Sun, K. Ruedenberg, and G. J. Atchity, J. Chem. Phys. **99**, 5276 (1993).

[93] R. Lindh, A. Bernhardsson, G. Karlström, and P.-Å. Malmqvist, Chem. Phys. Lett. **241**, 423 (1995).

[94] W. Humphrey, A. Dalke, and K. Schulten, J. Mol. Graphics **14**, 33 (1996).

[95] M. Schreiber, M. R. Silva-Junior, S. P. A. Sauer, and W. Thiel, J. Chem. Phys. **128**, 134110 (2008).

[96] G. Kachkovskyi et al., Synthesis of 9,10-dihydrophenanthrenes via photocatalytic decarboxylation, unpublished.

[97] G. Kachkovskyi, C. Faderl, and O. Reiser, Adv. Synth. Catal. **355**, 2240 (2013).

Appendix A

Coupled Cluster diagrams

Practical equations for the Lagrangian, which are the starting point for the derivatives with respect to the orbital variations in chapter 2 and nuclear displacements in chapter 3, are obtained using diagrammatic techniques as explained in detail in section 1.3. The diagrams were generated with the program `ccgen`.[57]

The diagrams for the ground state Lagrangian, i.e. the diagrams for the correlation energy,

$$E_0^{\mathrm{CC2}} = \langle 0|[\mathbf{H}, \mathbf{T_1}]|0\rangle + \frac{1}{2}\langle 0|[[\mathbf{H}, \mathbf{T_1}], \mathbf{T_1}]|0\rangle + \langle 0|[\mathbf{H}, \mathbf{T_2}]|0\rangle \ , \tag{A.1}$$

and the amplitude condition,

$$\tilde{\lambda}^0_{\mu_i}\Omega_{\mu_i} = \tilde{\lambda}^0_{\mu_1}\langle\tilde{\mu}_1|\hat{\mathbf{H}} + [\hat{\mathbf{H}}, \mathbf{T_2}])|0\rangle + \tilde{\lambda}^0_{\mu_2}\langle\tilde{\mu}_2|\hat{\mathbf{H}} + [\mathbf{F}, \mathbf{T_2}]|0\rangle \ , \tag{A.2}$$

are depicted in figures A.1 and A.2, respectively. As already mentioned in section 1.3, the diagrams project on the covariant CSFs, whereas the CC expressions project on the contravariant CSFs. This has to be considered in the resulting equations.

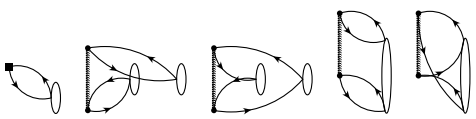

Figure A.1: Diagrams contributing to the ground state correlation energy E_0^{CC2} (all operators undressed).

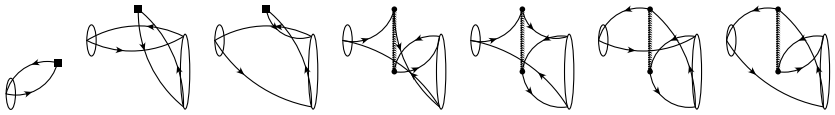

(a) Singles part.

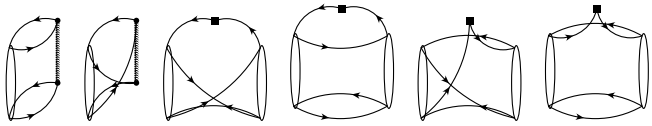

(b) Doubles part (Fock matrix is undressed).

Figure A.2: Diagrams contributing to the amplitude equations $\tilde{\lambda}_{\mu_i}\Omega_{\mu_i}$.

For the excited state Lagrangians practical equations for the excitation energy,

$$\begin{aligned}\tilde{L}_{\mu_i}A_{\mu_i\nu_j}R_{\nu_j} =&\tilde{L}_{\mu_1}\langle\tilde{\mu}_1|[\hat{\mathbf{H}},\tau_{\nu_1}]+[[\hat{\mathbf{H}},\tau_{\nu_1}],\mathbf{T_2}])|0\rangle R_{\nu_1}+\tilde{L}_{\mu_1}\langle\tilde{\mu}_1|[\hat{\mathbf{H}},\tau_{\nu_2}]|0\rangle R_{\nu_2}\\ &+\tilde{L}_{\mu_2}\langle\tilde{\mu}_2|[\hat{\mathbf{H}},\tau_{\nu_1}]|0\rangle R_{\nu_1}+\tilde{L}_{\mu_2}\langle\tilde{\mu}_2|[\mathbf{F},\tau_{\nu_2}]|0\rangle R_{\nu_2}\ ,\end{aligned} \tag{A.3}$$

the amplitude condition $\tilde{\lambda}^f_{\mu_i}\Omega_{\mu_i}$, and the norm of the left and right eigenvector,

$$\tilde{L}_{\mu_i}M_{\mu_i\nu_j}R_{\nu_j}=\tilde{L}_{\mu_1}\langle\tilde{\mu}_1|\nu_1\rangle R_{\nu_1}+\tilde{L}_{\mu_2}\langle\tilde{\mu}_2|\nu_2\rangle R_{\nu_2}\ , \tag{A.4}$$

are obtained from CC diagrams. The diagrams for the amplitude condition were already shown in figure A.2. The figures A.3 and A.4 contain the diagrams contributing to the excitation energy and the norm of the eigenvectors of singlet excited states.
The corresponding diagrams for triplet excited states are shown in the figures A.5 and A.6, where only diagrams with a non-zero weight are considered (cf. rule 5 in section 1.3). In the triplet case the equations deduced from the diagrams contain the nonsymmetrized doubles operators, which have to be replaced by the symmetric ones using the relation

$$U^{ij}_{rs}=\frac{1}{2}\overset{(+)}{U}{}^{ij}_{rs}+\overset{(-)}{U}{}^{ij}_{rs}\ . \tag{A.5}$$

The equations containing the symmetrized operators can often be drastically simplified due to the symmetry relations shown in eq. (1.28).

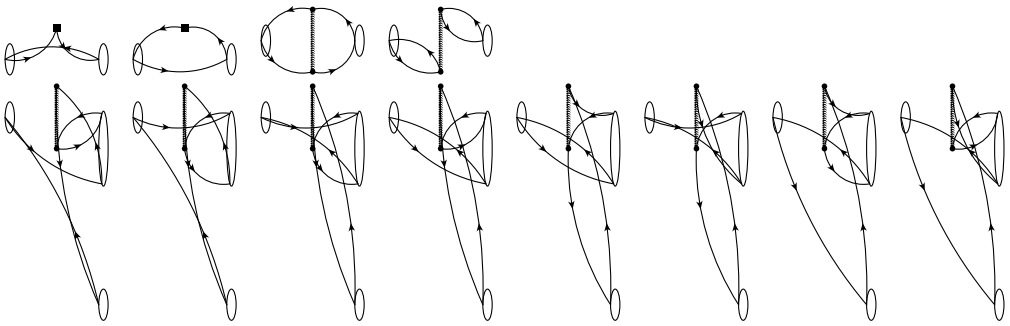

(a) Singles-singles part.

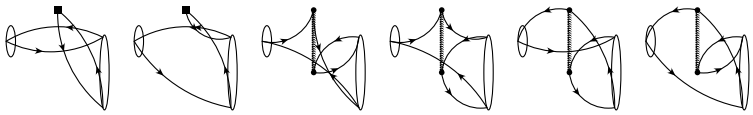

(b) Singles-doubles part.

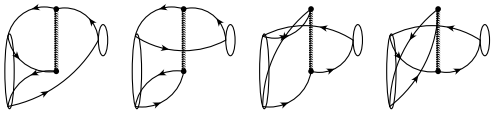

(c) Doubles-singles part.

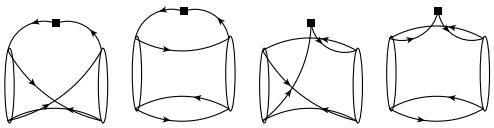

(d) Doubles-doubles part (Fock matrix is undressed).

Figure A.3: Diagrams contributing to the excitation energy $\omega = \tilde{L}\mathbf{A}R$ for singlet excited states.

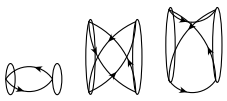

Figure A.4: Diagrams contributing to the norm of the left and right eigenvectors $\tilde{L}\mathbf{M}R$ for singlet excited states.

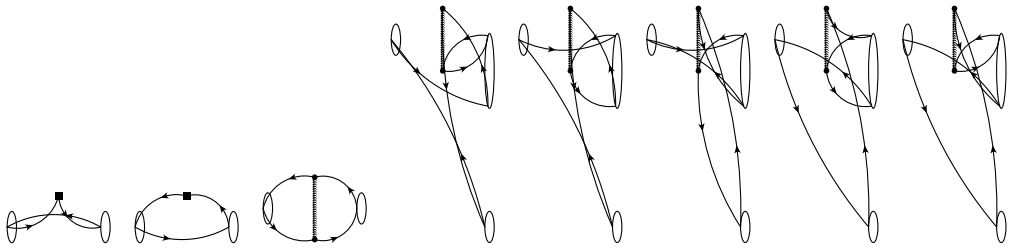

(a) Singles-singles part.

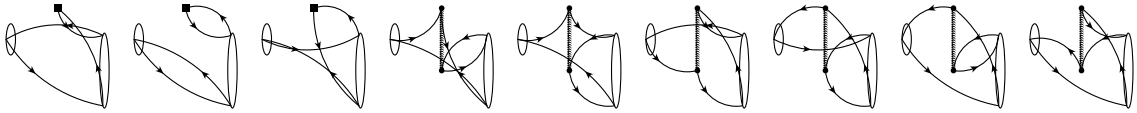

(b) Singles-doubles part.

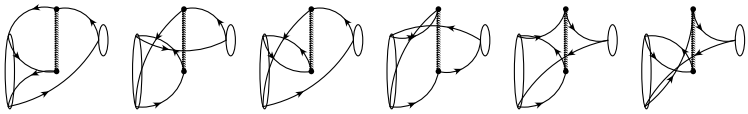

(c) Doubles-singles part.

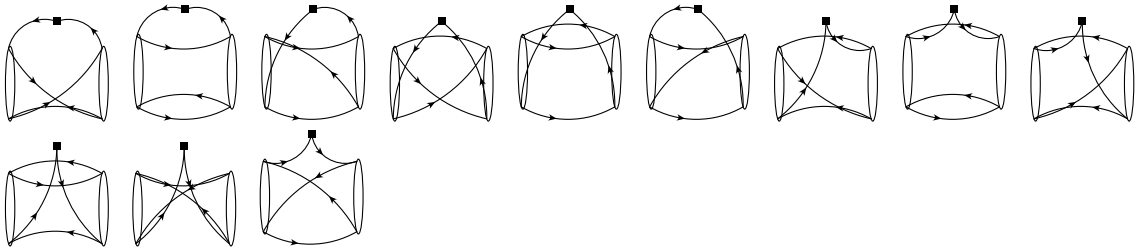

(d) Doubles-doubles part (Fock matrix is undressed).

Figure A.5: Diagrams contributing to the excitation energy $\tilde{L}\mathbf{A}R$ for triplet excited states (only diagrams with non-zero weight).

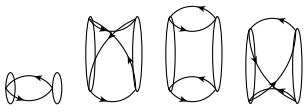

Figure A.6: Diagrams contributing to the norm of the left and right eigenvectors $\tilde{L}\mathbf{M}R$ for triplet excited states (only diagrams with non-zero weight).

Appendix B

Symmetry of the external-external part of B^0

A very useful relation, e.g. for debugging the code, is the symmetry of the intermediate quantity B^0_{ab},

$$B^0_{ab} = B^0_{ba} \ . \tag{B.1}$$

This relation is not obvious looking at the definition of B^0_{ab} according to eq. (2.22),

$$B^0_{ab} \ = \ C^v_{\mu a} B^0_{\mu r} Q_{rb} + C^v_{\mu a} S^{\mathrm{AO}}_{\mu\rho} \delta_{\rho r} B^0_{r\nu} C^v_{\nu b} \ , \tag{B.2}$$

but can be proved indirectly by building an auxiliary quantity Y_{ab},

$$Y_{ab} = \mathcal{R}^i_a t^i_b + \tilde{\lambda}^{i,0}_a \Omega^i_b \ , \tag{B.3}$$

including the amplitude and multiplier residual vectors, $\mathcal{R}^i_a$ and Ω^i_a. The residuals vanish for converged amplitudes t^i_a and multipliers $\tilde{\lambda}^{i,0}_a$, thus Y_{ab} is zero and consequently also symmetric ($Y_{ab} - Y_{ba} = 0$).
Explicitly writing down all terms of B^0_{ab} (starting from the working equations given in section 2.2.3, i.e. with local orbitals for the contractions inside and with all $\hat{f}$ dressed

only internally) yields

$$\begin{aligned}
B^0_{ab} =& 2f_{ka}t^k_b - \hat{f}_{ka}t^j_b\tilde{\lambda}^{j,0}_r S_{rr'}t^k_{r'} + \hat{f}_{ka}\tilde{\lambda}^{j,0}_r S_{rr'}\tilde{t}^{jk}_{r'b} + \hat{f}_{ak}\tilde{\lambda}^{k,0}_b + \hat{f}_{as}\tilde{\lambda}^{k,0}_b t^k_s + \hat{f}_{sa}\tilde{\lambda}^{k,0}_s t^k_b \\
&- 2t^k_b[(ka|ij) - 0.5(kj|ia)]\tilde{\lambda}^{j,0}_r S_{rr'}t^i_{r'} + 2t^k_b[(ka|rs) - 0.5(ks|ra)]\tilde{\lambda}^{j,0}_r t^j_s \\
&+ 2t^k_b[(ka|ri) - 0.5(ki|ra)]\tilde{\lambda}^{i,0}_r - 2t^k_b[(ka|ir) - 0.5(kr|ia)]\tilde{\lambda}^{j,0}_t S_{tt'}t^i_{t'}t^j_r \\
&+ 2t^k_b[(ka|ir) - 0.5(kr|ia)]\tilde{\lambda}^{j,0}_s S_{ss'}t^{ji}_{s'r} + \bar{\mathcal{D}}^{\xi}_{bs}(\lambda^0)f_{sa} + (ka\hat{|}ts)\tilde{t}^{kj}_{bs}\tilde{\lambda}^{j,0}_t \\
&-(ka\hat{|}jl)\tilde{t}^{kj}_{bs}S_{ss'}\tilde{\lambda}^{l,0}_{s'} + 4(ka|ls)t^k_b t^l_s - 2(ka|js)t^j_b t^k_s + (sa\hat{|}jt)\tilde{\lambda}^{k,0}_s\tilde{t}^{kj}_{bt} \\
&+ (ar|js)\tilde{\lambda}^{k,0}_b\tilde{t}^{kj}_{rs} + 2(ra\hat{|}sj)\tilde{\lambda}^{kj,0}_{rs}t^k_b + 2(ka|js)\tilde{t}^{kj}_{bs} + 2(ak\hat{|}sj)\tilde{\lambda}^{kj,0}_{bs} \\
&- (ka|jt)\tilde{\lambda}^{l,0}_s t^l_b S_{ss'}\tilde{t}^{kj}_{s't} \\
&+2(bk\hat{|}sl)\tilde{\lambda}^{kl,0}_{as} - 2(jk\hat{|}sl)\tilde{\lambda}^{kl,0}_{as}t^j_b + 2(kb|js)\tilde{t}^{kj}_{as} + (kb|\hat{ts})\tilde{\lambda}^{j,0}_t\tilde{t}^{kj}_{as} \\
&-(jl\hat{|}kb)\tilde{\lambda}^{l,0}_s S_{ss'}\tilde{t}^{kj}_{as'} + (jr|sb)\tilde{\lambda}^{k,0}_s\tilde{t}^{kj}_{ar} + \bar{\mathcal{D}}^{\xi}_{as}(\lambda^0)f_{sb} + \tilde{\lambda}^{k,0}_s S_{ss'}\tilde{t}^{kj}_{s'a}\hat{f}_{jb} \\
&+ \tilde{\lambda}^{j,0}_b\tilde{t}^{jk}_{ar}\hat{f}_{kr} - (is\hat{|}lk)\tilde{\lambda}^{k,0}_b\tilde{t}^{li}_{as} + \bar{d}^{D}_{ab}(f_{st}) - \bar{d}^{f}_{ab} \ . \qquad \text{(B.4)}
\end{aligned}$$

Considering the difference $B^0_{ab} - B^0_{ba}$, which has to be zero if B^0_{ab} is symmetric, the terms in the gray boxes cancel each other. Consequently, the entire quantity B^0_{ab} is symmetric, if the remaining terms of B^0_{ab} considered separatly are symmetric. These remaining terms of B^0_{ab} are in the following collected in $B^{0\,\prime}_{ab}$,

$$\begin{aligned}
B^{0\,\prime}_{ab} =& 2f_{ka}t^k_b - \hat{f}_{ka}t^j_b\tilde{\lambda}^{j,0}_r S_{rr'}t^k_{r'} + \hat{f}_{ak}\tilde{\lambda}^{k,0}_b + \hat{f}_{as}\tilde{\lambda}^{k,0}_b t^k_s + \hat{f}_{sa}\tilde{\lambda}^{k,0}_s t^k_b \\
&+ 2t^k_b[(ka\hat{|}ri) - 0.5(ki\hat{|}ra)]\tilde{\lambda}^{i,0}_r + 2t^k_b[(ka|ir) - 0.5(kr|ia)]\tilde{\lambda}^{j,0}_s S_{ss'}t^{ji}_{s'r} \\
&+ 4(ka|ls)t^k_b t^l_s - 2(ka|js)t^j_b t^k_s + (ar|js)\tilde{\lambda}^{k,0}_b\tilde{t}^{kj}_{rs} + 2(ra\hat{|}sj)\tilde{\lambda}^{kj,0}_{rs}t^k_b \\
&- (ka|jt)\tilde{\lambda}^{l,0}_s t^l_b S_{ss'}\tilde{t}^{kj}_{s't} - 2(jk\hat{|}sl)\tilde{\lambda}^{kl,0}_{as}t^j_b + \tilde{\lambda}^{j,0}_b\tilde{t}^{jk}_{ar}\hat{f}_{kr} - (is\hat{|}lk)\tilde{\lambda}^{k,0}_b\tilde{t}^{li}_{as} \ , \qquad \text{(B.5)}
\end{aligned}$$

using the relation

$$\begin{aligned}
2t^k_b[(ka\hat{|}ri) - 0.5(ki\hat{|}ra)]\tilde{\lambda}^{i,0}_r =& + 2t^k_b[(ka|ri) - 0.5(ki|ra)]\tilde{\lambda}^{i,0}_r \\
&- 2t^k_b[(ka|ij) - 0.5(kj|ia)]\tilde{\lambda}^{j,0}_r S_{rr'}t^i_{r'} \\
&+ 2t^k_b[(ka|rs) - 0.5(ks|ra)]\tilde{\lambda}^{j,0}_r t^j_s \\
&- 2t^k_b[(ka|ir) - 0.5(kr|ia)]\tilde{\lambda}^{j,0}_t S_{tt'}t^i_{t'}t^j_r \qquad \text{(B.6)}
\end{aligned}$$

for conciseness, with the indices r and i dressed on the left and undressed on the right hand side (k and a are always undressed, because $\Lambda^p_{\mu k} = L_{\mu k}$ and $\Lambda^h_{\mu a} = C^v_{\mu a}$). Note that

some of the summation indices were renamed on the right hand side of eq. (B.6).
To prove the symmetry of $B^{0\,\prime}_{ab}$, it has to be compared with Y_{ab}, which is known to be zero and thus symmetric,

$$\begin{aligned}
Y_{ab} =& \hat{f}_{ak}\tilde{\lambda}^{k,0}_{b} + \hat{f}_{as}\tilde{\lambda}^{k,0}_{b}t^{k}_{s} - \hat{f}_{ki}\tilde{\lambda}^{i,0}_{b}t^{k}_{a} - \hat{f}_{kr}\tilde{\lambda}^{i,0}_{b}t^{k}_{a}t^{i}_{r} + \hat{f}_{kr}\tilde{\lambda}^{j,0}_{b}\tilde{t}^{jk}_{ar} \\
& - (is\hat{|}lk)\tilde{\lambda}^{k,0}_{b}\tilde{t}^{li}_{as} + (ar|js)\tilde{\lambda}^{k,0}_{b}\tilde{t}^{kj}_{rs} - (ir|js)\tilde{\lambda}^{k,0}_{b}\tilde{t}^{kj}_{rs}t^{i}_{a} \\
& + 2\hat{f}_{ia}t^{i}_{b} - \hat{f}_{ki}\tilde{\lambda}^{i,0}_{a}t^{k}_{b} - \hat{f}_{kr}\tilde{\lambda}^{i,0}_{a}t^{k}_{b}t^{i}_{r} + \hat{f}_{sa}\tilde{\lambda}^{k,0}_{s}t^{k}_{b} - \hat{f}_{ka}t^{j}_{b}\tilde{\lambda}^{j,0}_{r}S_{rr'}t^{k}_{r'} \\
& + 2t^{k}_{b}[(ka\hat{|}ri) - 0.5(ki\hat{|}ra)]\tilde{\lambda}^{i,0}_{r} - (ka|jt)\tilde{\lambda}^{l,0}_{s}t^{l}_{b}S_{ss'}\tilde{t}^{kj}_{s't} - (ir|js)\tilde{\lambda}^{k,0}_{a}\tilde{t}^{kj}_{rs}t^{i}_{b} \\
& + 2t^{k}_{b}[(ka|ir) - 0.5(kr|ia)]\tilde{\lambda}^{j,0}_{s}S_{ss'}t^{ji}_{s'r} + 2(ra\hat{|}sj)\tilde{\lambda}^{kj,0}_{rs}t^{k}_{b} - 2(jk\hat{|}sl)\tilde{\lambda}^{kl,0}_{as}t^{j}_{b} \ . \qquad \text{(B.7)}
\end{aligned}$$

In analogy to B^0_{ab} local orbitals are used for the contractions inside Y_{ab}, and all $\hat{f}$ are dressed only internally in eq. (B.7). Again, there are some terms (in the gray boxes) which directly cancel each other, when building the difference $Y_{ab} - Y_{ba}$. The remaining terms are collected in Y'_{ab},

$$\begin{aligned}
Y'_{ab} =& \hat{f}_{ak}\tilde{\lambda}^{k,0}_{b} + \hat{f}_{as}\tilde{\lambda}^{k,0}_{b}t^{k}_{s} + \hat{f}_{kr}\tilde{\lambda}^{j,0}_{b}\tilde{t}^{jk}_{ar} - (is\hat{|}lk)\tilde{\lambda}^{k,0}_{b}\tilde{t}^{li}_{as} + (ar|js)\tilde{\lambda}^{k,0}_{b}\tilde{t}^{kj}_{rs} \\
& + 2\hat{f}_{ia}t^{i}_{b} + \hat{f}_{sa}\tilde{\lambda}^{k,0}_{s}t^{k}_{b} - \hat{f}_{ka}t^{j}_{b}\tilde{\lambda}^{j,0}_{r}S_{rr'}t^{k}_{r'} + 2t^{k}_{b}[(ka\hat{|}ri) - 0.5(ki\hat{|}ra)]\tilde{\lambda}^{i,0}_{r} \\
& - (ka|jt)\tilde{\lambda}^{l,0}_{s}t^{l}_{b}S_{ss'}\tilde{t}^{kj}_{s't} + 2t^{k}_{b}[(ka|ir) - 0.5(kr|ia)]\tilde{\lambda}^{j,0}_{s}S_{ss'}t^{ji}_{s'r} \\
& + 2(ra\hat{|}sj)\tilde{\lambda}^{kj,0}_{rs}t^{k}_{b} - 2(jk\hat{|}sl)\tilde{\lambda}^{kl,0}_{as}t^{j}_{b} \ , \qquad \text{(B.8)}
\end{aligned}$$

which consequently has to be symmetric, too. Finally, comparing $B^{0\,\prime}_{ab}$ (eq. (B.5)) and Y'_{ab} it can easily be seen, that they are equal, if eq. (1.19) is employed for the term $2\hat{f}_{ia}t^i_b$ in Y'_{ab},

$$\begin{aligned}
2\hat{f}_{ia}t^{i}_{b} =& 2t^{i}_{b}\left[h_{ia} + 2(ia\hat{|}kk) - (ik\hat{|}ka)\right] \\
=& 2t^{i}_{b}\left[h_{ia} + 2(ia|kk) + 2(ia|kr)t^{k}_{r} - (ik|ka) - (ir|ka)t^{k}_{r}\right] \\
=& 2f_{ia}t^{i}_{b} + 4(ia|kr)t^{k}_{r}t^{i}_{b} - 2(ir|ka)t^{k}_{r}t^{i}_{b} \ . \qquad \text{(B.9)}
\end{aligned}$$

Hence, $B^{0\,\prime}_{ab}$ and B^0_{ab} are symmetric, and eq. (B.1) is fulfilled.